$5

QEX

INCLUDING: COMMUNICATIONS QUARTERLY

Forum for Communications Experimenters

September/October 2000

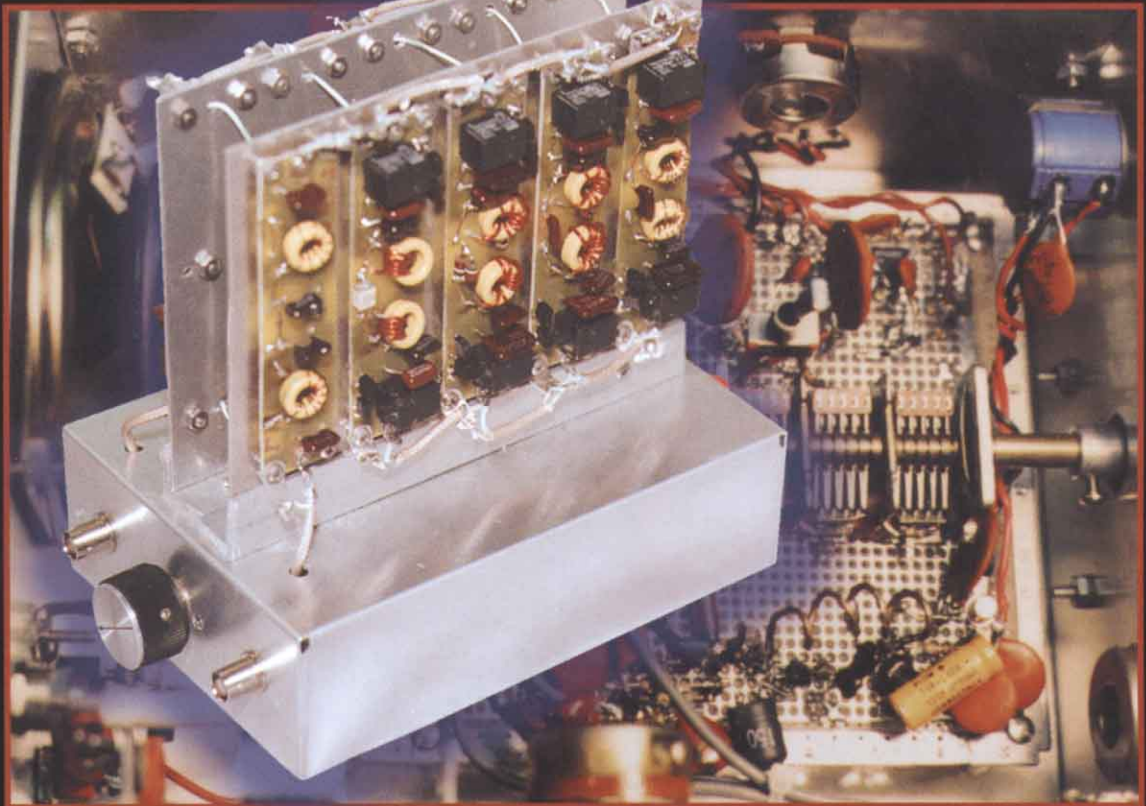

WØIYH's HF Filter floats over N1TEV's 88-180 MHz Super-Regen Receiver—Look Inside!

ARRL The national association for AMATEUR RADIO
225 Main Street
Newington, CT USA 06111-1494

QEX

INCLUDING: COMMUNICATIONS QUARTERLY

QEX (ISSN: 0886-8093) is published bimonthly in January, March, May, July, September, and November by the American Radio Relay League, 225 Main Street, Newington CT 06111-1494. Yearly subscription rate to ARRL members is $22; nonmembers $34. Other rates are listed below. Periodicals postage paid at Hartford, CT and at additional mailing offices.

POSTMASTER: Form 3579 requested. Send address changes to: QEX, 225 Main St, Newington, CT 06111-1494

Issue No 202

Offices

225 Main St, Newington, CT 06111-1494 USA
Telephone: 860-594-0200
Telex: 650215-5052 MCI
Fax: 860-594-0259 (24 hour direct line)
e-mail: **qex@arrl.org**

Subscription rate for 6 issues:

In the US: ARRL Member $22, nonmember $34;

US, Canada and Mexico by First Class Mail: ARRL member $35, nonmember $47;

Elsewhere by Surface Mail (4-8 week delivery): ARRL member $27, nonmember $39;

Elsewhere by Airmail: ARRL member $55, nonmember $67.

Members are asked to include their membership control number or a label from their *QST* wrapper when applying.

In order to ensure prompt delivery, we ask that you periodically check the address information on your mailing label. If you find any inaccuracies, please contact the Circulation Department immediately. Thank you for your assistance.

About the Cover

Bill Sabin's narrow-band-pass HF filter article begins on p 13. Charles Kitchin's discussion of super-regen receivers begins on p 18.

Features

Columns

Sept/Oct 2000 *QEX* Advertising Index

Empirically Speaking

Lately, I've been through a sort of crash course in high-speed, wireless networking. Commercial entities world-wide are on a bandwidth binge fueled by increasing demand for wireless Internet access, digital voice and video. Some recent studies predict a compound growth rate as high as 55% per year for the next five years in wireless LANs alone.

In a free market, rising demand for products usually brings down equipment costs through larger production volumes. As the cost of high-speed radios (in buck-seconds per bit) comes down, more folks are encouraged to dream up new uses for spectrum, many of which may become popular. On CSPAN recently, Former FCC chairman Reed Hundt said that he sees significant pressure coming for additional spectrum. It's not too hard to imagine that the bands we share with some of these other services will become crowded soon.

I've heard from many who are interested in fast digital modes. Interest in digital voice also seems high. Well, hams have always been good at building wide-area networks! It would be nice if Amateur Radio experimenters were fielding more systems to try to keep our stake in certain bands, especially 13 cm and 5 cm.

The League has made a significant commitment to experimentation with software-defined radios (SDRs). An SDR is a radio that "knows" many different frequencies and modulation formats, and whose software may be readily updated to "learn" others yet unforeseen. It looks as if we have an article or two lined up on this topic and we'll be looking for more. Note that it's an excellent opportunity for analog and digital designers to cooperate on both hardware and software. Each may be standardized to some extent—a valuable benefit to those working on applications for the future.

Among key ingredients in SDRs will be adaptive DSP algorithms that not only find signals and analyze their modulation, but also detect and correct distortion effects, such as multipath. "Adaptive beam-forming" arrays may be employed that automatically alter their patterns according to preset criteria, such as direction of arrival. An adaptive array may be programmed to automatically build a sharp null in the direction of interference the moment it appears. This leads directly to an extremely effective form of direction finder that exhibits very fine angular resolution. It will be interesting to see what impact SDR technology has on radio design in the coming years.

In This Issue

From his perspective as a long-time experimenter in the field, Bar-Giora Goldberg delivers a technical overview of frequency-synthesis techniques, past and present. Giora concentrates on the prime goal of producing a clean signal. He discusses loop noise shaping and fractional-N methods in detail. Current trends in research and development are also treated.

Broadband front ends in receivers have been prevalent for some time now. SDRs are likely to continue on that path; but to minimize interference and reduce processing horsepower, interest in narrow-band preselectors is likely to resurge. Bill Sabin, W0IYH, brings us a bank of narrow band-pass filters for use in reducing second-order IMD and other problems. Bill uses relays to select the filters. Linearity factors are closely examined.

Unfortunately, Part 3 of R. P. Haviland, W4MB's series on quad antennas has been delayed until the next issue.

Charles Kitchin, N1TEV, has some updates on super-regenerative receivers. He discusses many of their traditional drawbacks and the ways he and others have found to overcome them. New work on VHF and NBFM is presented.

Sam Ulbing, N4UAU, continues his series on UHF remote control by expanding his bandwidth and choice of operating modes. We're quite pleased to have an article from Chen Ping, BA1HAM, about improved commutating filters. Chen Ping shows how to deal with aliasing problems in an interesting and, we believe, unique way.

Matt Reilly, KB1VC's paper from the 25th Eastern States UHF/VHF Conference *Proceedings* introduces a Web site that calculates and returns line-of-sight radio paths based on USGS digital elevation information. Now, who wants to get in the record books?

In RF, Zack Lau, W1VT, writes about feeding a dipole with TV twin lead and presents a 70-cm band-pass filter. In his column, Peter Bertini, K1ZJH, re-introduces himself and brings us a piece about baluns from Rick Littlefield, K1BQT.—*73, Doug Smith, KF6DX,* **kf6dx@arrl.org**.

Frequency Synthesis Technology and Applications: A Review and Update

Look to the future—smaller, cleaner, less costly frequency generation.

By Bar-Giora Goldberg
VITCOM CORPORATION

Signal generation and frequency synthesis (FS) are basic functions in all radio and timing products. They are used to generate transmitted signals, as local oscillators and clocks for timing circuits. Three main techniques are used to synthesize signals from a reference: direct analog (DA), direct digital (DDS), and phase-locked loop (PLL). Frequency synthesis is a mature but fast-evolving technology. The last few years have seen rapid advances in PLL and fractional-n principles, technology and chips. This article reviews and compares the different FS techniques, elaborates on the nature of signals and phase-noise theory, reviews new PLL technology (all-digital fractional), demonstrates computer-simulation results and attempts to forecast future evolution of the technology.

3521 Mercer Ln
San Diego, CA 92122
giora18@tns.net

A Review of FS

Signal generation and control is a fundamental function in any radio. Years ago, most applications used free-running oscillators for LOs or to generate transmitted signals, but in the last quarter century, the art and science of FS has developed and matured. Now, FS has become ubiquitous even in hand-held consumer electronics, as cost, size and performance have improved. Compared to free-running oscillators, FS is a mechanism that may generate many frequencies from a single crystal reference. The output frequency—always a rational multiplier of the reference's—acquires the accuracy and stability of the reference:

$$F_0 = F_{xtal}\left(N + \frac{K}{L}\right) \qquad \text{(Eq 1)}$$

where F_0 is the output frequency, F_{xtal} the reference and N, K and L are all natural numbers. Compared to free-running types, synthesizer signals have improved accuracy and stability by orders of magnitude.

Modern wireless networks require very tight spectral control, accurate timing and very little jitter; therefore, the use of FS is necessary. In addition, FS allows better spectral purity (phase noise), the most important parameter of FS. Phase noise affects not only jitter, signal-to-noise ratio

(SNR) and bit-error rate (BER) of the signal we receive, but also has an adverse effect on adjacent channels, hence its significance in wireless networks.

The engineering task involved in designing FS always has a built-in requirement for economy, variously with respect to size, power, complexity and cost. The designer must weigh all available options to resolve the issue and come up with the most economical solution. Wireless handheld devices have much less demanding requirements and are usually served by a single-chip solution, while instrumentation, base stations, "satcom" terminals and LOS radio links can have very demanding specifications, calling for more complex designs.

The technology has matured immensely in the last decade. Single-chip PLL devices, running at 3.5 GHz or more, now consume very low power (5-6 mA at 3 V dc) and require only an external crystal, VCO and loop filter to operate. There are already designs that even integrate the VCO and loop filter into the chip! Some manufacturers integrate two or even three complete PLL circuits into a single device, enabling RF and IF or timing generation using a single part, thus saving power and space.

DDS technology has also matured greatly. Single-chip devices including all functions—with quadrature multipliers, CW and chirp built in and extremely high control-interface speeds —are already available in CMOS at clock speeds exceeding 300 MHz. So chip technology and CMOS processes are accelerating the utility of FS chip technology; increases in functionality, frequency range and economy of power are expected to rise quickly in the coming years.

Generally speaking, FS is concerned with the improvement of a signal's spectral purity. We will therefore start with a short review of phase-noise theory; later we will look at phase-noise modeling of VCOs and PLLs. Of all FS techniques, PLL is most often the technology of choice, so PLL will get more attention in this article.

Introduction to Phase-Noise Theory

All signals are narrow-band noise! The concept of ideal periodic signals of the form:

$$y = A\sin(\omega_0 t) \qquad \text{(Eq 2)}$$

is only theoretical and convenient for modeling and analysis; it is erroneous in principle. All oscillators are actually positive feedback amplifiers with a resonator in the feedback path; all oscillators start oscillations because there is noise inherent in the active device. (See Fig 1.) Ultimately, their spectra are the products of the noise and resonator transfer functions. Therefore, a more accurate description of real signals is given by:

$$y = A\sin[\phi(t)] \qquad \text{(Eq 3)}$$

While there is also noise in amplitude variations (AM noise), it is practically negligible compared with phase noise.

Note then, that real signal energy is not concentrated in one frequency (the *delta* function in the frequency domain); rather it has a noisy spectrum. A more concentrated spectrum yields better signal quality. Thus, signals can be described only in statistical terms. Their phase:

$$\phi(t) \approx \omega_0 t + \varphi(t) \qquad \text{(Eq 4)}$$

has an *average* angular frequency of ω_0. This is what we refer to as the center frequency. Note that this is a statistical average; its instantaneous value may change with time. The quality of the signal is defined by the standard deviation of this statistically varying parameter.

Now, to better our understanding of the effect, let's briefly derive phase-noise theory from FM theory. We will model the "corrupted" signal as:

$$y = \sin[\omega_0 t + m\sin(\omega_m t)] \qquad \text{(Eq 5)}$$

where the first term represents an "ideal phase" and the second represents phase fluctuations or noise. We always assume that the noise is low; m is the *modulation index* of a general FM signal, thus $m<<1$. This signal is periodic, therefore its Fourier series is generally given by:

$$\sin[\omega_0 t + m\sin(\omega_m t)] = J_0\sin(\omega_0 t) + J_1\sin(\omega_0 \pm \omega_m)t + J_2\sin[(\omega_0 \pm 2\omega_m)t] + \ldots \qquad \text{(Eq 6)}$$

J_0, J_1, J_2, etc are *Bessel functions* and their value depends on m. For $m<<1$, Bessel coefficients are $J_0=1$, $J_1=m/2$; and others are virtually negligible. Therefore, our model shows a perfect carrier with two sidebands, each with peak amplitude $m/2$. These sidebands represent the noise perturbation in our model. See Fig 2 for a spectral depiction of this signal representation. The phase deviation clearly has RMS power given by:

$$E\{[m\sin(\omega_m t)]^2\} = \frac{m^2}{2}\ \text{rad}^2 \qquad \text{(Eq 7)}$$

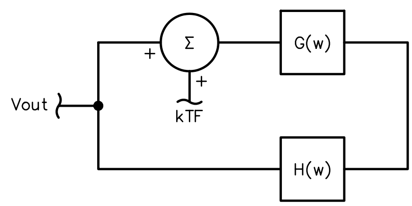

Fig 1—Oscillator model with forward gain *G*, feedback resonator *H* and device noise *kTF*. *F* is the noise factor of the active device.

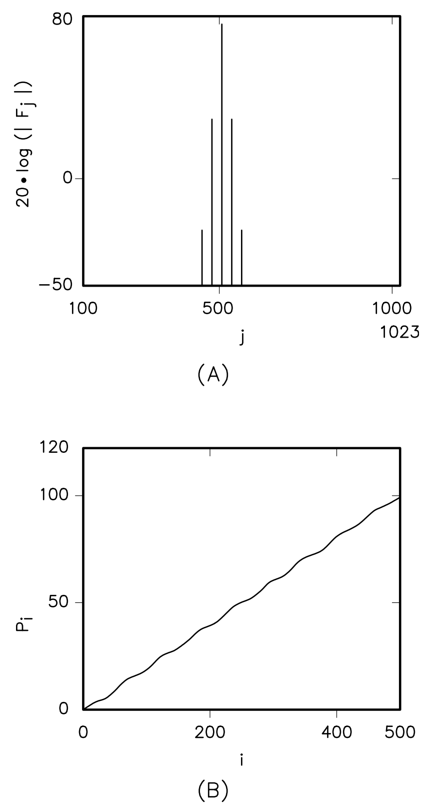

Fig 2—Spectral representation of an FM-modulated signal, showing 0th, 1st, and 2nd terms of Bessel functions.

Each sideband has relative power of $m^2/4$. We can shortly summarize that the phase error, in radians^2, is equal to the relative power of the sidebands.

Extension of this analysis is easily made from sine-wave modulation of the carrier (deterministic) to noise modulation (random). Thus, we can summarize that for a real signal, with reasonably good spectral purity (m<<1), the phase jitter, in radians^2, is equivalent to the relative power of the noise spectrum.

Phase-Noise Examples and Simulation

Most signal sources and synthesizers have a phase-noise spectrum monotonically declining with increasing frequency offset, such as shown in Table 1. Close to the carrier, the noise embodies slow fluctuations such as crystal drift with temperature or time and flicker noise of active devices. These slowly varying (long-term) noise components can usually be tracked, and therefore corrected, in the receiver. As we move away from the center frequency, noise components become faster (short-term) and add to the noise that always exists in any communication channel. The noise in the signal itself, therefore, is already a limiting factor in the quality of the communication link and must be specified carefully. The noise spectrum of a signal is usually defined by the function $L(f_m)$, which indicates the SSB noise distribution—in a 1 Hz bandwidth relative to total power—at an offset f_m from center frequency. $L(f_m)$ is given in dBc/Hz (the "c" indicates that carrier power is the reference). So a 1-GHz synthesized signal having $L(f_m)$ = –90 dBc/Hz at f_m = 10 kHz means that at an offset of ±10 kHz from 1 GHz, the signal's SSB power, in a 1-Hz bandwidth, is 90 dB below the signal's total power. If this signal's total power level is +10 dBm, its spectral components at 10-kHz offset are at a level of (+10–90) = –80 dBm/Hz.

Table 1—An Example of an Oscillator's Phase-Noise Characteristic

$L(f_m)$ (dBc/Hz)	f_m (Hz)
–20	1
–30	10
–55	100
–72	1 k
–85	10 k
–95	100 k
–125	1 M

To measure the total contribution of this noise in anything but a 1-Hz BW, we must define the frequency range (bandwidth) of interest. Therefore, according to the principles we developed before:

$$\phi_j^2 = 2\int_{f_1}^{f_2} L(f_m)\,df_m \ \text{rad}^2 \qquad \text{(Eq 8)}$$

This is the RMS phase deviation for the frequency range (f_2–f_1), obtained by integrating (summing) the noise contributions at every frequency in the range. Once we have a given noise profile, a computer program may be employed to calculate this integral.

For example, take a signal having phase-noise characteristics as given in Table 1. The phase jitter from 10 Hz to 100 kHz can be calculated to be 0.117 radians, RMS. (CAD programs to calculate this integral are reasonably easy to write.) This means that in a perfect channel, with no noise, the signal will already contribute 0.117 radians of noise. In a four-phase (QPSK) modulated signal, where phase difference between states is $\pi/2$ radians and $\pi/4$-radian deviations cause error, such a signal will already have a maximum SNR of:

$$SNR_{\max} = 20\log\left(\frac{\frac{\pi}{2}}{0.117}\right) \approx 16.5 \text{ dB} \qquad \text{(Eq 9)}$$

clearly not enough for most applications!

Those spurious signals appearing on a signal that are deterministic but not related to the carrier add phase jitter exactly as random noise does. For example, an ideal signal with a single spur at –60 dBc will cause phase jitter of ϕ_j^2 = –60 dBc or a factor of 10^{-6}, so $\phi_j = \sqrt{10^{-6}} = 10^{-3}$ radians. Noise and spurious signals add incoherently, thus the total contribution of phase noise and spurious will be given by:

$$\phi^2_{j\,\text{total}} = \phi^2_{j\,\text{noise}} + \phi^2_{j\,\text{spurs}} \qquad \text{(Eq 10)}$$

We consequently conclude that all signals have a noise profile. This noise affects signal quality and may interfere with adjacent channels. Once this profile is measured, it is easy to convert its value to phase or time jitter and check if it meets system requirements. We will see later that in a PLL circuit, it is possible to control the profile of a signal's noise spectrum in its generation.

FS Design: Specifications

Synthesizers are specified by many parameters. The following is a short summary:

- Frequency range
- Resolution or step size: specifies the smallest frequency step the synthesizer can generate. In instrumentation, this parameter is 0.1-10 Hz; in cellular, it's 5-200 kHz.
- Accuracy: usually measured in ppm. This parameter is sometimes given in ppm/day or ppm/year as an aging rate. Most cellular radios use ±2.5 ppm-accuracy crystals. In SSB service, frequency errors up to 5 Hz may be allowed. At 100 MHz, this translates to 5×10^{-8} or 0.05 ppm. Accuracy depends on reference quality.
- Switching speed: specifies the time taken to switch across the band of interest. This is sometimes given in µs/MHz and is defined as settling to within a specific frequency tolerance (say within 1 kHz) or phase (say 0.1 radians). This parameter is specified this way because all settling processes may be represented as convergences taking the form $A\bullet e^{-\alpha t}$, where A usually depends on the excursion: Larger excursions yield larger As. (Hopping 10 kHz is much faster than hopping 10 MHz.)
- Phase noise: specifies signal purity and noise profile; this can be related to RMS phase fluctuations as defined above.
- Spurious responses: specifies the maximum level of discrete, unwanted spectral lines such as line-frequency, switching-power-supply frequency and PLL reference-frequency offenders as well as mixing and intermodulation products.
- Power, voltage, interface, environmental conditions and mechanical structure.

The following is a short review of FS techniques, namely direct analog, direct digital and PLL.

FS Design Principle Summary

Historically, DA is the first FS technology. Direct (PLL has been coined "indirect") means that the frequencies are derived directly from the reference, mainly by using multiplication (comb generation), division and mix-and-filter operations. Direct synthesizers generate sets of reference frequencies that are used repeatedly to generate resolution. Such blocks usually perform the generation of 10 frequencies, at which point the output is divided by 10 and connected to the next, similar block. Consequently, every block increases resolution by a digit and control is usually in BCD. Reference frequencies are generated by a comb generator: A comb line is selected, filtered and sometimes mixed with another. An alternate technique used in DA synthesis is drift cancellation, as shown below. This allows economical and rapid selection of a specific comb line. (See Figs 3 and 4.) Direct analog synthesis uses comb generators and mix-and-filter operations extensively, thus DA circuits are generally large and use extensive filtering.

DA synthesizers offer very good spectral purity and fast switching speed. However, they are usually complex, large, expensive and require very careful grounding and shielding. Because they lack any filtering mechanism like that in a PLL, their noise floor is usually quite limited.

DDS, invented in 1970 by MIT scientists,[1] is a DSP technique that builds the signal numerically, converting the digital samples to analog via a digital-to-analog converter (DAC) and low-pass filter (LPF). The DDS tracks signal phase, $\phi(t)$, as a linear function of time in a phase accumulator. A digital integrator adds a phase increment, $d\phi$, at each sample time. The slope of the line representing phase versus time is equal to the output frequency, ω_0. The phase samples then serve as the addresses into a look-up table, mapping them to output amplitudes of a sine or cosine wave. Because the look-up ROM can become quite large, many compression algorithms have been devised that achieve compression ratios of up to 50:1. A very popular ROM size, transforming 14 bits of phase input to 12 bits of amplitude output and requiring a raw 12×214 = 196 kbits, can be implemented using approximately 3 kbits of compressed memory. Highly integrated chips are available at low cost and small size from Analog Devices (a clear leader in CMOS DDS products) and others such as Stanford Telecom, Harris (Intersil) and Qualcomm. These devices, running at clock speeds up to 300 MHz, cost in the $20-$50 range and have many useful features such as FSK, phase modulation, chirp capabilities, digital amplitude control and more.

Very-high-speed DDS products are available from Plessey (SP2002) and Stanford Telecom (GaAs) with clock speeds up to 2 GHz, but these are quite expensive ($1000s). Arbitrary function generators, capable of generating programmable waveforms, operate on the same principle and are now available with clock rates exceeding 1 GHz.

PLL is usually the FS technology of choice for economical generation of signals in local-oscillator and timing circuits. PLL is a feedback-mechanism technology used to multiply signals but also enable control of their output spectra, since it acts as a band-pass filter. (See Fig 7.) While DA and DDS produce phase noise similar to that of the reference (but multiplied), PLL enables control of the noise profile. We will later outline basic PLL theory. In a classical (integer) PLL, the relationship between the output and reference frequency is always given by $F_0 = NF_{ref}$, where N is an integer. An extension of this principle—called *fractional-n* PLL—enables reduction of N, the multiplier, thus reducing phase noise; this technique has been the focus of significant research and development by chip manufacturers. Analog fractional-n implies analog compensation of the error signal (second-order fractional), while a new DSP technique (third-order fractional) has caught the attention and imagination of many designers.[2]

Classical PLL chips from National Semiconductors, Fujitsu, Philips, Texas Instruments, Motorola, Analog Devices and many others constitute a large array. There are a few second-order fractional-n chips in the market from Philips, National and Texas Instruments. There are no third-order (all-digital) chips in the market yet. Hewlett Packard, Marconi and Synergy Microwave have working parts and supply complete synthesizers. Chips are expected on the market this year.

PLL chips are very economical in power, size and cost. Complete PLL chips, covering up to 3.5 GHz and requiring an external reference crystal, VCO and loop filter, usually operate from 3-5 V dc, require 4-6 mA and cost $3-4.

VCO and Phase-Noise Modeling

Almost all models for VCO noise use the Leeson model,[3] given approximately by:

$$L(f_m) \approx 10 \log \left[kTF \left(1 + \frac{f_c}{f_m} \right) \left(1 + \left\{ \frac{f_0}{2Q f_m} \right\}^2 \right) \right] \quad \text{(Eq 11)}$$

where F is noise factor, f_c is VCO flicker-

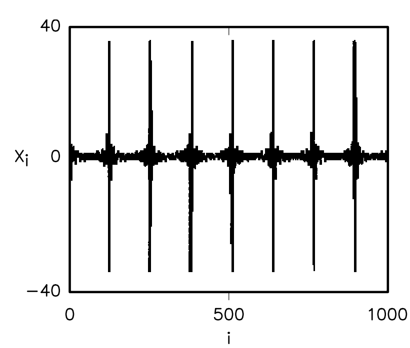

Fig 3—A time series of the comb-generator output.

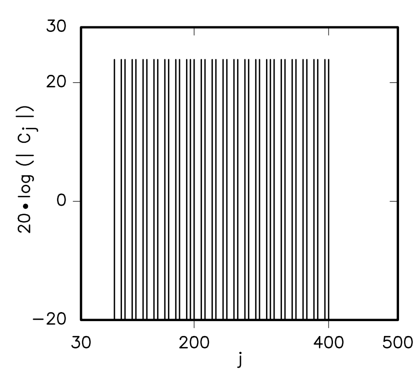

Fig 4—Comb-generator output spectrum.

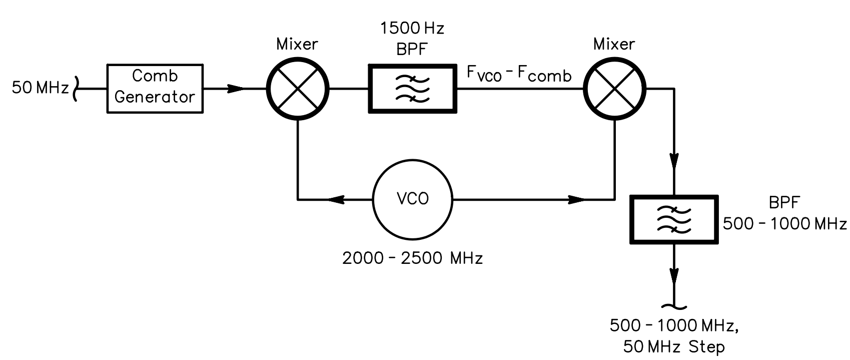

Fig 5—A block diagram of a drift-cancellation loop.

[1]Notes appear on page 12.

frequency corner, f_0 is output center frequency, Q is resonator loaded Q, and f_m is offset from center frequency. Of course, there are new CAD models that are more accurate, but many VCO designs are still an "art." A VCO noise profile at 2 GHz, with Q=50, is shown in Fig 6. Though monotonically declining, the VCO noise eventually reaches a floor, close to –155 dBc/Hz in this case. Across a 10-Hz to 1-MHz offset, the VCO noise profile covers 130-140 dB of dynamic range, hence there is a difficulty in measurement.

VCO noise is highly dependent on Q and tuning sensitivity (in MHz/V). Lower tuning/modulation sensitivities yield better phase-noise performance. For most cellular/PCS VCOs, this number is in the 4-20 MHz/V range, depending on the application. Now, let's try to demonstrate what this noise floor means in the radio.

In cellular phones, VCOs must be very economical; let's assume that the noise floor is –155 dBc/Hz. The phone is full duplex and transmits approximately 1 W (+30 dBm). This means that without filtering, the transmitter noise floor is +30–155 = –125 dBm/Hz. Compare this level to the "kTB" or thermal noise, –174 dBm/Hz, and see immediately that without significant filtering (usually with a diplexer in cellular phones), the transmit VCO phase noise would reduce receiver sensitivity by more than 40 dB!

Phase noise and noise floor also have adverse effects on adjacent channels. Thus, there are two related problems mainly concerning us in radio-networking applications: close-in phase noise, which usually affects data and BER quality; and the need for greater transmit/receive frequency offsets as noise floor affects network performance. In PLL applications, it is easy to show that the loop attenuates VCO phase noise within the loop bandwidth. See Fig 7, a loop simulation showing the individual contributions of crystal-reference, phase-detector and VCO noise using *Eagleware* software. Beyond the loop bandwidth—300 Hz in this example—the VCO becomes the dominant noise source and the loop has no effect on this parameter. Close to the carrier, reference- and phase-detector noise contributions are dominant, while VCO noise is attenuated heavily.

Basic PLL Theory: Noise-Cancellation Effects

A PLL is a simple negative-feedback circuit that allows extremely economical generation of frequencies up to 15 GHz. (A block diagram is shown in Fig 8.) When the loop is locked, the condition $f_0 = Nf_{ref}$ must be satisfied; hence, changing the division ratio N changes the output frequency. In addition, PLLs allow some control of the output spectrum. I assume the reader is familiar with basic PLL math, so the following is a short summary. PLL parameters are:

- Phase-detector constant k_d (V/rad)
- VCO constant kv (Hz/V)
- Division ratio N
- Loop filter response

For a second-order loop filter, the type most commonly used, the transfer function is:

$$F(s)=\frac{1+st2}{st1} \qquad \text{(Eq 12)}$$

Second-order PLL loop response is given by:

$$\frac{\varphi_o}{\varphi_i}=\frac{NK[F(s)]}{1+K[F(s)]}$$
$$=\frac{N\left(2\xi\,\omega_n s+\omega_n^2\right)}{s^2+2\xi\,\omega_n s+\omega_n^2} \qquad \text{(Eq 13)}$$

where $K=k_v\,k_d$, V is the loop damping

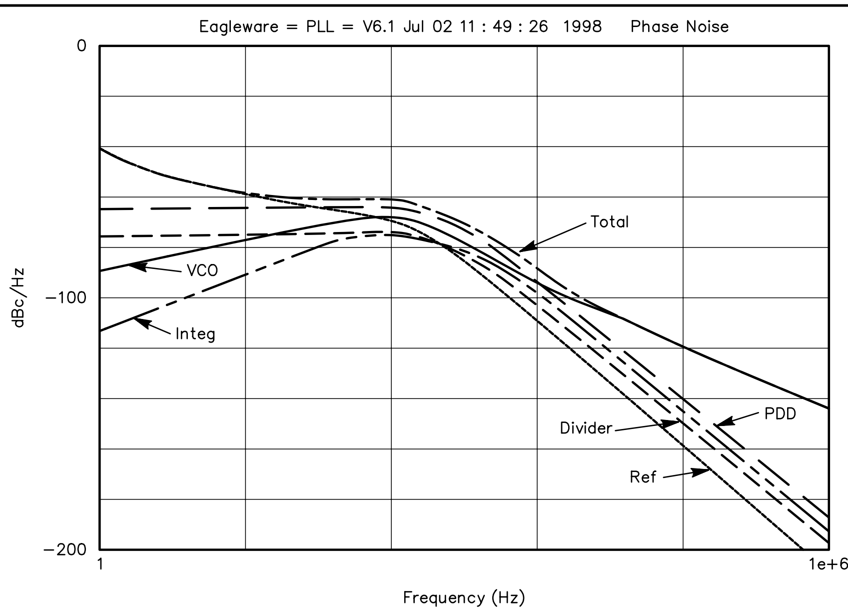

Fig 7—PLL noise components and composite (highest line) simulation with loop BW = 300 Hz, using *Eagleware* software. Note VCO noise is heavily attenuated inside the loop bandwidth.

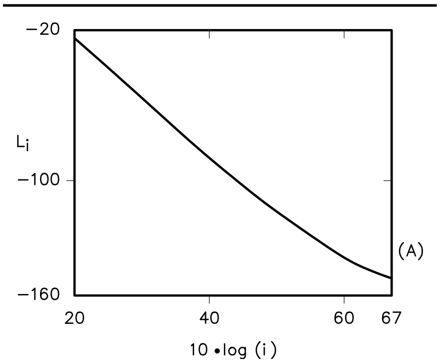

Fig 6—2-GHz VCO noise model results, Q=50, 10 Hz≤f_m≤5 MHz.

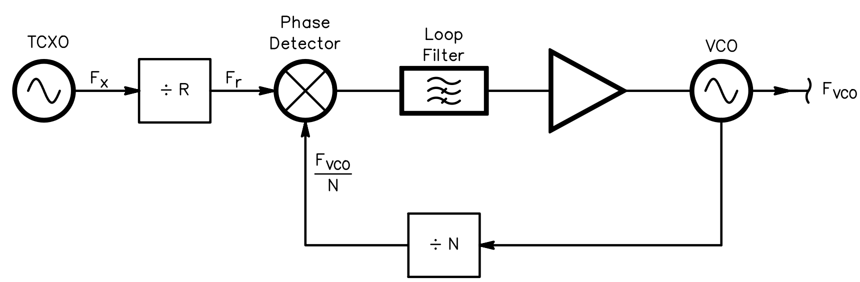

Fig 8—Basic PLL block diagram.

factor, and ω_n is its natural frequency.

PLL phase noise is mainly affected by phase-detector/divider noise within the loop bandwidth. This noise, usually assumed flat, is multiplied by the loop transfer function, causing a 20log(N) degradation within the loop. Beyond the loop bandwidth, though, it is filtered out. VCO noise is highly attenuated within the loop bandwidth. (See Fig 7.) Outside the loop bandwidth, the VCO noise is not effected by the loop. Inside, the VCO attenuation transfer function is given by:

$$\frac{s^2}{s^2+2\xi\,\omega_n s\,\omega_n^2} \quad \text{(Eq 14)}$$

Thus, close to the carrier, VCO noise is attenuated at the rate of 40 dB decade. This effect is one of the "miracles" of PLL.

Fractional-n PLL

As already mentioned, the main challenge of FS is the improvement of phase noise and spectral purity. In a PLL, when resolution is high because of very high values of N, phase noise can be very corrupted, even if parameters are designed well. For example, a cellular-radio PLL, running at 900 MHz with 10-kHz steps must set N=90,000. With phase-detector noise of –165 dBc/Hz, noise multiplication of 20 log(90,000) corrupts noise inside the loop bandwidth by almost 100 dB, from –165 to –65 dBc/Hz!

One of the ideas developed some 20-25 years ago was to increase the reference f_{ref} so that N could be lowered to allow the output frequency to be a fraction of the reference, so that $f_0 = f_{ref}(N+K/L)$. Now, the reference can be L times higher than before and still get the same resolution f_{ref}/L. L is the circuit *fractionality*. Since there are no dividers that divide by fractions, fractionality can be achieved only by generating an average division of K/L. This is done by dynamically changing the divisor between N and N+1. If we divide (in a single cycle consisting of L subcycles) K times by N+1 and L–K times by N, then the average division is given by:

$$\frac{K(N+1)+N(L-K)}{L}=N+\frac{K}{L} \quad \text{(Eq 15)}$$

exactly what we wish to achieve. The problem that we create by doing it is that we generated the correct phase slope by an average (step-wise) process. (See Fig 9.) This problem of fractional circuits has been resolved by two methods: analog (second-order) and digital (third-order) compensation.

First, let's review the workings of a fractional circuit to understand these correction mechanisms. Compared to classical PLLs, fractional PLLs use an extra accumulator (size L) and change the division ratio from N to N+1 every time the accumulator overflows and carries. When the accumulator reaches a preset value under our control, the ratio is set back to N. This is sometimes called *dual-modulus* division. Say, for example, we make the preset (K) value equal to 1; then the divider will operate with a divisor of N+1 for 1 of the 8 counts, a divisor of N for 7 counts.

Now if we change K to 3, the divider will change ratios 3 times in 8 counts. Note that the accumulator will always overflow K times in L increments where $0 \le K < L$. Also, note that the content of the accumulator indicates the exact phase error from the ideal phase. For example, in the first case, K=1, we wish the phase to generate an ideal slope of 1/8 so that at each sample, the phase will increment by $2\pi/8$. Instead, the basic fractional circuit does not increment the phase at all for seven cycles, then gives us the complete 2π in one shot. (Incrementing the count from N to N+1 forces the counter to swallow 1 more cycle of the VCO, which is exactly 2π.) However, if we also note the accumulator contents, it goes 0, 1, 2, 3, ...7, exactly the phase we need to compensate (times $2\pi/8$ of course).

Second-order fractional-n circuits, therefore, use the accumulator carry out to modulate the divider, but also use the accumulator contents to instantaneously increment the phase by pumping current into the phase detector according to the value of the accumulator contents. The accuracy of these circuits—in large-volume manufacturing of low-cost products—is limited to about 35-40 dB, so fractional spurious products are limited to these numbers and require external filtering to meet the 60-70 dB levels usually necessary.

This problem has, however, another solution: an all-digital one developed only in the last decade, but still not available in mass production. To understand it, we need to explore principles of oversampling and noise shaping.

Oversampling and Noise Shaping

The sampling theorem provides that if a signal is sampled at a rate at least twice its bandwidth, it can be fully reconstructed from its samples. I cannot offer an intuitive explanation, but the math is 50 years old and not too complicated (see the referent of Note 1 if you are not familiar). The theorem is now widely used in all electronics and DSP. Analog sampling is followed by digital quantization, that is, the sampled signal is converted to digital format, represented by b bits. A sine wave represented by b bits can be writ-

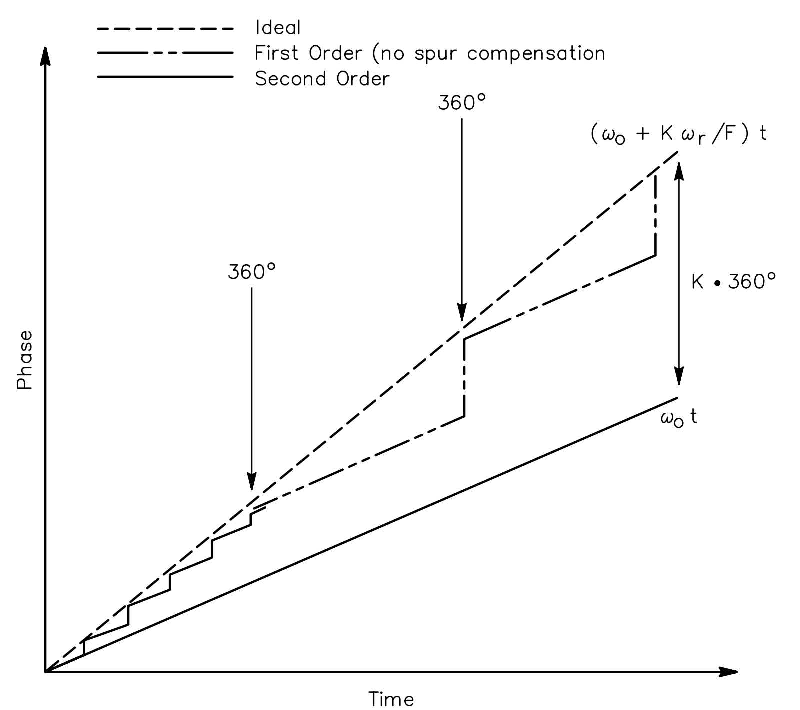

Fig 9—A large phase excursion in a fractional PLL.

ten as $2^{b-1}\sin(\omega t)$. This signal has power:

$$\left(\frac{2^{b-1}}{\sqrt{2}}\right)^2=\frac{2^b}{8} \qquad \text{(Eq 16)}$$

When the signal is quantized, we introduce a quantization error that is evenly distributed in the range –0.5 to +0.5 bits. The error power is given by:

$$E_\chi=\int_{-0.5}^{+0.5}\chi^2 d\chi \frac{1}{12} \qquad \text{(Eq 17)}$$

Therefore, the signal-to-quantization error ratio is given by:

$$\frac{2^b}{8E_\chi}=3(2^{b-1}) \qquad \text{(Eq 18)}$$

or $6b$+1.76 dB: This is a fundamental ratio in DSP. This indicates that for every extra bit we add to the quantizer, we improve the SNR by 6 dB.

Another way to improve SNR is to sample the signal faster. This way, we preserve the signal energy but spread the quantization noise spectrum over a wider bandwidth. So if the signal bandwidth is b_s and sampling rate f_s, the noise energy will spread over the entire sampling bandwidth, $f_s/2$. When we reconstruct the signal back, with a filter of bandwidth b_s, we gain SNR by the ratio f_s/b_s. Doubling sampling frequency improves SNR by 3 dB.

Now let's review some numbers. If we use a 10-bit quantizer, our SNR will be approximately 60 dB. If we use a one-bit quantizer and multiply the sampling frequency by two 10 times (each time by 2, so overall ratio f_s/b_s=1024), quantization SNR improves only by 30 dB. Thus, replacing bits by speed carries a significant deficit.

One of the common one-bit quantizers is the *delta modulator*, shown in Fig 10A. Analog signal X is connected to the input of the negative-feedback circuit (RC integrator in the feedback) and the error is quantized to a single bit, Y (see the waveform in Fig 11). E_q is the total quantization error. Clearly, as the clock frequency increases, quantization error decreases, but we saw that the improvement is only 3 dB per doubling of f_s. An improvement is found in delta-sigma modulation, which places the integrator before the quantizer. (See Fig 10B.)

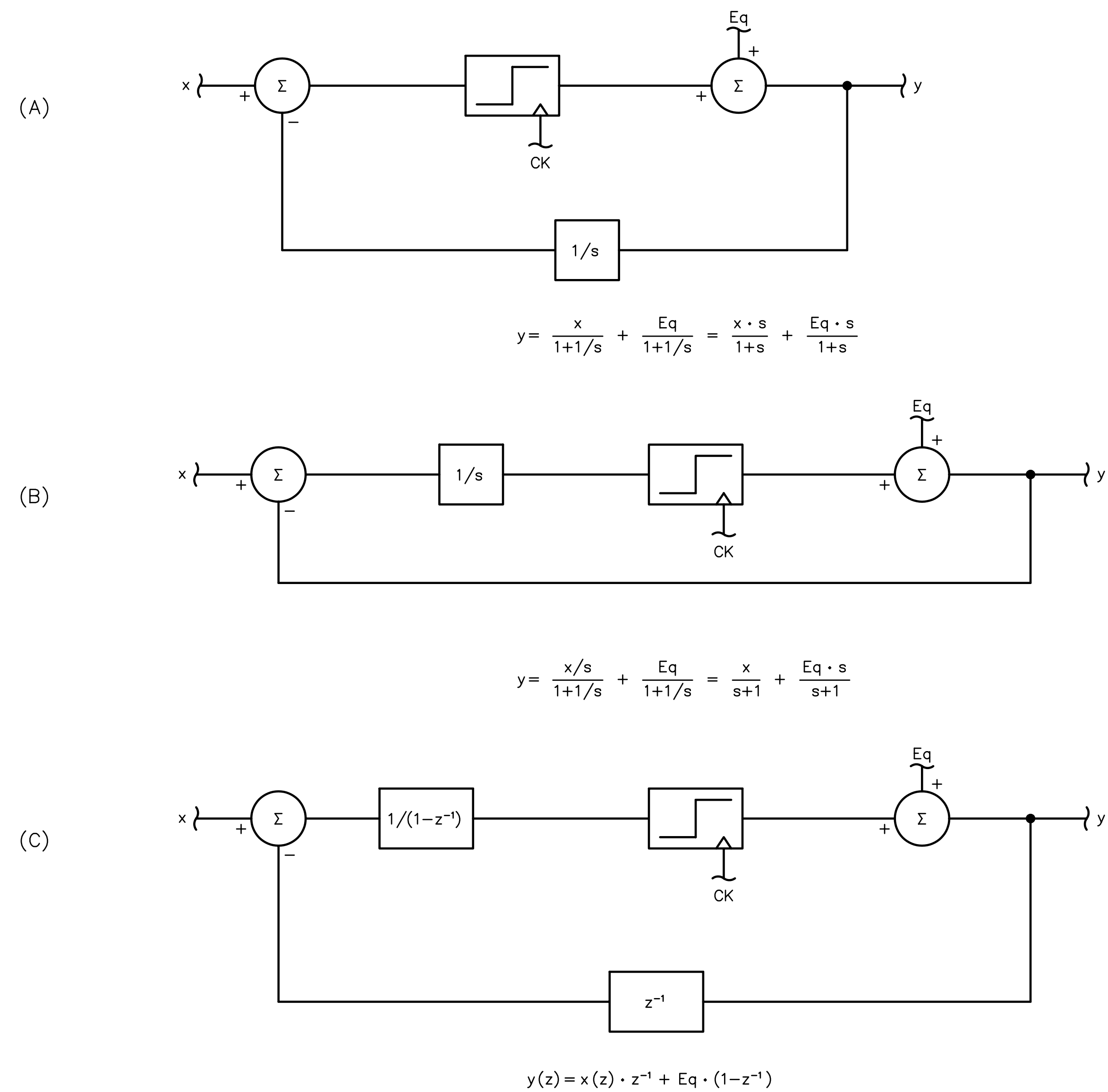

Fig 10—Single-bit quantizers: (A) a delta modulator, (B) a delta-sigma modulator, (C) a third-order delta-sigma modulator.

The transfer function of Y now becomes more interesting. It is given by: $Y \approx (X + E_q s)/(1+s)$. This means that while the signal input X is coming out unchanged as we wish, the quantization error is multiplied by a high-pass function; that is, the noise spectrum is attenuated at low frequencies and "pushed" to higher frequencies. Since the reconstruction of X will be followed by a low-pass filter ($f_s >> BW$), the majority of quantization noise energy will be attenuated. Most CD players use single-bit DACs and similar noise-shaping principles. For economy, your ear is the filter. Usually in such circuits, audio bandwidth is 15 kHz and clock frequency is 15-20 MHz so the ratio f_s/b_s is indeed 1000:1. Now in PLLs, we have a similar situation. If the ratio of the reference frequency (especially in fractional circuits) to the loop bandwidth is 100:1 or more, we can use similar principles, creating the slope K/L, and attenuating noise significantly. In fact, third-order fractional-n circuits use third-order delta-sigma modulation circuits, achieving a transfer function that is approximately $Y \approx X + s^3 E_q$. (See Fig 10C.)

Third-Order, All-Digital Fractional-n

These circuits use third-order delta-sigma modulators that control the dual-modulus device in the PLL's feedback path such that it can take on values N, $N\pm1$, $N\pm2$, $N\pm3$ and so forth. The modulating sequence is very fast compared with the slope K/L and generates the desired phase slope on average, but with a noise spectrum that has almost no energy inside the loop bandwidth. This system has been pioneered in England by Marconi (for which the company received the Queen's award) and later re-arranged by Hewlett Packard (see the referent of Note 3). Fig 12 illustrates a simulation of the quantizer-noise-shaped spectrum.

The delta-sigma modulator generates pseudo-random numbers whose average is the desired slope K/L, but with a shaped noise spectrum having minimal energy close to the carrier. Because these sequences must be long to be pseudo random, L must be a large number. Since the delta-sigma modulator is approximated by the carry out of a binary accumulator, the size of the accumulator is usually 2^{18} to 2^{32}. Therefore, it is immediately evident that the resolution of such designs is excellent and can actually be selected arbitrarily. Here we have an all-digital design with excellent phase noise (low N), and arbitrary resolution. (Fig 13 is a block diagram of an all-digital fractional divider.) In the case where f_{ref} = 10 MHz and accumulator size is 2^{24}; step size is approximately 0.6 Hz! So at the cost of increased digital complexity (while economical and consuming little power), performance is improved greatly. When these devices start to show in the market, they will create a revolutionary step in signal generation. Availability is expected this year.

Fractional Difficulties

Not all is roses in the fractional universe! While theoretically we gain 20 log(L) in phase noise, phase/frequency-detector characteristics depend on f_{ref} speed and lose performance at the rate of 10 log(f_{ref}). This means that while we increase the reference rate by L (the fractionality) to gain 20 log(L), we give back 10 log(L) for a total advantage of 10 log(L). This is still very good: For L=8, the gain is 9 dB and for L=16, 12 dB. In practice, fractional-n parts have failed so far to keep this promise. It is most possible that the addition of the analog compensating circuit at the most sensitive point in the circuit causes additional noise. Improvements have been done, but there is a lot of work in front of us. Third-order fractional FS is still just a dream. Very few companies own the technology and most don't share it.[4] That is to say: They either use it in their equipment as a competitive advantage or sell only the complete

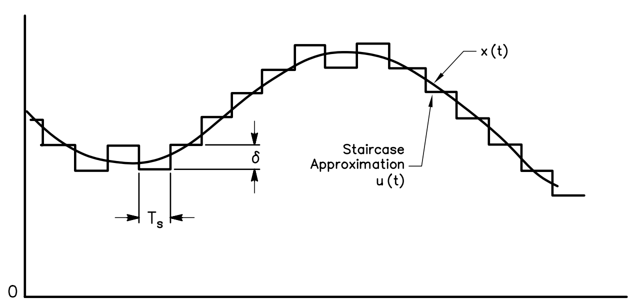

Fig 11—A delta modulator output response to sine-wave input.

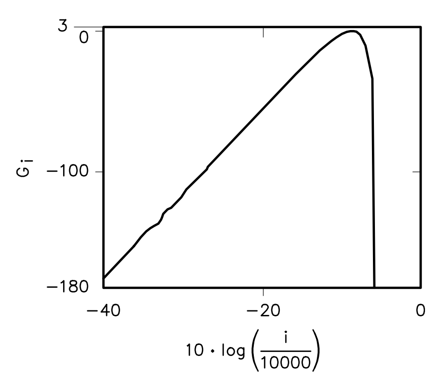

Fig 12—Simulated noise profile of a third-order delta-sigma modulator.

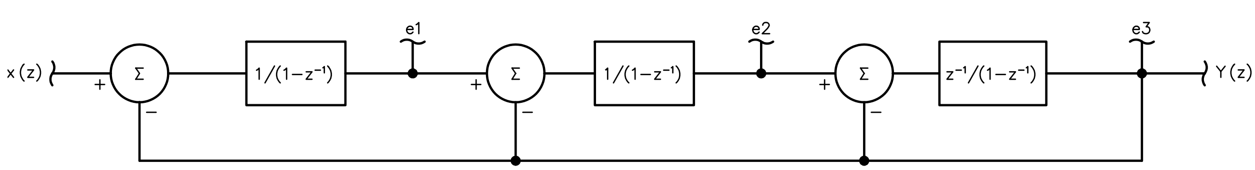

Fig 13—Structure of an all-digital fractional divider.

synthesizer. In a while—the best estimate is 8 to 12 months—such parts will be available in the market, and they will be competitive.

Hybrid FS Techniques

For more demanding specifications, it is sometimes required to increase the complexity of the synthesizer to achieve better performance. One pair in the set of conflicting goals is that of resolution and phase noise. In PLLs, increased resolution usually implies a lower reference, which increases N and thus also 20 log(N). If this is not tolerable, more complex designs need be employed.

Example #1: mix-and-count-down. Suppose we have to generate a 4 to 4.1 GHz signal with 0.1 MHz steps. If we wish to use a single loop, then we'll need to divide the VCO first by two, then connect the divider output to a synthesizer chip that has a programmable divider (there are no variable dividers at 4 GHz yet). As a consequence, the reference in the PLL circuit must be at least 50 kHz and total division is 4000/.05 = 80,000. Noise corruption will be on the order of 20 log(80,000) = 98 dB. An approach to lower division, and thus improved phase noise, is shown in Fig 14, a mix-and-count-down scheme.

The creation of a new LO, at a fixed frequency, can use a much higher reference in its PLL circuit, but now division ratio can be reduced by a ratio of 50:1. Now the synthesizer processes 200-300 MHz with 100 kHz steps, thus using division ratios of 2000-3000.

PLL+DDS

Another technique that has been mentioned is to use the PLL as a multiplier and "cleaning mechanism" for a DDS. Here, rather than a fixed crystal reference, the PLL is driven by a DDS that serves as the reference for the loop. (See Fig 15.) Since DDS has very fine steps, a PLL circuit will have good resolution even after multiplication and will act as a cleaner for DDS spurious responses that are outside of the loop bandwidth. This method is not recommended, as DDS spurious are usually strong and, if multiplied by a high number, will be very significant within the loop bandwidth at some points. There might be special applications where this can be used, but complete characterization of the DDS over very narrow bands should be considered.

Phase-Noise Measurements

Phase noise is a complicated and tedious measurement because of the wide dynamic range required. Three main methods are used to measure phase noise:

1. Measure phase noise $L(f_m)$ directly on a spectrum analyzer. All synthesized spectrum analyzers have an automatic function that measures and calculates $L(f_m)$. This can be done as long as the analyzer has better phase noise than the measured source.
2. Lock a better source to the same frequency, then mix them and measure the phase-noise profile using an FFT analyzer. In this case, the unit under test and the reference are mixed first, with a frequency difference of, say 1 kHz, and the power of the signal is measured. This enables calibration of the system and measurement of signal total power. Then the two signals are brought to the same frequency and a 90° offset (where the measurement sensitivity is highest). The main energy in the carriers cancel thus enabling increased dynamic range, and the spectrum of the noise can be measured after amplification on a spectrum analyzer or FFT. Such systems are available from HP, Comstron/Aeroflex and others. This is the most sophisticated system to measure phase noise, with the best sensitivity and noise floor in the –175 dBc/Hz range; however, measurement is lengthy and the equipment very expensive. The reference source used for the measurement must be of supreme quality (very expensive).

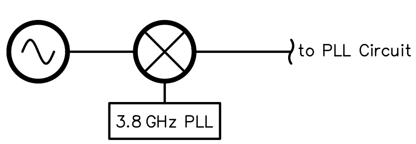

Fig 14—Mix-and-count-down synthesizer scheme.

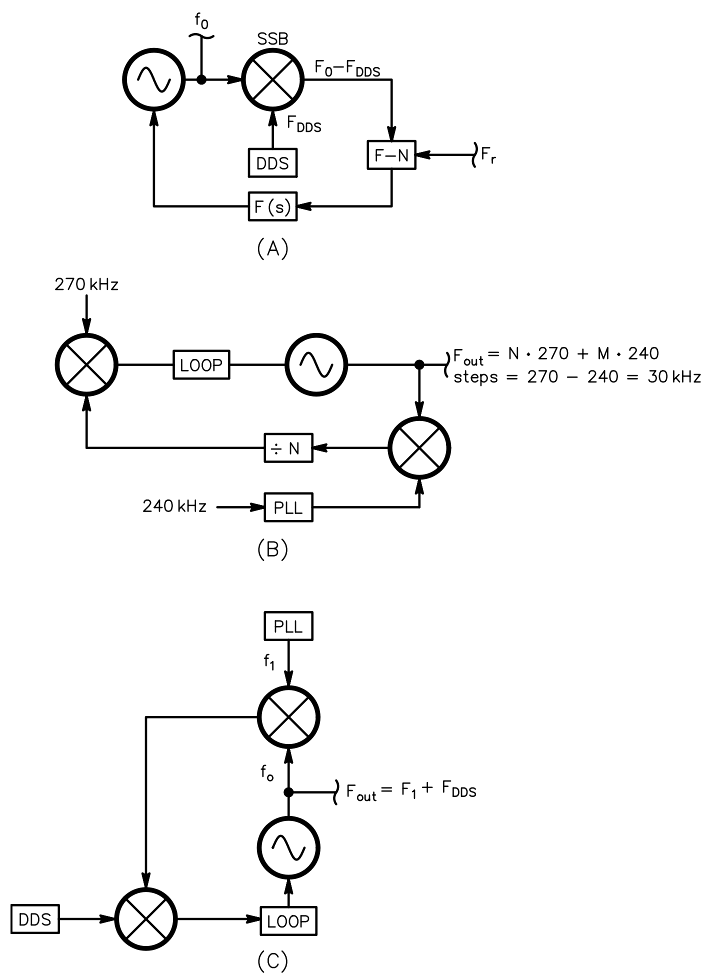

Fig 15—Block diagrams of alternative PLL schemes: (A) A PLL multiplies and "cleans" a DDS signal, (B) a typical two-loop synthesizer, (C) a typical DDS+PLL synthesizer.

3. Use the discriminator method and compare the signal to a delayed version of itself (quadrature detector). In this scheme, the signal is split and one leg delayed. (See Fig 16.) First, one leg is offset by, say 1 kHz, and a calibration measurement is taken. Then the two legs are brought back to same frequency at a 90° phase offset and the noise is measured and calculated. It can be shown that in such measurements, phase noise is given by:

$$L(f_m) = L'(f_m) \bullet \frac{K}{f_m \tau} \qquad \text{(Eq 19)}$$

$L'(f_m)$ is the direct measurement of the discriminator output, K a calibration constant, and τ the delay.

Clearly, this measurement is limited for close-in offsets (when we mix a signal with itself delayed, we cancel a lot of the close-in noise), with practical limitations of –50 dB and –80 dB at 10- and 100-Hz offsets, respectively. Usually it does not measure above 1 MHz offsets from the carrier (in most cases the delay line τ is in the 0.5-ms range).

Delay is implemented using coaxial cables, which have significant attenuation above 1 GHz, so a direct measurement (with no conversion) is practical to 1 GHz. The advantages of such measurement are its speed, relatively low cost, and the easy ability to check free-running VCO phase noise without the need to lock. We believe such measurement systems that do not require an excellent synthesizer for reference can be developed to be very practical and economical. Its performance is not the best, but is sufficient for measurement of most cellular, wireless and satcom VCOs and synthesizers.

Future Evolution

FS is clearly a very mature technology. DDS and PLL chips are economical in voltage, power and cost. Where are we headed?

Toward integration: So far, PLL and FS parts are separated from the rest of the RF portions of radios. PLLs have many digital parts that corrupt RF sensitivity by radiation, if too close. This will be soon overcome. Silicon Labs, an innovator in chip design, has recently introduced to the market a PLL chip that integrates all functions. Loop filter and even the VCO are included in the device (requires an external inductor). Performance is excellent. The next step is the inclusion of the inductor and maybe even the crystal reference in the package.

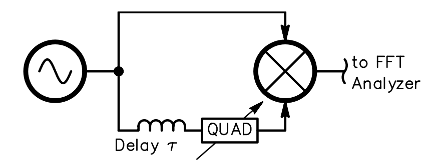

Fig 16—A delay-line discriminator for phase-noise measurements.

"Fractionality" still requires a lot of work before it matures. Third-order fractional techniques may revolutionize the field altogether. The focus of development should be on integration, spectral purity and improving agility and switching speed. Frequency-hopping spread spectrum (FHSS) is a critical technology that still faces limitations due to FS speed issues.

Conclusion and Challenges

Phase noise is a fundamental and critical parameter of signals, especially in radio-network applications. Lately, synthesizer designers also see market interest in fast switching speeds as wireless networks mature. VCO technology continues to evolve with better resonator materials, noise-cancellation techniques, smaller size and lower power requirements. Close-in phase noise affects signal performance while high-offset phase noise and noise-floor effects impact network performance and adjacent-channel interference. Economical solutions for low-noise VCOs are a continuously standing challenge. Even more critical is the need for economical instrumentation for fast phase-noise and noise-floor measurements.

Obviously, phase-noise numbers in the –165 dBc/Hz range are difficult to measure as they are close to kTB levels. However, these measurements are necessary very commonly, and their improvement is quite critical to the evolution of wireless telecommunications. I believe that necessity will drive the evolution of new generations of VCO and resonator technology as well as economical phase-noise measurement systems and testers. BiCMOS PLL parts continue to evolve in frequency coverage (now close to 4 GHz) while still maintaining low cost, power and size. DDS technology evolves in parallel, with CMOS parts already running at 300 MHz, and 500 MHz speeds forecasted in the next two years. Development in silicon and SiGe will continue to improve device speed, power and economy.

The greatest excitement awaiting the field is the introduction of third-order fractional, all-digital PLL technology, which will certainly revolutionize signal-generation speed, resolution and economy.

*Bar-Giora Goldberg is President of VITCOM Corporation, a company dedicated to signal generation, measurement and training. He authored six US patents, published a book, Digital Frequency Synthesis Demystified, (now in its third edition with LLH Publishing) and numerous articles. VITCOM's specialty is PLL and DDS products. Giora also cooperates with GMS, a radio company based in Oceanside, California, involved in audio-visual development (**www.gmsinc.com**) and with Besser Associates, giving seminars in the US and abroad.*

Notes

[1]B. Goldberg, *Digital Frequency Synthesis Demystified*, LLH Technology Publishing, 3578 Old Rail Rd, Eagle Rock, VA 24085; **http://www.llh-publishing.com/catalog/books/dfsd.html**.

[2]B. Miller and B. Conley, "A Multiple Fractional Divider," *Proceedings of the Annual Symposium on Frequency Control* (44th, 1990). The Proceedings are order number AD-A272 017/5INZ available from the National Technical Information Service (NTIS) 5285 Port Royal Rd, Sills Bldg, Springfield, VA 22161; tel 703-487-4650, fax 703-321-8547; e-mail **info@NTIS.fedworld.gov**, URL **http://www.fedworld.gov/ntis/search.htm**.

[3]B. Razavi, *Monolithic PLL and CDR*, (New York: IEEE Press, 1996).

[4]U. L. Rohde, "A High-Performance Fractional-N Synthesizer," *QEX*, Jul/Aug 1998, pp 3-12.

Narrow Band-Pass Filters for HF

Band-pass filters can be critical components in competitive stations. This setup may help put your station on the map.

By William E. Sabin, W0IYH

There are nine relatively narrow HF Amateur Radio frequency bands. In homebrew equipment designed for these bands, a narrow band-pass filter (NBPF) that attenuates frequencies above and below a particular band can be very useful. Harmonic, sub-harmonic, image, intermodulation, overload and mixer spurious products (harmonic intermodulation) are problems that these filters can greatly alleviate in receivers and transmitters. This article describes simple filters at medium cost and performance levels that are suitable for many of the kinds of homebrew projects Amateurs build. They can be cascaded in filter-amplifier-filter arrangements for highly advanced performance.

Construction details, including simulated frequency responses of the filters, can be downloaded from the *QEX/Communications Quarterly* Web page.[1] The plots can be studied to see if they are adequate for the task at hand. A 32 MHz low-pass filter is included that provides additional attenuation beyond the HF region. My actual filters agree quite closely with simulations down to the –60 dB level, except for small differences in the passbands.

[1]Notes appear on page 17.

1400 Harold Rapids Dr SE
Cedar Rapids, IA 52403
sabinw@mwci.net

The filters use two resonators. In the interest of simplicity, low parts count, low dc power consumption (0.9 W for any number of filters, one at a time) and low internally generated intermodulation distortion (IMD), a pair of inexpensive, miniature RadioShack SPDT relays (275-241) is used in each filter. A PIN-diode switching approach for lower-level applications will be discussed later. Fig 1 shows simulated, idealized responses of three types of two-resonator filters. One has greater selectivity on the "high" side and one is better on the "low" side. These types are quite useful in various applications. The symmetrical response is not as easy to implement in practice in a NBPF, but very easy on a computer. Because the frequency scale is logarithmic, the shape of these plots is constant as they "slide" horizontally.

The filters will deliver 10 W continuous output with negligible warming. On each band, and at S = +37 dBm (5 W) input for each of two in-band tones, a third-order input intercept point (I_3 in dBm) was determined. A 40 dB each-tone-to-intermod ratio (IMR_3) computes to an I_3 of about +57 dBm, using Eq 1. A value of IMR_3 for other values of input per tone can be estimated also from Eq 1. Do not "hot-switch" the relays. I also suggest using type-2 (μ=10) or type-6 (μ=8) powdered-iron cores.

$$I_3(\text{dBm}) = S(\text{dBm}) + 0.5 \bullet IMR_3(\text{dB})$$
$$IMR_3(\text{dB}) = 2.0 \bullet \left[I_3(\text{dBm}) - S(\text{dBm})\right] \qquad \text{(Eq 1)}$$

NBPF Circuits

Fig 2A is a typical high-side filter. The shunt C_S couples the two resonators. Since its reactance decreases as frequency increases, the resonators become more isolated from each other at higher frequencies. Fig 2B uses a top-coupling capacitor C_T and the low side is improved because the reactance of C_T increases at low frequencies. Capacitive dividers C1 and C2 provide a desirable broadband interface with adjacent circuits.

The filters are designed to operate between two 50-Ω resistances, but we begin the design with *R* much greater than 50 Ω. The filters are based on the Butterworth approach. There are certain approximations involved in the design of narrow-band coupled resonators[2,3,4] that are related to the ways that coupling reactances and impedance-transforming networks vary with frequency. The method used here gets very close to the final filter using simple design equations and a program like *Mathcad,* then tweaks the design with *ARRL Radio Designer*. A simple test setup is used to make final adjustments to the hardware.

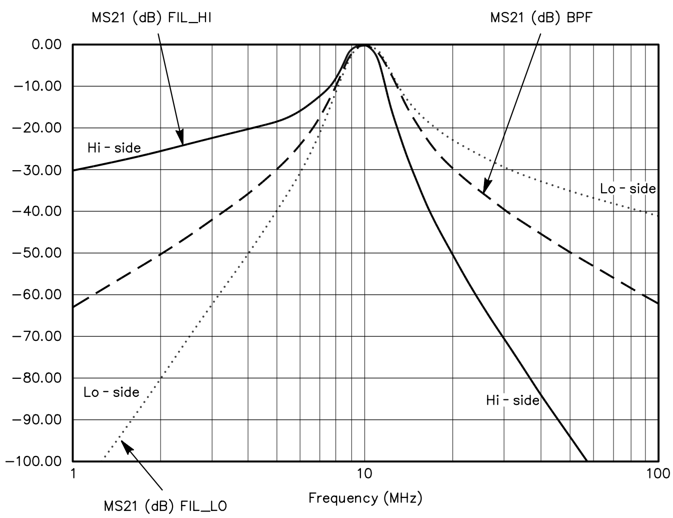

Fig 1—*ARRL Radio Designer* predicted response of symmetrical, low-side and high-side band-pass filters.

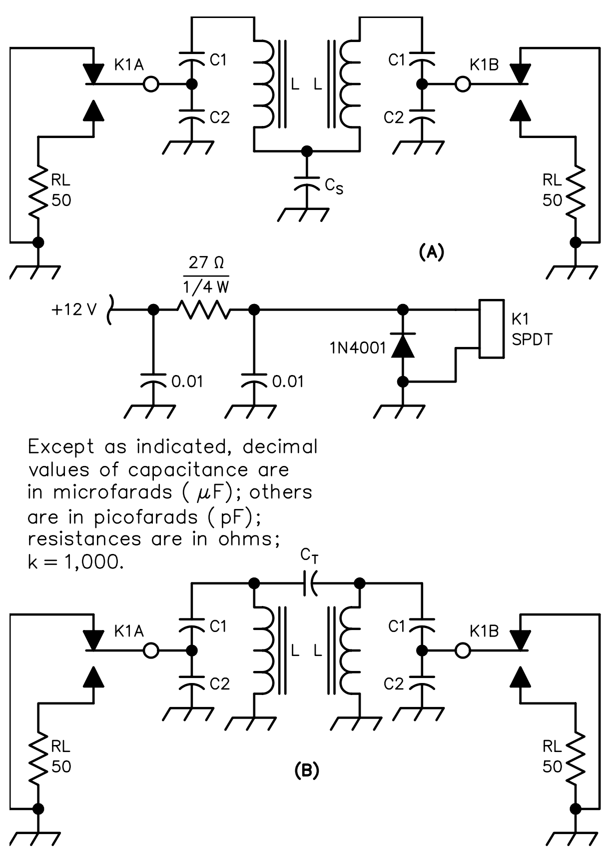

Fig 2—Two-resonator NBPF circuits. (A) is a bottom-coupled "high side" filter; (B) is a top-coupled "low-side" filter.

Low-pass and NBPF Prototypes

Comparisons between Chebyshev and Butterworth filters

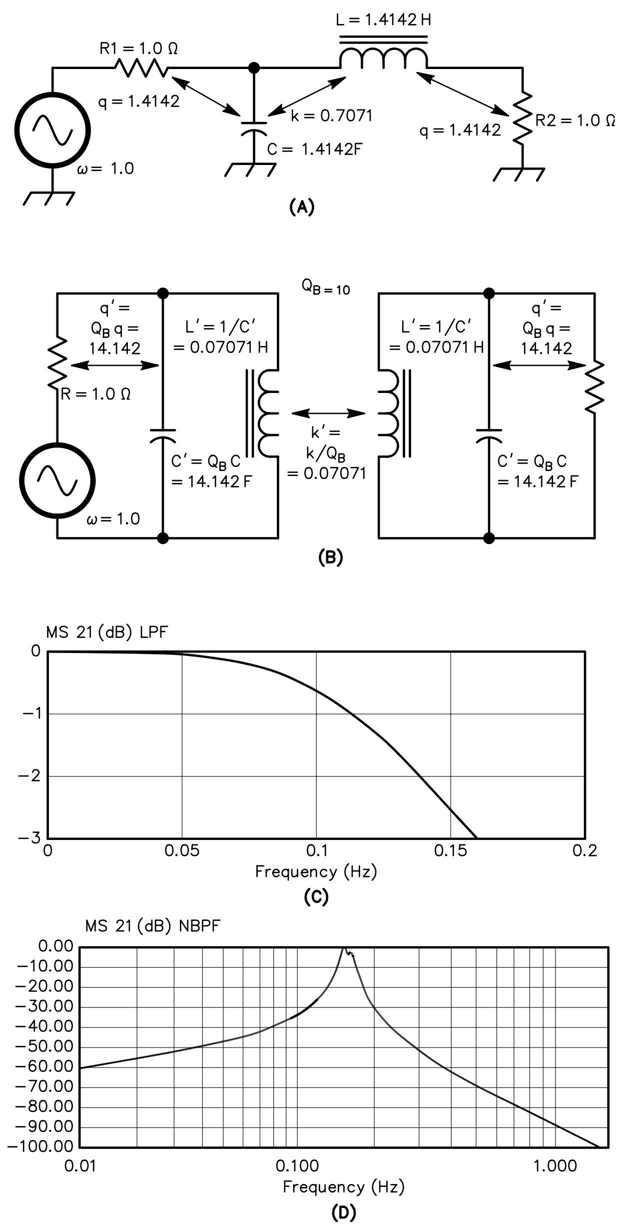

Fig 3—Prototype filters: (A) low-pass filter; (B) narrow band-pass filter; (C) a low-pass response; (D) a narrow band-pass response.

led me to the Butterworth as a better choice for the NBPF. We use two numbers to get started: q and k. For the Butterworth, q = 1.4142 and k = 0.7071. The significance of these numbers is seen in Fig 3A, the two-element Butterworth prototype LPF from which the NBPF is derived. Variable q is the "Q" of C in parallel with R1 at ω = 1.0:

$$q = R\frac{1}{X_C} = R\bullet\omega\bullet C = (1.0)(1.0)\bullet C = 1.4142;\ C = 1.4142\ F \qquad \text{(Eq 2)}$$

k is the "coefficient of coupling" (explained later) from C to L; L is given by:

$$L = \frac{1}{\omega^2 k^2 C} = \frac{1}{(1.0)^2(0.7071)^2(1.4142)} = 1.4142\ H \qquad \text{(Eq 3)}$$

$R2$ is found by noting that q is also the Q of L in series with $R2$ at ω =1.0:

$$R2 = \frac{\omega L}{q} = \frac{(1.0)(1.4142)}{1.4142} = 1.0\ \Omega \qquad \text{(Eq 4)}$$

The response of Fig 3A is down 3 dB at ω =1.0 rad/s (0.1592 Hz) as shown in Fig 3C.

The numbers q and k also apply to the NBPF. If the coefficient of coupling (k in Fig 3A) could be achieved without a direct connection between C and L, we could remove this connection. First, we must do the following: Multiply q by a large number, which we call Q_B, for example 10, and divide k by Q_B. To keep the discussion brief, Fig 3B shows the method and the component values. The response (Fig 3D) of Fig 3B is centered at ω = 1.0 rad/s (0.1592 Hz). Close to this frequency, above and below, the response is very nearly the Butterworth. Far away from the center frequency the similarity changes; that is, the NBPF is a *narrow-band approximation* to Butterworth *near* ω = 1.0. At low frequencies, the response is –20 dB per decade and at high frequencies the response is –40 dB per decade. The 3-dB bandwidth of Fig 3D is nearly:

$$\frac{1}{Q_B} = 0.1 \text{ rads/sec } (0.0159 \text{ Hz}) \qquad \text{(Eq 5)}$$

The next task is to scale this NBPF prototype to its final HF values. For small HF filters that use low-cost inductors and capacitors, values of Q_B from 4 to 30 are practical.

Designing the Two-Resonator NBPF

Refer now to Fig 4. We need the value of Q_B for the final filter

$$Q_B = \frac{F_0}{BW_{3dB}} = \frac{\sqrt{F_{HI}\bullet F_{LO}}}{F_{HI} - F_{LO}} \qquad \text{(Eq 6)}$$

where F_{LO} and F_{HI} are the 3-dB edges of the filter's passband. F_{LO} and F_{HI} are positioned so that the frequency response over the amateur band varies no more than a few tenths of a decibel. They should also be selected initially so that the filter is centered near the geometric center of the amateur-band limits. For example, F_0 (in MHz) for the 80-meter band is $\sqrt{3.5\bullet 4.0} \approx 3.74$. We will need to fine-tune these numbers later. We now need Q_N, the Q of each resonator when loaded by R, and K, the coefficient of coupling between the resonators.

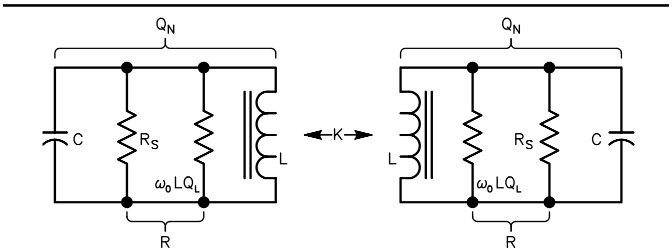

Fig 4—Coupled, loaded resonators.

$$Q_N = q\bullet Q_B;\ K = \frac{k}{Q_B} \qquad \text{(Eq 7)}$$

In Fig 4, there are three values to be determined: C, L and R, which are related as shown in Eq 8:

$$C = \frac{1}{\omega_0^2\bullet L} = \frac{Q_N}{\omega_0\bullet R};\ \omega_0 = 2\pi\sqrt{F_{HI}\bullet F_{LO}} \qquad \text{(Eq 8)}$$

For a selected value of Q_N, it is clear from this equation that after C is chosen, L and R are both determined. The goal is to make all three "reasonable" values that are inexpensive and appropriate for the particular frequency band. For example, we would not choose C = 1000 pF for the 10-meter band because that would make L unreasonably small and difficult. We would not choose C = 10 pF for the 160-meter band. Experience and "feel" are valuable tools for this. Having made an educated choice for C, L can then be achieved by winding the right number of turns on the right toroid core. R is then constrained to the value found in Eq 8 and should be between 500 Ω and 2500 Ω.

In Fig 4, the next step is to couple the two resonators so that the desired bandwidth and passband response are achieved. For the top-coupled filter (as in Fig 2B), C_T is used and C is reduced to the value C':

$$C_T = \frac{C\bullet k}{Q_B} = C\bullet K;\ C' = C\bullet(1-K) \qquad \text{(Eq 9)}$$

For the shunt-coupled filter (as in Fig 2A), C_S is used and L is increased to L':

$$C_S = \frac{1}{K\bullet\omega_0^2\bullet L};\ L' = L\bullet(1+K) \qquad \text{(Eq 10)}$$

Refer to Fig 5. In Eq 8 we found that, having chosen a reasonable C, R is determined. So the final step is to use capacitive dividers to transform R to R_L = 50 Ω; but first, R must be broken up into two parts. One is the resistance of the coil and the other is R_S, the external loading resistance as shown in Fig 5.

$$R_S = \frac{1}{\left(\frac{1}{R} - \frac{1}{\omega_0\bullet L\bullet Q_L}\right)};\ \omega_0\bullet L\bullet Q_L >> R \qquad \text{(Eq 11)}$$

where Q_L is assumed to be known by measurement at ω_0. Note that the coil resistance must be much greater than R, which implies that L and Q_L cannot be too small. R_S is then to be transformed to R_L. For the capacitor dividers, I use exact equations rather than the approximate ones that are found in many references. The values of C2 and C1 (C_F is defined below) are given by:

$$C2 = \frac{\sqrt{\frac{R_L}{R_S}\bullet\left[1+(\omega_0\bullet C_F\bullet R_S)^2\right]-1}}{\omega_0\bullet R_L};\ C1 = \frac{1+(\omega_0\bullet C2\bullet R_L)^2}{\omega_0^2\bullet R_L\bullet(C_F\bullet R_S - C2\bullet R_L)} \qquad \text{(Eq 12)}$$

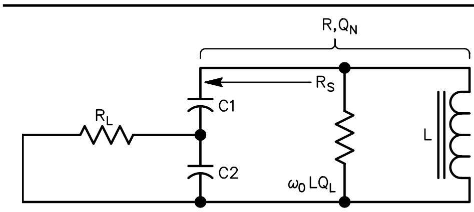

Fig 5—A capacitor-divider impedance transformer.

If different values of R_L at either end of the filter are desired, Eq 12 can be used to find new values for C1 and C2, with no changes elsewhere. Two conditions must be satisfied in Eq 12:

$$\frac{R_L}{R_S} \bullet \left[1+(\omega_0 \bullet C_F \bullet R_S)^2\right] > 1 \text{ and } \frac{R_S}{R_L} > 1 \quad \text{(Eq 13)}$$

In Eqs 12 and 13, C' from Eq 9 is the correct value of C_F to use if top coupling is used. C from Eq 8 is the correct value if C_S is used. C_S replaces a coupling inductor L_M as shown in Note 3, Fig 6.15. This substitution causes very little error within the narrow passband but greatly increases high-side attenuation, as Fig 1 shows.

Final Design

The filter design is now almost complete and looks like Fig 2A or 2B, and the losses due to the coils (measured Q_L from 160 to 220) have been adequately accounted for. The coil losses affect the attenuation in the passband, which is to be 2 dB or less. I adjusted Q_B (Eq 6) and C (Eq 8) and used *ARRL Radio Designer* and my lab equipment to get the desired passband response and to get standard C values, if possible. I then slightly adjusted L to get reasonably close to the desired response. There is also a small mismatch loss because the input and output impedances are not exactly 50 Ω. *Mathcad* quickly recalculates the component value improvements using the equations in this article. I run *Mathcad* and *Radio Designer* simultaneously and click back and forth. One problem to avoid is making the passband too narrow, in which case the passband attenuation increases more than we might want. In general, it is much better to let the powerful software that is available take care of the design tweaking than to get involved in a purely experimental approach. The *Mathcad* (a spreadsheet program is also good) and *Radio Designer* worksheets that I used are included in the data package (see Note 1) and are very convenient for those who want to design or modify filters. For more in-depth material on the NBPF, look at the references in Notes 2, 3 and 4.

Core Flux

For a power input of P_{IN} watts, the capacitive divider increases the input voltage V_{IN} to V_{TOP} at the top of the coils according to Fig 6:

$$V_{TOP} = \sqrt{P_{IN} \bullet R} \quad \text{(Eq 14)}$$

and the capacitors are appropriately rated. The question occurs whether the powdered-iron-core inductors will have too much flux at the higher impedance. The answer is no; for a *specific* core, the flux is nearly constant. Suppose one circuit has resistance value R_A and another has R_B. The voltage ratio is:

$$\frac{V_B}{V_A} = \sqrt{\frac{R_B}{R_A}} \quad \text{(Eq 15)}$$

and the inductance ratio is:

$$\frac{L_B}{L_A} = \frac{R_B}{R_A} = \left(\frac{N_B}{N_A}\right)^2 \quad \text{(Eq 16)}$$

The flux, ϕ, in a particular core is equal to a constant, K_ϕ, times the volts per turn, V/N, of the winding. Combining Eqs 15 and 16 into this relationship, we get the resulting flux ratio:

$$\frac{\phi_B}{\phi_A} = \frac{V_B}{V_A} \bullet \frac{N_A}{N_B} = \sqrt{\frac{R_B}{R_A}} \bullet \sqrt{\frac{R_A}{R_B}} = 1 \quad \text{(Eq 17)}$$

which is approximately correct for the filters described in this article. This question often occurs because of the influence of core flux levels on nonlinearities.

Construction

Fig 7A is a close-up of two of the high-side (shunt-coupled) filters and Fig 7B shows two of the low-side (top-coupled) filters. Each filter is 1×4 inches, and a standard 4×6-inch PC board provides five individual filter boards. These individual boards are available in any quantity from FAR Circuits.[5] Fig 8 shows the construction of my filter assembly on a 5×7×2-inch chassis. The band switch, the low-pass filter and the method of mounting the filters, five to each side, are shown. The idea was to minimize the chassis footprint of the filter assembly by using the vertical style of construction.

The filters should be connected by short lengths of miniature 50-Ω coax. This method is somewhat tedious to implement, but helps to preserve the 50-Ω interface and

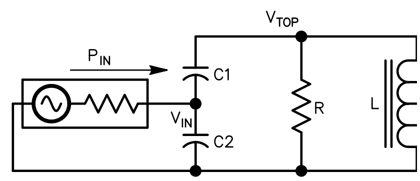

Fig 6—Voltage and flux transformation in a capacitive divider.

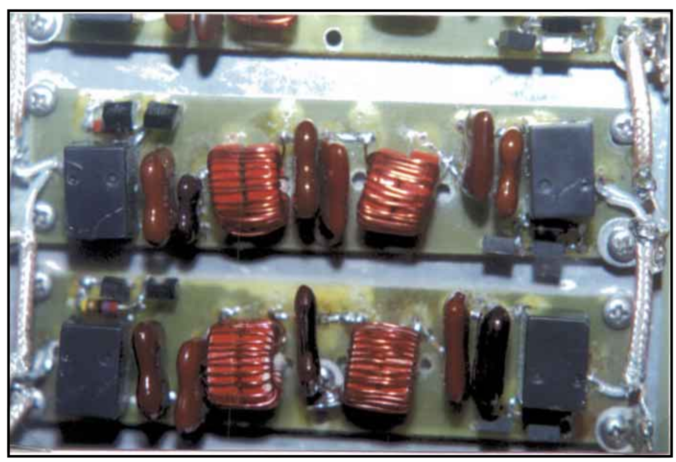

(A)

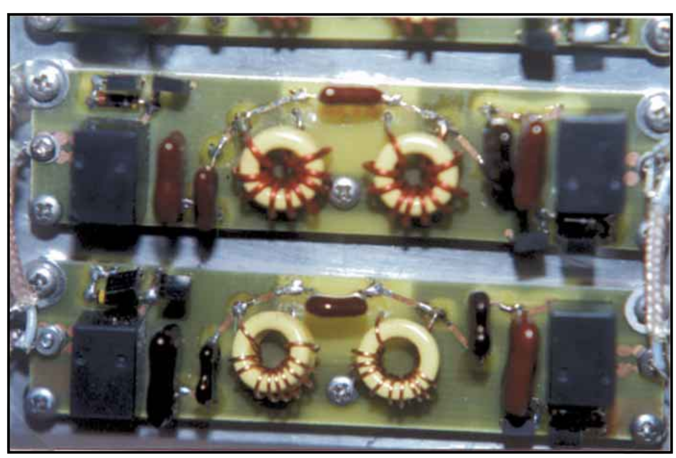

(B)

Fig 7—(A) Shunt-coupled NBPFs. (B) Top-coupled NBPFs.

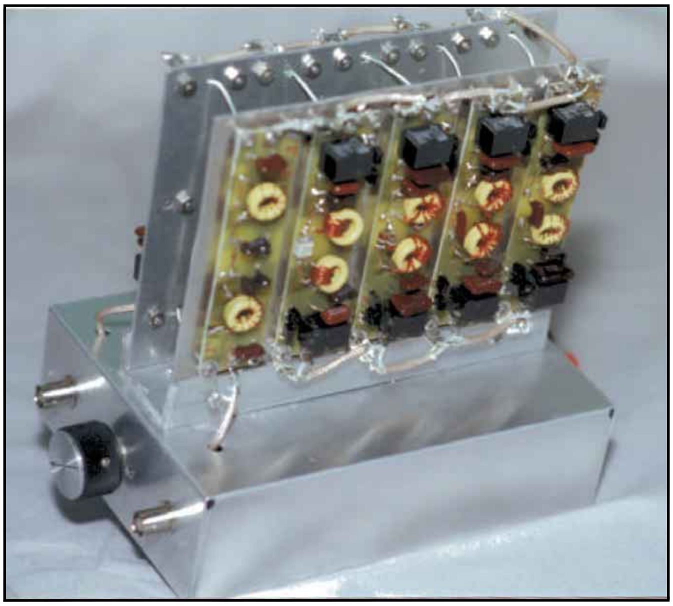

Fig 8—A complete NBPF assembly. The 32-MHz LPF is at the left.

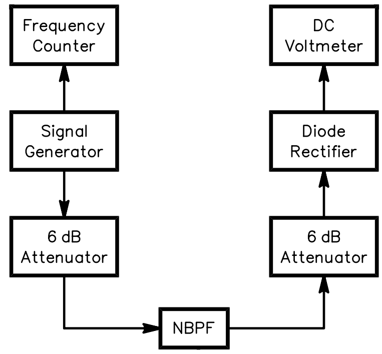

Fig 9—Block diagram of a test setup to adjust the NBPF passband.

effectively reduces stopband leakage. The **IN** connector coax goes to the 160-meter input first, then to the other inputs. The filter outputs all go to the LPF input and the LPF output goes to the **OUT** connector (of course, **IN** and **OUT** may be reversed). Notice the single-point grounding of the coax braids at the input and output of each filter (verified effective). The relay-coil switching can be done electronically, under software control, in an actual application. The low-pass-filter board is an NBPF board, slightly modified (see Fig 8); a separate board design is not necessary.

Fig 9 is a simple test setup that can be used to finalize the passband response and is highly recommended if the use of a spectrum analyzer and tracking generator is not feasible. The capacitors should ideally be within 2% of the values that are suggested in the datasheets. A digital or analog capacitance meter that has an accuracy of better than 1% is a valuable asset for filter construction. Because of the tolerances of capacitors, this selection process is a source of some difficulty that requires patience and an assortment of parts from which to choose. If necessary, use two capacitors in parallel: a "main" low-side value and a small "tweak" value. You can modify slightly the Cs values in Eqs 6, 7, 8, 9, 10, 11, 12 and 13 to values that match what you have on hand or can easily get. Use *Radio Designer* to fine-tune the inductance, using the capacitance values you have chosen.

Filter tests within the passband, using the setup of Fig 9, will require some minor adjustments of the inductors by spreading or compressing turns. I found this procedure to be less effective on the 160 and 80 filters than on those for the higher frequency bands. A turn more or less on the toroid cores may be indicated (start with an extra turn and remove it if necessary). Experimental adjustments of C_S (for shunt-coupled) or C_T (for top-coupled) can be made to fine-tune the shape of the passband, if necessary. The accumulation of small uncertainties ("fuzziness" is the operative word these days) in the actual filter module often makes this process desirable and quite permissible.

Here are some suggestions that will improve the broadband attenuation of the filter boards. For the high-side filter, Fig 7A, remove the printed-circuit traces that go the location where a top-coupling capacitor C_T would be located. Be sure to use C_S capacitors that have low self-inductance.

For the low-side filter (Fig 7B) remove the two strips that go to the shunt capacitor (C_S) location. Connect each coil ground lead directly to ground by running the coil wires through the pads and soldering them to the ground plane. Be sure to use the grounding screw from the center of the PC board to the metal mounting plate. I use #4-40 hex nuts and #4 flat washers as spacers in five locations. In addition, it is important to avoid stray coupling between the filters and adjacent metal surfaces and circuits that might degrade the stopband (verified).

For the simple style of construction shown in Figs 7 and 8, an ultimate attenuation of 70 dB from 1.8 through 30 MHz, is a reasonable expectation that is good enough for many applications. For more-stringent needs, a filter-amplifier-filter arrangement will provide enough ultimate attenuation for just about any application. I prefer this approach to more elaborate individual filters because the actual hardware's ultimate broadband attenuation is much better. The amplifier can be a low-gain (4-6 dB), unilateral, grounded-gate amplifier that has a 50-Ω dynamic (loss-less) input resistance, a physical 50-Ω output resistance and dynamic range suitable to the application. Calculate the cascaded noise figure and intercepts.

Another option is to sharpen the selectivity of the filter. This can be done by narrowing the passband (Eq 6) and calculating new component values (Eqs 7, 8, 9, 10, 11, 12 and 13). *Radio Designer* will show that the passband attenuation may in-crease by a decibel.

For low-level applications, such as medium-performance receivers, the filters can be switched with PIN diodes, although I much prefer the relays. The download file (see Note 1) shows an approach that I have used; it works quite well in the HF bands. The references in Notes 6 and 7 should be consulted for further information on this approach.

Notes

[1]You can download this package from the ARRL Web **http://www.arrl.org/files/qex/**. Look for NPBF.ZIP.

[2]H. J. Blinchikoff and A. I. Zverev, *Filtering in the Time an Frequency Domain* (Wiley and Sons, 1976) Chapter 4.

[3]A. I. Zverev, *Handbook of Filter Synthesis* (Wiley and Sons, 1967), pp 300-306.

[4]W. E. Sabin, W0IYH, "Designing Narrow Band-Pass Filters with a BASIC Program," *QST*, May 1983.

[5]FAR Circuits, 18N640 Field Ct, Dundee, IL 60118; tel 847-836-9148 (Voice mail), fax 847-836-9148 (same as voice mail); e-mail **farcir@ais.net**; URL **http://www.cl.ais.net/farcir/.**

[6]*The ARRL Handbook*, 1995-2000 editions, p 17.31. ARRL publications are available from your local ARRL dealer or directly from the ARRL. Check out the full ARRL publications line at **http://www.arrl.org/catalog**.

[7]W. E. Sabin, W0IYH, "Mechanical Filters in HF Receiver Design," *QEX*, Mar 1996.

New Super-Regenerative Circuits for Amateur VHF and UHF Experimentation

A super-regen party! Three circuits cover 38-54 MHz, 118-136 MHz and 88-180 MHz. Add a TV UHF downconverter for 450-910 MHz. Check out the new Squelch and NBFM designs!

By Charles Kitchin, N1TEV

Although many radio amateurs enjoy building their own shortwave receivers, very few attempt to construct radios for frequencies above 30 MHz. There are several reasons for this present lack of activity. The very few VHF and UHF circuits that are published today tend to be complex, superheterodyne designs. Even when PC boards are made available, these projects are often too difficult for the average ham to construct. Although a superheterodyne receiver is entirely sensible for a commercial design, the complexities of building even a simple superhet are formidable at VHF frequencies.

26 Crystal St
Billerica, MA 01821
charles.kitchin@analog.com

This lack of amateur experimentation in VHF has only occurred in recent times. In the 1930s and '40s, many hams built their own VHF equipment. In fact, radio amateurs were the pioneers responsible for the development of the first practical VHF and UHF communications gear. I believe that the number-one reason for the decline in VHF homebrewing is the abandonment of super-regenerative receivers in favor of the much more complex superheterodyne—and there were some very good reasons for this change.

Ever since their introduction in the early 1920s, *super-regens* (super-regenerative receivers) have had some serious problems. When vacuum tubes were used in these sets, their relatively high power levels resulted in serious interference to nearby receivers. In addition, the traditional super-regen circuit suffers from very poor selectivity; it also has a very loud and annoying background noise. Even the performance of commercial super-regen designs, such as those used in low-cost, hand-held transceivers, has traditionally been very poor. Nonetheless, the super-regen circuit does have some great advantages. These easy-to-build circuits are very sensitive, even at VHF and UHF. They cover a very wide frequency range, and their very low supply-current requirements make them ideal portable receivers.

This article features some new circuits that greatly help minimize the traditional shortcomings of super-regens. We'll see circuits for the reception of narrow-band FM (NBFM) that operate over a very wide frequency range and can detect virtually every common transmission mode. I'll also introduce a simple, but effective, squelch circuit that mutes the super-regen's very loud undesired background noise.

With careful design, adequate controls and some operator skill, modern super-regen circuits can provide surprisingly good performance. Today, the availability of excellent low-cost semiconductors allows us to re-examine the potential of this technology.

The designs and information provided in this article are based on several years of construction and experimentation, rather than on a theoretical or mathematical analysis. I believe that this follows the traditional spirit of the radio amateur: to discover practical new technologies and methods of radio communication.

Finally, this article shows that many previously published "facts" about super-regeneration are false; they have simply been printed over and again without anyone challenging their truth. I also hope to show that the super-regen circuit remains a fascinating and misunderstood technology that is ideal for amateur experimentation.

[1]Notes appear on page 32.

Regeneration and Super-Regeneration

Regenerative receivers use a detector that is an RF oscillator to which an input signal has been coupled. Discovered by Edwin Howard Armstrong in 1914,[1] regeneration allowed radio amateurs to build very sensitive receivers in an age when the cost of radio components was very high and RF amplifier performance was dismal by today's standards.

In the modern regenerative circuit of Fig 1, the RF input signal from the antenna is amplified by Q1 and then coupled to the detector by L1. Winding L2 and capacitors C3a and C3b tune the input signal frequency. A portion of the detector's amplified RF output is then fed back to its input, in phase (so the signals add), by tickler winding L3. The signal is then amplified repeatedly, building-up (regenerating) to very high levels, until a critical point is reached where a self-sustaining oscillation begins. After that point, amplification of the input signal stops increasing and starts decreasing as most of the detector's energy is now devoted to generating this internal oscillation.

The actual mechanism of regeneration is complex. Regeneration has the effect of introducing a negative resistance into a circuit, which cancels out its positive resistance. Since the circuit's selectivity, or Q, is equal to its net reactance divided by its net resistance, the circuit's selectivity is increased along with its gain when regeneration is introduced. So, when properly adjusted, a single stage can be highly selective and avoid the use of several tuned stages, which are usually required in more complex receivers.

The amount of gain an individual regenerative stage can provide is limited by the introduction of these self-sustaining oscillations into the circuit. The free oscillations, once started, will build up to the limiting capacity of the amplifying device. Therefore, in a straight regenerative receiver, the operator must adjust the amount of feedback to a point just below self-oscillation, if the highest gain and selectivity are desired. For CW and SSB reception, the detector is adjusted so that it is operating just above the oscillation threshold. The detector's oscillations then mix with the input frequency, producing an audio beat note for CW or the local BFO signal needed for SSB reception. Typical circuit gains in a straight regenerative detector are 1000 times greater than the same detector operating without regeneration. Using modern components, practical circuit gains of 20,000 (86 dB) and higher are normal.

In 1922, Armstrong came up with yet another invention based on regeneration, but whose actual mechanism

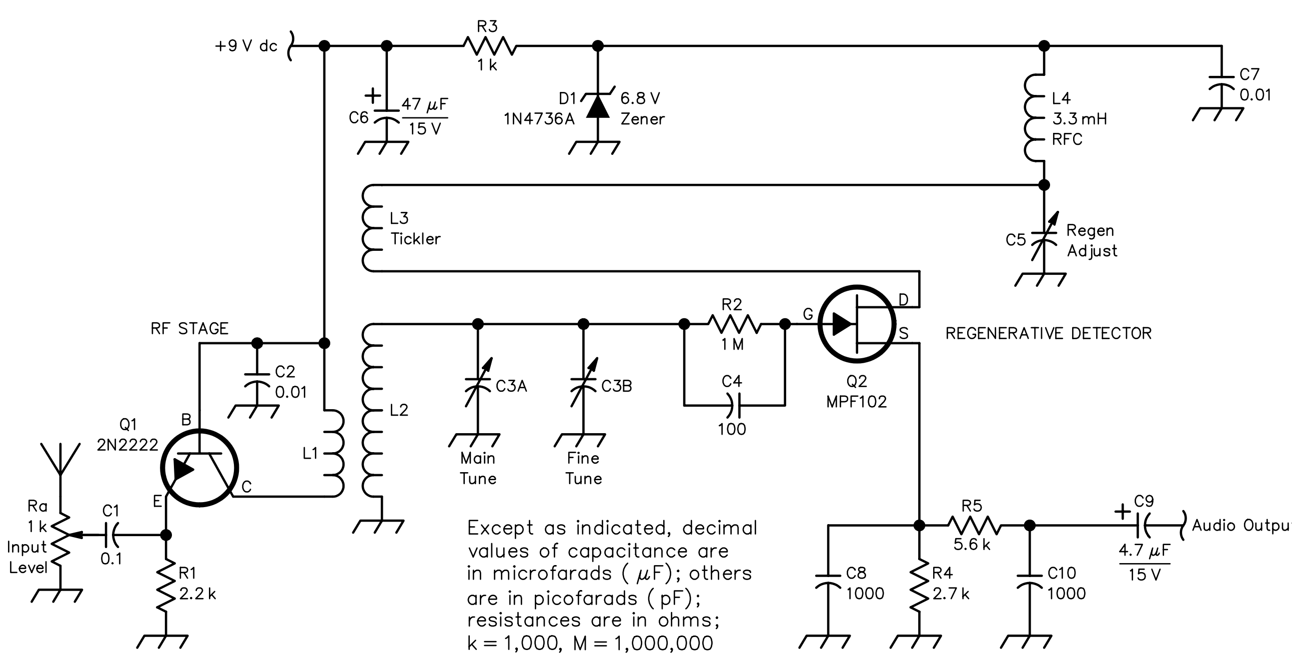

Fig 1—A modern regenerative detector circuit using semiconductors.

opened up an entirely new field of research: super-regeneration.[2] This is a modification of the straight regenerative circuit; the detector is set to an oscillating condition and then periodically shut down or *quenched* by a second oscillator operating at a lower frequency. In its simplest form, the circuit is essentially a modulated oscillator whose input is coupled to an antenna. Super-regeneration allows the input signal to build up to the oscillation point over and over again, providing single-stage circuit gains of close to one million (120 dB). As long as there is enough gain to begin oscillations, very sensitive receiver circuits can be built at frequencies where would be much too difficult for the average ham to construct other types of receivers, such as the superheterodyne.

Super-regens are classified into one of two general categories, depending on how their oscillations are interrupted: separately quenched and self-quenched (as shown by Fig 2). In Fig 2A, the separately quenched variety uses a separate quench oscillator, Q2, to generate an alternating voltage (historically a sine wave) that is above the audio range but still far lower than the signal frequency. This modulates the drain voltage of Q1 at the quench frequency. The JFET is periodically cycled on and off at the quench-frequency rate. The quenching oscillations are simply a form of AM that periodically interrupts the main oscillation, allowing the RF signal to repeatedly build up to the oscillation point.

Although the separately quenched variety provides high sensitivity and permits the operator to adjust both quench frequency and amplitude, it requires building, powering and adjusting a separate quench oscillator. This adds quite a lot of complexity to an otherwise simple circuit. Fortunately, modern ICs make a separate quench oscillator cheap and easy to construct.

Fig 2B shows the self-quenched variety. In a self-quenched circuit, a secondary *relaxation oscillation* is produced in the detector so that it is simultaneously oscillating at two frequencies: the RF signal frequency and the quench frequency.

In the self-quenched circuit, the RC time constant of C1 and R1 is deliberately set long enough so that C1 cannot discharge fast enough to prevent a build-up of a reverse-bias voltage across R1. This bias voltage eventually increases enough to shut down the RF oscillation. C1 is then discharged through R1 until the bias

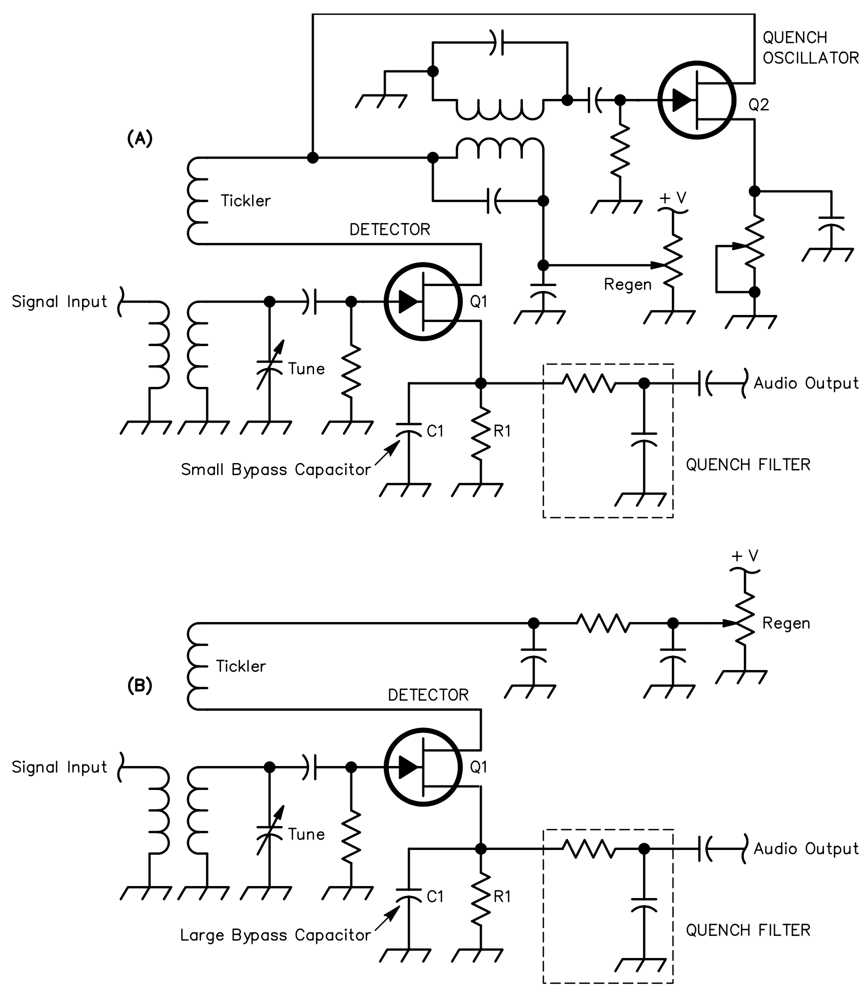

Fig 2—Basic super-regen circuits. (A) Separately quenched detector circuit. (B) Self-quenched detector circuit.

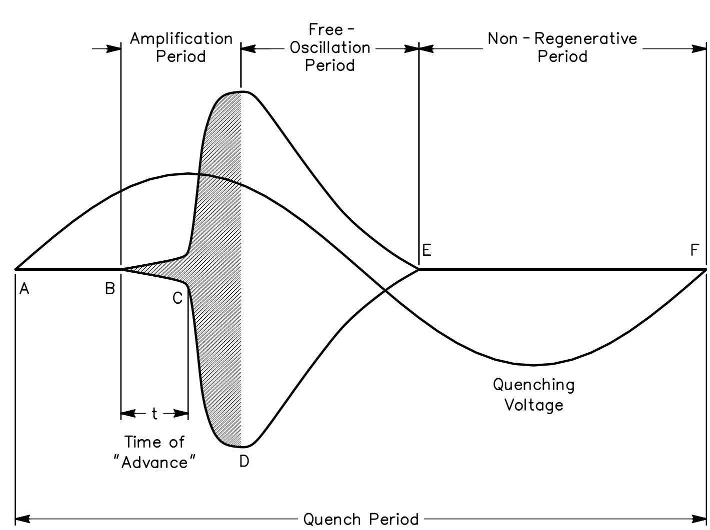

Fig 3—The characteristic RF envelope of a super-regen detector.

voltage is low enough for RF oscillations to begin again. The RC time constant of R1 and C1, along with any resistance and capacitance in the power-supply line, determine the frequency and wave shape of these quenching oscillations.

The Actual Mechanism of Super-Regeneration

Fig 3 is derived from a 1935 article by Hikosaburo Ataka.[3,4] It provides a detailed representation of the oscillation envelope of a super-regen detector circuit being externally quenched by a sine-wave voltage. This resembles the pattern that you would actually see on an oscilloscope. The area within the shaded region of the envelope is where the received signal is actually amplified.

When there is no signal present, noise in the detector initiates a build-up of a free oscillation that starts around point C and builds to the carrying capacity of the active device. The detector is now in a state of free oscillation; this continues until the circuit is quenched and the oscillations die (point E).

When an input signal is applied, the dynamics of the shaded region change. The build-up of oscillation now starts sooner—at point B; this added time of build up, t, by which the oscillation starts early in the presence of a signal, is termed the time of *advance*. The greater the magnitude of the input signal, the greater will be the time of advance. Greater times of advance yield longer amplification time periods (B to D). Weak noise sources require longer for oscillation to begin than do stronger radio signals. Therefore, given the limited time between quench intervals, the signal sources are amplified much more than the background noise. The time of advance directly affects detector sensitivity and is a function of the strength of the applied input signal and both the frequency and amplitude of the quench voltage.

Note that the unshaded (oscillatory) portion of the envelope (D to E) contains by far the greatest area, but does not contribute to any actual amplification of the signal. The non-regenerative time interval (E to F) is that period when the quench signal has completely stopped oscillations.

Oscillations must be allowed to completely cease before recommencing. This is why high-Q tuned circuits ahead of super-regen detectors can theoretically prevent the detector from operating correctly. They hold the signal, preventing it from being totally quenched: Super-regeneration stops and the circuit oscillates continuously. In practical circuits using hand-wound coils, however, there are always enough circuit losses to prevent this problem.

The audio output from the detector is directly related to the area of the shaded region (B to D). With no signal applied, the noise initiating the build up of oscillations is random; thus the time of advance—the area of the shaded region—and the output of the detector will also be random. This explains the characteristic back ground hiss—termed *rush noise*—of a super-regen detector. It is very noticeable with no signal and disappears completely on strong signals.

Both the amplitude and frequency of the interruption (*quench rate*) affect performance. Ideally, the detector should be quenched at a point just after it has broken into free oscillation, or

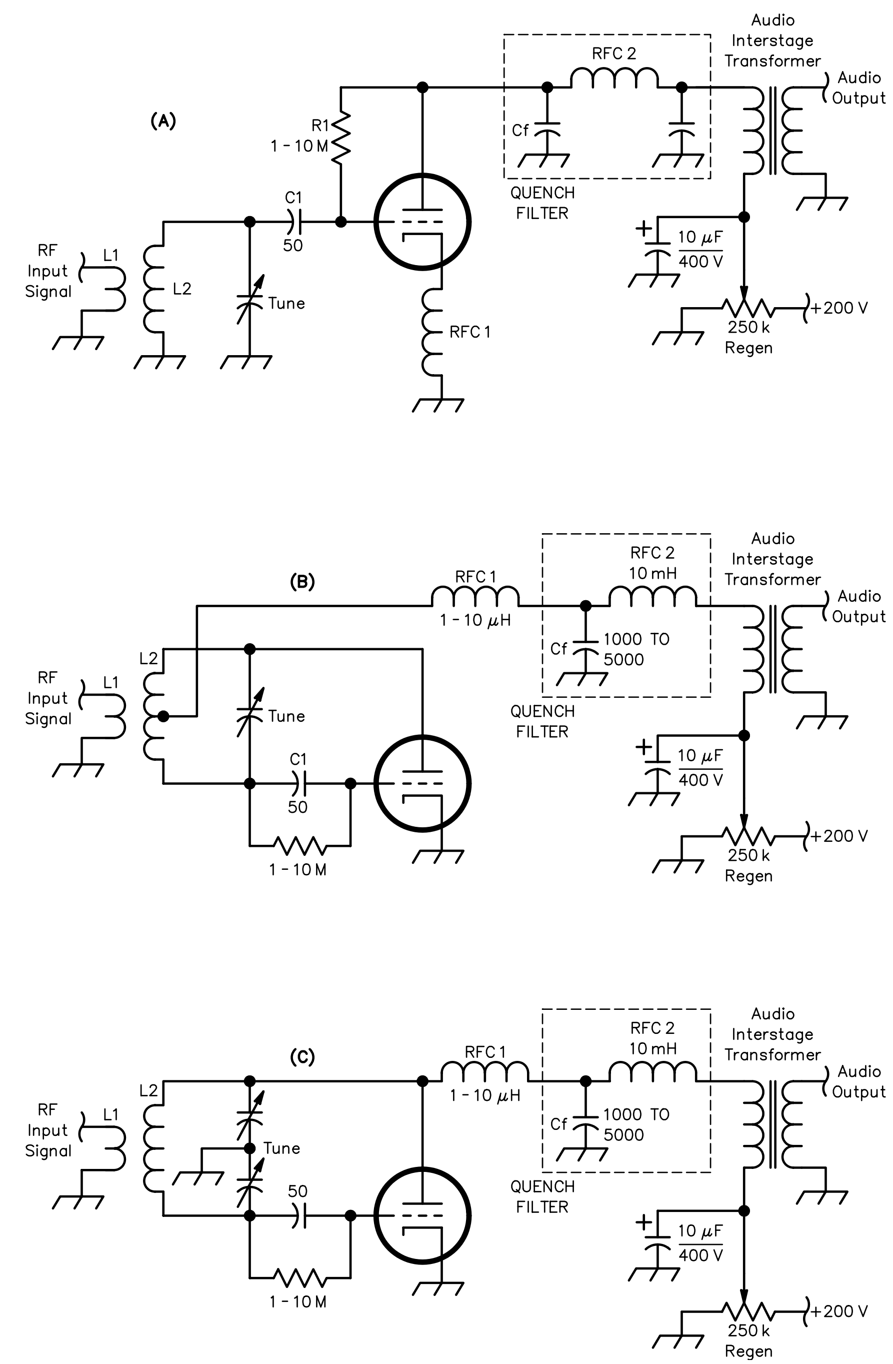

Fig 4—Classic self-quenched vacuum-tube super-regen detector circuits. (A) Floating-cathode circuit, (B) Hartley and (C) Colpitts.

just beyond point D in Fig 3: This should provide the greatest sensitivity. With these circuits, though, sensitivity is so great that it is almost never an issue. Selectivity is the big challenge; it has been the subject of confusion and misinformation for many years.

Traditional Super-Regen Circuits

Fig 4 shows some of the many vacuum-tube super-regen detector circuits that were common in the 1930s and ’40s. In all these circuits, the frequency of the RF oscillations (the receiving frequency) is set by coil L2 and the tuning capacitor. Regeneration is controlled by varying the detector’s supply voltage.

Fig 4A is the classic “floating-cathode” circuit. Here RFC1 keeps the cathode of the tube above ground for RF. This destabilizes the circuit by allowing the build-up of RF energy at the cathode. The tube’s plate is bypassed to ground. The internal tube capacitance (plus any stray circuit capacitance) between the cathode and ground, together with the capacitance between the tube’s cathode and grid, create a Colpitts oscillator. When the **REGEN** control is set high enough, RF oscillations begin.

The circuit of Fig 4B uses a center-tapped coil in a Hartley oscillator configuration. Notice that this time, the cathode is at ground potential. The plate is at one end of L2 while the grid is at the other. The plate current flows through the tap on the coil back to the supply. This induces a signal into the other half of the coil—which is now in phase with the input—so that oscillation can occur.

The circuit of Fig 4C is based on a Colpitts oscillator. It uses a split-stator tuning capacitor, rather than a center-tapped coil, to provide phase inversion. Here, a capacitive divider is formed between plate and grid with the tube’s cathode—which is grounded—at the center. This connection has an obvious advantage: It allows the tuning capacitor’s frame to be grounded.

All these circuits suffer from serious construction and operational problems. Variations in individual layout will change the stray capacitances at the tube’s grid and cathode, requiring that the builder try different values of RFC1 and Cf to get the detector to oscillate (and quench) properly. Fig 4B has an added complication: Both sides of the tuning capacitor are floating. This requires that the tuning capacitor have an insulated shaft long enough to prevent any frequency change from hand capacitance. Although the tap of L2 is occasionally bypassed directly to ground, an RF choke (RFC1) is usually recommended between this point and the bypass capacitor. I believe this is so because—with the center of L2 bypassed—the stray circuit capacitance between either side of the coil and the tap would have a fairly direct connection to ground. If these stray capacitances were unbalanced, RF oscillation might be inhibited. In addition, with a “floating” tap (using the RF choke), a higher maximum oscillation frequency could be achieved.

Reducing Interference

Because a super-regen breaks into oscillation as part of its normal

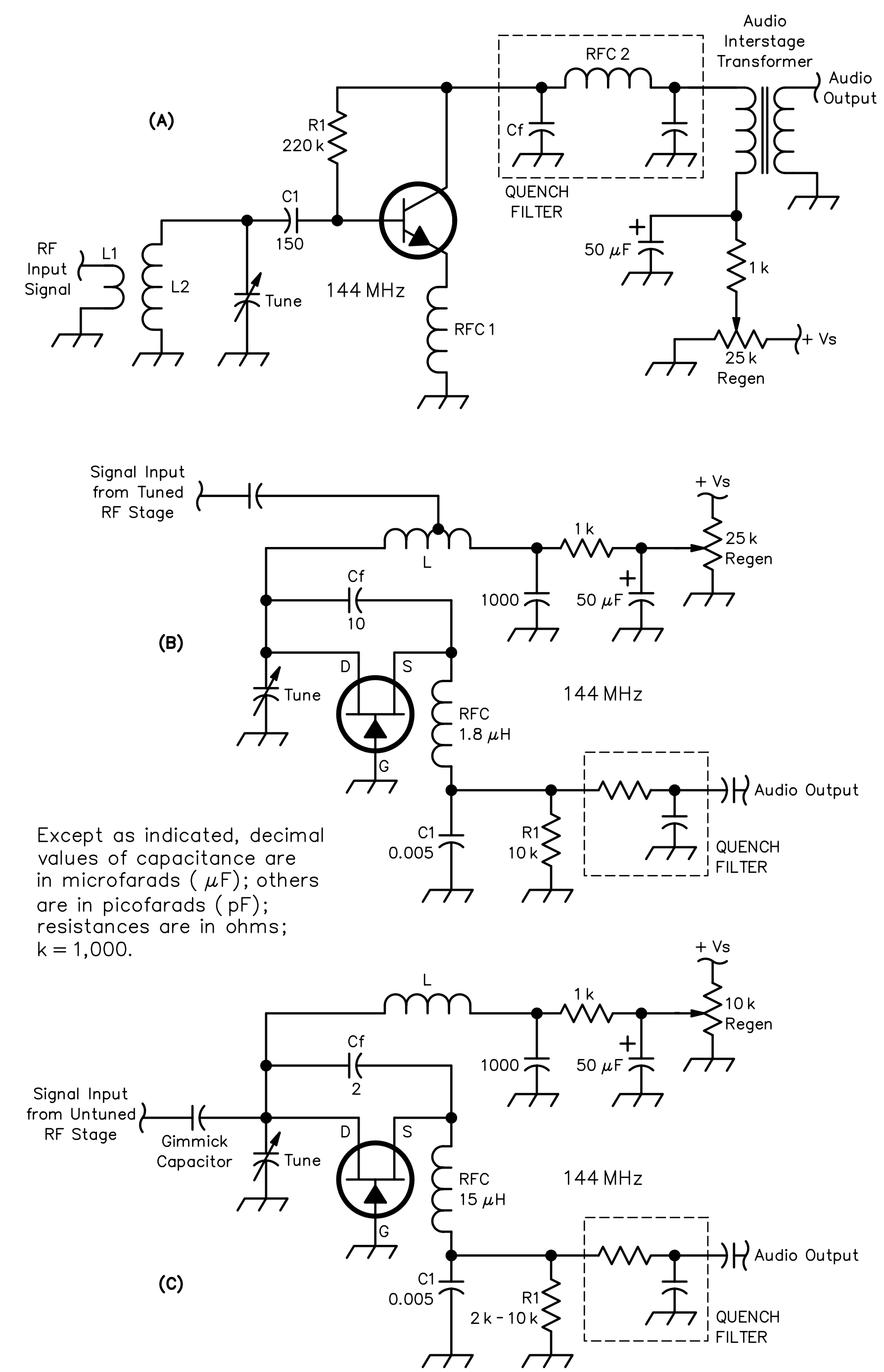

Fig 5—Some modern VHF super-regen detector circuits using semiconductors. (A) shows a typical bipolar circuit of the early 1960s, (B) an original DeMaw circuit of 1967, (C) a modified DeMaw circuit.

operating cycle, it will radiate some of its own signal. When vacuum-tube detector circuits are directly coupled to the antenna, serious interference often resulted. Using a tube such as the 6J5, operating at several milliamperes and 100-200 V, power levels could be as high as a watt, or more!

Today, we have excellent low-power semiconductors that offer much better performance than vacuum tubes while operating at far lower power levels. The JFET detectors described in this article typically consume 200 µA at 6 V or less, which is only 1.2 mW. Despite this significant reduction in potential interference, all super-regen receivers built today should also include an RF stage to provide additional isolation of the detector's oscillations from the antenna. (QRP enthusiasts make many QSOs with 1.2 mW—*Ed*)

Super-Regen Detectors Using Semiconductors

Fig 5 shows some solid-state super-regen circuits that were introduced in the 1960s. Fig 5A is very similar to the floating-cathode circuit of Fig 4A. Here, an NPN bipolar transistor is the active device. Note that RFC1 floats the transistor's emitter above ground, which promotes oscillation and helps prevent the fairly low impedance of the transistor's emitter-base junction from loading L2. In actual use, regeneration is difficult to control in all of these bipolar designs. The change of the transistor gain with variations in supply voltage is far too abrupt for smooth regeneration control.

Although these transistor designs are small and portable, all of these traditional circuits—both tube and solid state—suffer from very poor selectivity. A few homebrew receivers built in the 1940s and '50s used very-high-Q tuned coaxial lines.[5] These offered much better selectivity than the traditional sets, but building the lines was fairly complicated, and this idea never became very popular.

Fig 5B shows a circuit introduced by Doug DeMaw, W1FB/W1CER, in 1967.[6] It has some real advantages over previous designs. It uses a JFET device, which has less gain but normally has much greater stability than bipolar transistors. The JFET is operated in a grounded-gate configuration, which further improves stability and provides greater bandwidth than a comparable common-source amplifier connection. DeMaw's circuit has some similarities to the old floating-cathode circuit. Extra capacitance added between the source and drain helps initiate RF oscillations. This connection is unique in that it uses, R1, a large (10-kΩ) source resistor to: set a high level of dc bias for the JFET, work with C1 to set up quenching oscillations and allow the audio to be extracted easily from the JFET source.

Trying to build a 1990s version of this circuit, I was unable to find a commonly available source for the 1.8 µH RF choke specified; so the design needed to be modified. The result is shown in Fig 5C. Here, I increased the value of the RF choke and decreased the value of Cf (to provide about the same amount of feedback). Now, larger-value commercial chokes could be used for the RFC.

Instead of a tuned RF stage tightly coupled to the detector, as in DeMaw's design, an untuned RF stage is used along with a very small gimmick capacitor for interstage coupling. The untuned RF stage provides more than enough gain to drive a super-regen detector, is very stable and easy to build. The use of the tiny gimmick capacitor reduces sensitivity somewhat, but it prevents any loading of the LC circuit, thus preserving its Q. This increases the detector's selectivity and provides additional isolation of the detector's oscillations from the antenna.

I found this variation of DeMaw's basic circuit very useful for constructing small, portable receivers for AM reception on the VHF aircraft band (118-136 MHz), but selectivity was still poor and NBFM signals on 2 meters could not be detected. Only the NBFM signal's carrier could be received; its modulation was too weak to be readable.

A Super-Regen Circuit for Narrow-Band FM

Fig 6 shows a new self-quenched circuit that has several important differences from the traditional, unselective super-regen. All previous articles and references I have seen on super-regens credit the Q of the LC tank circuit as the primary determinant of receiver selectivity. Quench frequency is usually listed as non-critical, while the wave shape of the quenching oscillation is not mentioned. As with any receiver, the Q of the tuned circuit is always important; however, as my own experiments have shown, *the most important variable affecting the selectivity of a super-regen detector is the wave shape of the quenching oscillation* [emphasis added—*Ed*]. I have found that the use of a very clean sine-wave quenching oscillation greatly increases selectivity and allows detection of NBFM signals.

The first new feature the circuit of Fig 6 provides is potentiometer, Rqw, the *quench-waveform* control. It introduces a small resistance in series with the quench capacitor, C1. This added resistance varies the wave shape of the quenching oscillations from the usual sawtooth to something much closer to a sine wave. Once Q1's oscillations start in this self-quenched circuit, the long time constant set by C1/R1 causes the source dc bias level to increase until it stops the detector's RF oscillations. This bias voltage then discharges through R1 until oscillations to start again. The values of R1 and C1, plus

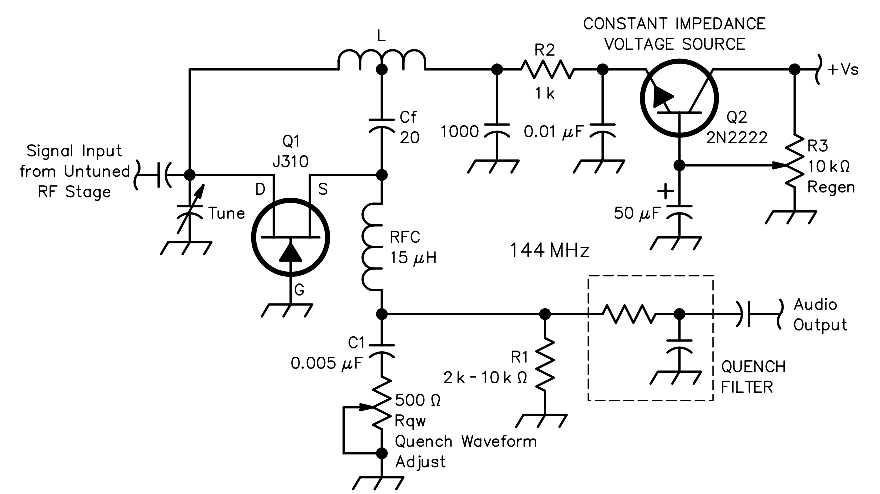

Fig 6—A super-regen circuit for NBFM.

any resistance and capacitance in the detector's power-supply line, set the frequency and wave shape of this relaxation oscillation. Both are critically important in determining the receiver's selectivity.

The oscilloscope photos of Fig 7 show the quench waveforms of the Fig 6 detector circuit. To sample the waveforms a small pick-up loop was made by tying together the ground wire and tip of an oscilloscope probe. This loop was placed near the main tuning coil, L. The top waveform is the detector's RF oscillation envelope as sensed by the loop; the bottom waveform is the voltage at the JFET source, where the RC time constants that create the secondary quenching oscillations are located.

Fig 7A shows the waveform of the Fig 6 detector circuit with RQW set to 0 Ω. Note that this produces a sawtooth modulation envelope: The detector breaks into full oscillation very quickly and then slowly decays. This sawtooth modulation produces wide sidebands on either side of the detector's carrier (its primary oscillation at the receiving frequency). These sidebands contain many harmonics. Any sidebands present will *interfere* with a narrow-band input signal, and the reduction of these sidebands is essential for the detection of NBFM signals.

With the introduction of RQW into the self-quenched circuit, however, both the wave shape and amplitude of the quenching voltage developed within the detector change. This results in a clean-looking (smoothed-out) modulation of the RF oscillation (see Fig 7B). Since this waveform now more closely resembles a sine wave, it has much less harmonic content than a sawtooth, and the sidebands generated are much narrower. This reduces self-interference (where the detector is effectively jamming itself) and greatly improves the detector's ability to copy narrow-band signals.

Note that most previous super-regen circuits have used high-resistance regeneration controls, typically 25 kΩ in transistor circuits and up to 250 kΩ in tube circuits. When the control was not at the top of its range, it introduced a large series resistance in the power-supply line. In a self-quenched detector circuit, this further distorted its RF envelope, making selectivity even worse.

The use of Q2, a simple voltage source, helps prevent any large changes in the series resistance of the detector's supply line as regeneration is varied. R3, a 10-turn potentiometer, varies the voltage at Q2's base, which will be approximately 0.7 V higher than that at its emitter. As a lower-cost alternative, two standard potentiometers—a 1-kΩ and a 10 kΩ—may be substituted for the 10-kΩ, 10-turn potentiometer. Simply connect the wiper and one side of the 1-kΩ pot together and wire it in series with the 10-kΩ main regeneration control. The 1-kΩ pot then allows you to fine-tune the regeneration level. By experimentation, I have found that resistor R2 should be around 1-kΩ. This amount of series resistance appears to provide the best demodulation of NBFM signals.

The second major improvement over conventional circuits is the use of a super-regen detector operating grounded-gate in a modified Hartley oscillator configuration. The detector's drain is connected to one end of L, while L's other end is bypassed to ground, which effectively connects it to the JFET gate. The JFET source is coupled to a tap on the coil. The tap provides the necessary phase inversion between gate and drain, so that positive feedback is introduced into the stage. The RF choke "lifts" the JFET source above ground for RF and allows the audio to be extracted from the JFET source without loading the detector.

This circuit (Fig 6) is much easier to get functioning correctly than the source-to-drain capacitance-feedback scheme of Fig 5C. Now, the amount of feedback may be easily adjusted simply by changing the point where capacitor Cf connects to coil L. For the vast majority of circuit layouts, connecting Cf to the center of the coil gives excellent results. This circuit is much less dependent on variations in the values of Cf and the RFC.

When receiving NBFM, the detector is tuned to one side of the carrier and the regeneration control is carefully adjusted to permit slope detection. Slope detection is a method for receiving FM signals using an AM detector. The sidebands on either side of the carrier can be tuned in and since their amplitude decreases the further their frequency is from the carrier, the amplitude of the detected signal varies with frequency modulation.

Slope detection usually works poorly with superhets because their selectivity cannot be easily changed, but the user-controlled selectivity of a super-regen set allows the reception of NBFM, and virtually all common transmissions. Like traditional regenerative sets operating on shortwave frequencies, this narrow-band circuit requires careful adjustments of tuning and regeneration by the operator. Nonetheless, learning to tune and operate a regen is considerably easier than building a sensitive, broadband superheterodyne receiver for VHF.

Increasing the Selectivity of Externally Quenched Circuits

A very interesting effect occurs when

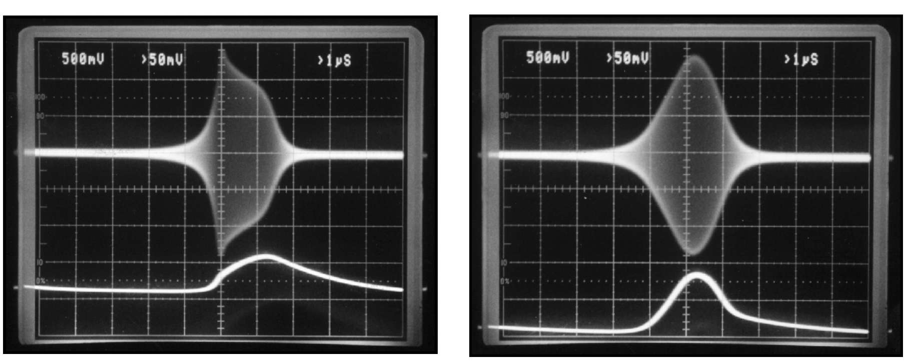

(A) (B)

Fig 7—The effect of the QUENCH-WAVEFORM (RQW) potentiometer on the shape of the detector's RF envelope. At A, RQW is set to 0 ; at B, 250 Ω.

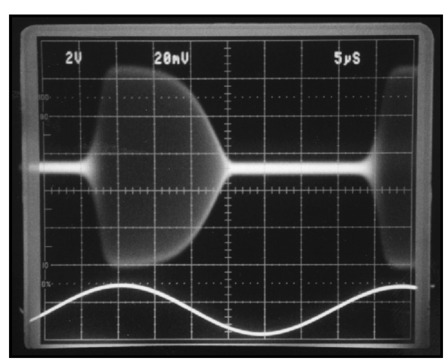

Fig 8—The RF envelope of a typical super-regen detector being separately quenched by an external sine-wave voltage.

an *external* voltage waveform, from a separate sine-wave oscillator, is used to quench the detector circuit of Fig 6. Although the detector remains very sensitive and its no-signal background noise is lower than that of the traditional self-quenched circuit, the receiver remains unselective and unable to detect NBFM signals. I believe the reason for this is that modulation of an oscillator (the detector) is not the same as modulation of an RF amplifier. When an oscillating super-regen detector is quenched (modulated) by an external sine-wave voltage, a very distorted sine-wave RF envelope is produced. (The upper trace of Fig 8 shows the RF envelope of a typical super-regen detector being separately quenched by an external sine-wave voltage, which is shown in the lower trace.) This occurs because the detector's oscillation frequency is being varied as well as its amplitude and because the rise and fall times of this RF oscillation are not linear. What is needed is a wave form and duty cycle that results in a clean sine-wave RF envelope on the detector. This area is still open to amateur experimentation.

A Super-Regen Mixer/ Demodulator for NBFM

A New Zealand ham, Nat Bradley, ZL3VN, has built many VHF and UHF super-regen receivers and has made several important discoveries. Perhaps the most interesting of these is—until now—unpublished. If a *suitable* local RF oscillation is mixed into a super-regen detector, the detector will provide very strong audio output from NBFM. (*Suitable* oscillations are offset from the receive frequency by the quench frequency of the detector.) I have verified Nat's findings using a signal generator located close to a receiver (no direct connection is needed). With the signal generator set approximately 100 kHz (the quench frequency of my set) to either side of the received signal, NBFM is recovered at a very high level, with low distortion and little need to adjust the regeneration control.

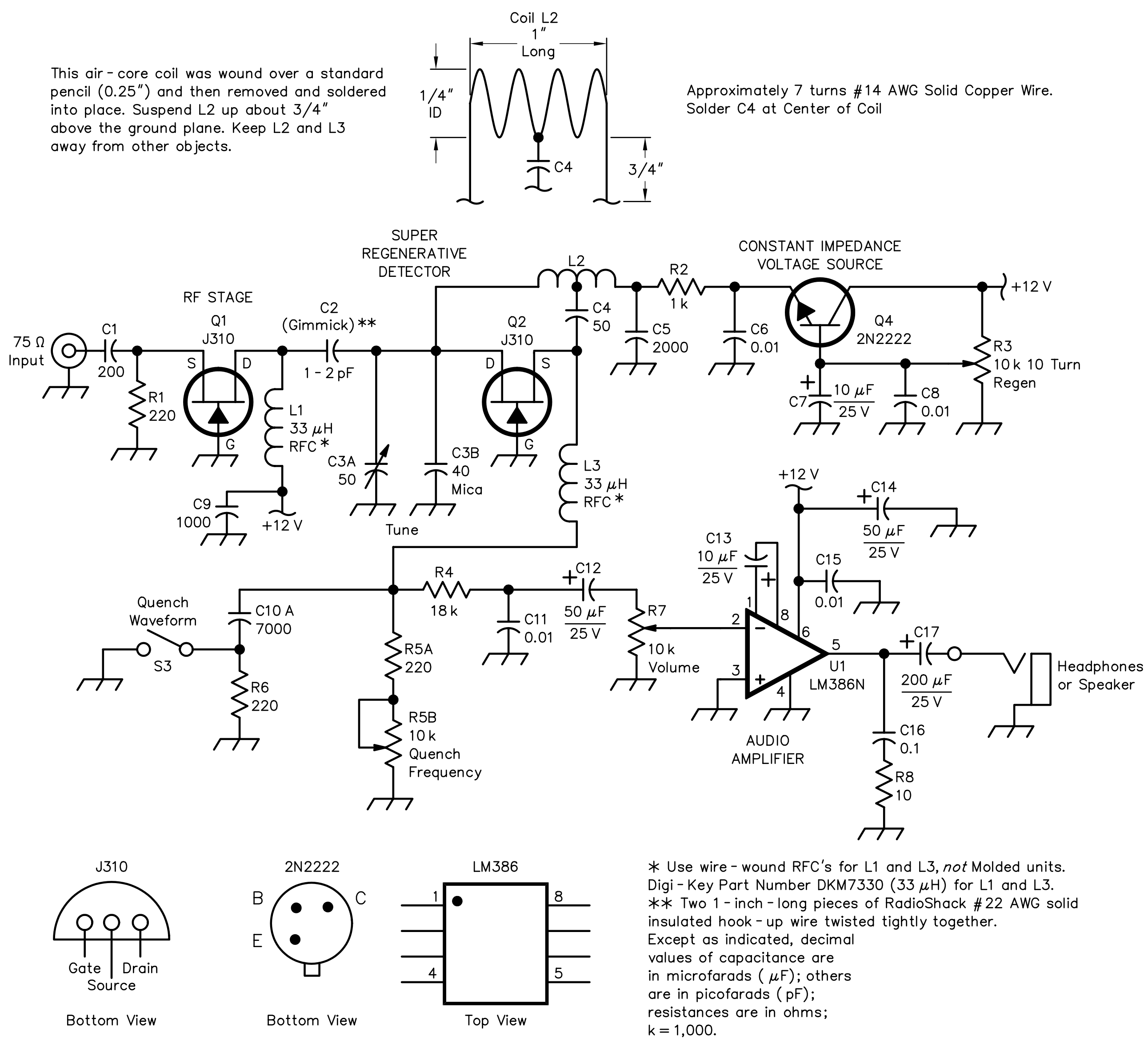

Fig 9—A 38 to 54 MHz super-regen VHF receiver.

Although the exact mechanism is unknown, we believe that the super-regen detector is mixing the two signals. This produces two RF signals at the detector's output: a 100-kHz "IF" (the difference between the local oscillation and the received carrier) and a second RF signal, which is the detector's quench frequency. The quench frequency is modulated ±5 kHz by the received NBFM transmission. The two signals then mix within the detector's quenching oscillation. This removes the 100-kHz *quench carrier*, leaving the original NBFM modulation.

This discovery implies that very sensitive super-regen mixer/detectors could be built that directly demodulate NBFM at extremely high frequencies. This at a fraction of the cost and power consumption of conventional superhet designs. Notice however, that although this provides a mixer of great sensitivity, it still suffers from problems inherent in all superhet designs. The local oscillator must closely track the mixer tuning as the received frequency is changed. Hence, the homebrewer needs to build two oscillators, one conventional and one super-regen, using a two- or three-gang tuning capacitor. Even so, this could produce a very nice receiver for a limited tuning range such as a single ham band.

A VHF Receiver Circuit for 38-54 MHz

The circuit shown in Figs 9 and 10 provides good coverage of the 6-meter ham band and other lower VHF frequencies. These include fire, police, snow plows, maintenance/repair crews, older cordless telephones, telephone paging and a variety of other local communications. The circuit will demodulate AM, wide-band FM, NBFM and phase-modulated signals with the **REGEN** control set for super-regen and—when set to a straight regeneration mode—it will detect CW and SSB, as well. The entire circuit operates on only 20 mA and has a sensitivity of around 0.5 µV.

The circuit may be built using a low-cost PC board from FAR circuits.[7] This is *highly* recommended, since it greatly simplifies construction and helps prevent any layout or wiring errors. This board may also be used to build the VHF Aircraft Band and 88- to 180-MHz circuits, as well. For that reason, similar components have the same designations in all three circuits.

In Fig 9, RF signals enter via a 75-Ω coaxial cable and are ac coupled to the source of the RF amplifier, Q1. Although this stage has no current gain, its common-gate connection does provide modest voltage gain over a wide frequency range. The great sensitivity of the super-regen detector makes up for any losses here. Low noise, freedom from oscillation, immunity to strong-signal overload, multiband operation and good input-to-output isolation are the important design issues for this stage. It also has a low input impedance (to match the coax line) and a high output impedance, which minimizes loading on the detector.

R1 provides protective dc bias to the JFET source. L1 is an RF choke, which extracts the amplified RF signal from the JFET Q1's drain. The choke's value is not critical, but it's a good rule of thumb to use the same value as that of L3 in the detector circuit. A gimmick capacitor, C2, couples the signal from the RF stage to the detector. The gimmick was made by twisting together two 1-inch-long pieces of RadioShack #22 AWG solid, insulated hook-up wire. Its value is somewhere around 1 pF. Compared to a larger fixed-value capacitor, the gimmick lightly couples signals into the detector. This prevents overcoupling, which would reduce detector selectivity and often creates reception "holes" in the tuning range of a super-regen receiver.

Q2 operates as a super-regen detector in a modified Hartley oscillator configuration. Capacitors C3b, C4 and

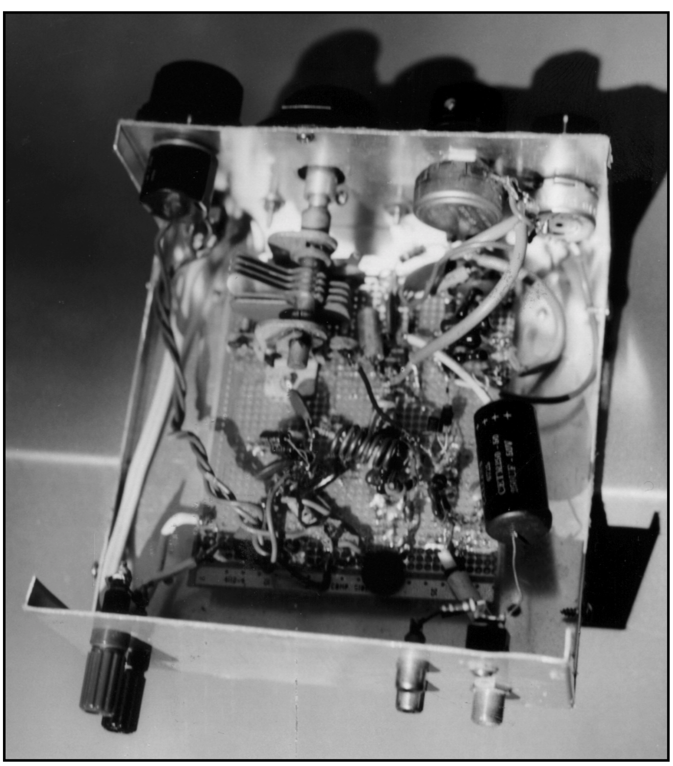

(A)

(B)

Fig 10—38 to 54MHz receiver (A) interior and (B) exterior views.

C5 should be mica (or NP0 ceramic), as they need to be low-drift, high-Q devices. R6 introduces a small resistance in series with C10a, which modifies the self-quenched waveform into a sine wave for high selectivity. Q4 reduces any variations in quench waveform shape when the regeneration control is adjusted.

Audio output is extracted and low-pass filtered by R4 and C11. This filtering prevents the quenching oscillations from reaching the audio stage. The filter also "rolls off" the higher audio frequencies, which improves the audio quality and reduces background noise. C12 ac couples the filtered audio signal to volume control R7. An LM386 audio amplifier IC provides an audio gain of 200 with enough power to drive Walkman-style headphones or a small speaker.

A Practical Squelch Circuit for Super-Regen Receivers

Since its widespread use in 1930s VHF ham receivers, the super-regen detector has been notorious for its high background noise. This rushing noise can be annoying over long periods, such as when monitoring control-tower fre-

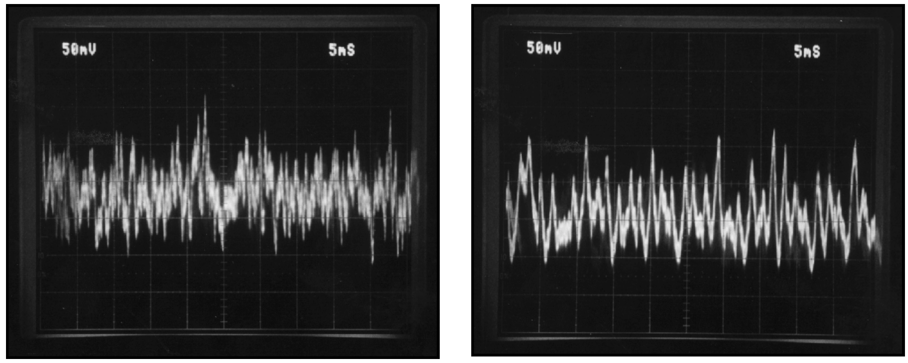

(A) (B)

Fig 11—Audio output from a typical super-regen detector with (A) no signal and (B) when receiving an RF signal.

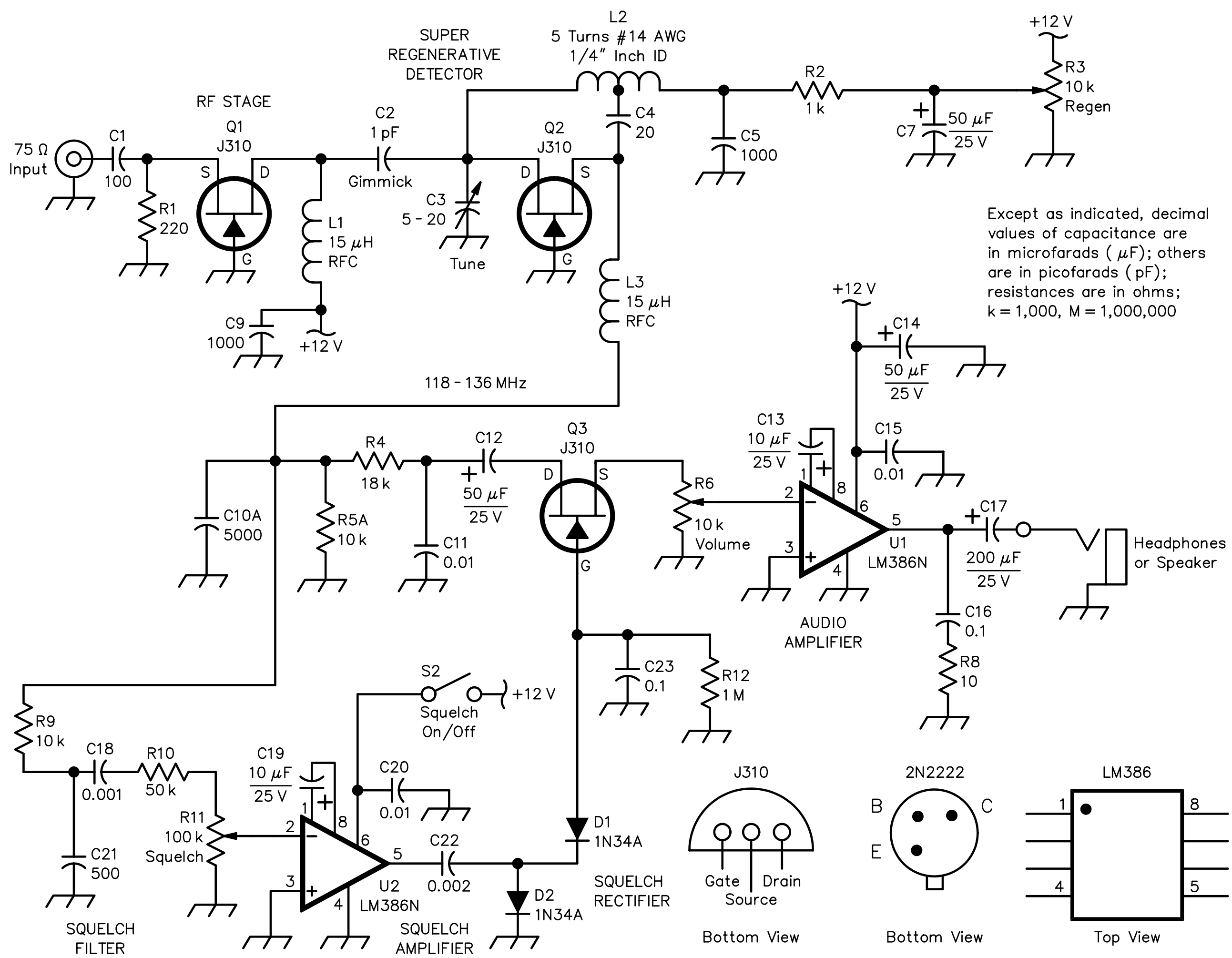

Fig 12—A super-regen VHF aircraft-band (118-136 MHz) receiver with squelch.

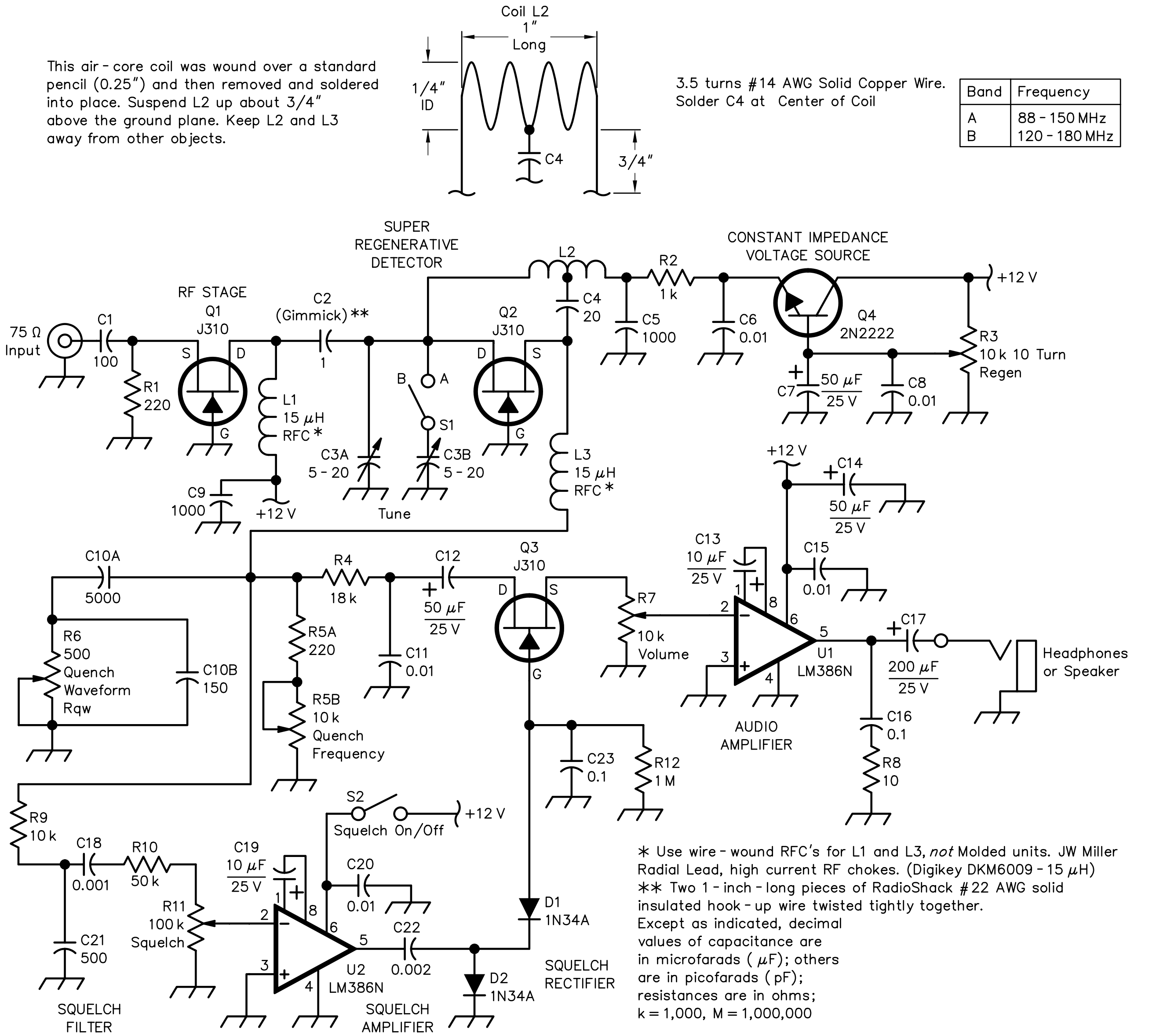

Fig 13—A two-band 88-180 MHz VHF receiver with squelch.

quencies on the aircraft band. Notice, however, that this is generally *not* a problem when listening to wide-band FM (such as stations on the FM broadcast band), since signal levels are very high and the station carrier is on all the time. When listening to NBFM signals, the detector is adjusted to a low regeneration level that greatly reduces the background noise.

Nonetheless, weak NBFM signals—and especially AM signals on the aircraft band—still need a squelch circuit for listener comfort. This can be achieved through a curious characteristic of the super-regen. By nature, the super-regen detector is a very effective AGC amplifier, bringing both no-signal (noise) and with-signal inputs to virtually the same audio output level. Under no-signal conditions, the detector's audio output is fundamentally a constant-amplitude, very-wide-bandwidth signal similar to white noise. This is shown in the oscilloscope photo of Fig 11A. When a signal is received (Fig 11B), the audio output changes and consists mainly of lower audio frequencies, with quiet periods when no one is talking.

The audio output level of the detector, therefore, stays nearly constant, but the audio-frequency balance (high versus low audio frequencies) varies greatly. So simple audio filtering and rectification may be used to create a control voltage that varies directly with the amount of high-frequency audio content. This voltage may then be used to mute (squelch) the audio amplifier.

Just such a circuit is shown in Fig 12. Here, approximate component values for the 118-136 MHz aircraft band are provided. Two outputs are taken from the detector. The first is the usual audio output, which runs through quench filter components R4 and C11, then to the **VOLUME** control and LM386 audio amplifier. The other output runs through a second filter consisting of R9, C21, C18, R10 and R11. This RC bandpass filter removes the quench frequency and the lower audio frequencies. The output of the squelch control R11 contains mainly the higher audio frequencies. The RC filter could be replaced with a high-Q active filter for better results, but the present circuit appears to func-tion quite well.

IC2, a second LM386, amplifies this signal and drives a simple voltage-doubler circuit built around D1 and D2. This rectifies the signal and produces a negative voltage output that varies directly with the amount of higher audio frequencies present in the output of the detector. R12 and C23 filter the rectified voltage, which is then applied to the gate of Q3. This JFET's source and drain are wired in series with the main audio output from the detector.

In operation, the **SQUELCH** control is advanced (with the receiver in a no-signal condition) until the negative-voltage output from the voltage doubler just cuts off the JFET, which mutes the audio. When a signal is received, the detector's high-frequency background noise level drops dramatically, lowering the doubler output voltage and the JFET conducts, restoring the audio.

If there is a need to receive very weak RF signals, the **SQUELCH** control may be adjusted so that only partial muting occurs; but even with partial muting, background noise is reduced considerably. Because female voices usually contain higher audio frequencies than those of their male counterparts, female-voice programming may require a lesser **SQUELCH** adjustment. The squelch portion of the receiver consumes only about 4 mA of supply current.

A Two-Band, 88-180 MHz VHF Receiver with Squelch

The circuit of Fig 13 is a VHF receiver that features a very wide tuning range: much wider than that of a homebrew superhet design. It covers 88-180 MHz in two bands. Photos of a finished receiver are shown in Fig 14.

Because it operates at the higher end of VHF, this circuit uses a main tuning coil (L2) with fewer turns than that used in the 38-54 MHz unit of Fig 9. The coil should be approximately the same length, though. The turns can easily be stretched so that the coil is about one inch long. After the circuit has been built and the detector is operating correctly, the turns of L2 can be compressed or expanded to raise or lower the tuning range. The values of L1 and L3 are lower in this circuit than those of the 38-54 MHz receiver. Likewise, the values of C1, C4, C10a and C5 have been reduced. C10b is optional; it serves to minimize any effects caused by stray capacitance in the wiring of R6.

The value of C3 is not critical. A two- or three-gang capacitor salvaged from an old FM radio will work nicely. Other small variable capacitors may be substituted, as long as their maximum capacity is not too great. A small mica capacitor may be wired in series with the tuning capacitor to reduce its maximum value; likewise, a turn or two may be added or subtracted from L2 to change the tuning range.

Band switching is accomplished simply and easily, using a miniature toggle switch to connect either one or two gangs of the tuning capacitor. The bandswitch was wired directly onto the hot terminals of the tuning capacitor using two very short lengths of #14 AWG copper wire. These support the switch quite well. With this arrangement, it is necessary to build the receiver with an open top, so you can reach in to change bands. Of course, a relay could be wired to switch in the second gang with a switch controlling

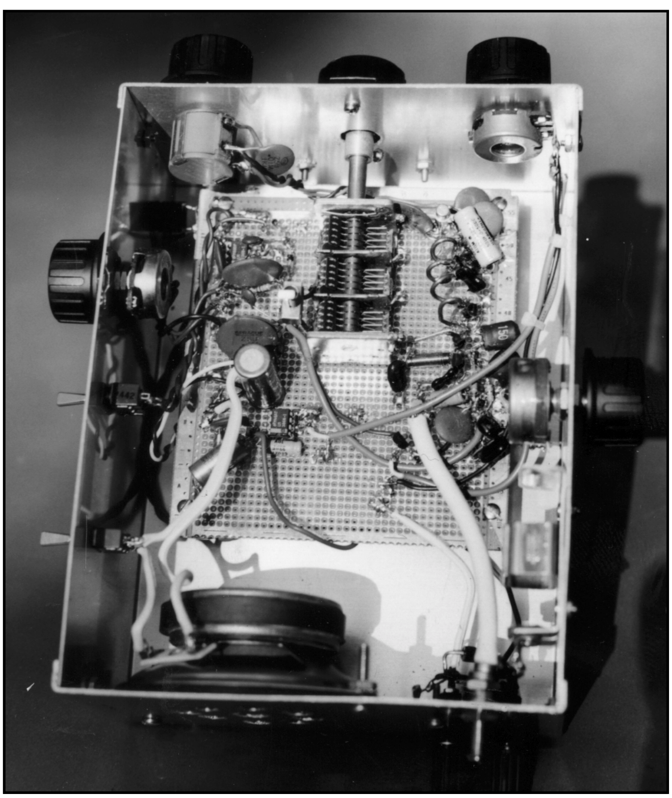

(A)

(B)

Fig 14—88-180 MHz receiver (A) interior and (B) exterior views.

it from the front panel, but this would greatly increase the power consumption of the receiver.

By using fewer turns on L2 and a lesser value for L3, operation may be extended up to about 350 MHz. Above that, stray circuit capacitances between the detector and the PC board prevent it from oscillating and super-regenerating properly. R5b can be a trimpot on the PC board. Set it to a value that allows smooth regeneration control throughout the range of the receiver. For the best possible reception of NBFM signals, it could be a standard 10-kΩ potentiometer installed on the front panel.

As shown in the photos, the enclosure for this receiver was made by placing the top half of a metal box inside its bottom section. These two sections are connected using small screws and nuts. This produces a very rigid four-sided box with an open top. The use of a good, solid box greatly improves the receiver's frequency stability. Were the front panel allowed to move around, the received frequency might shift when the radio controls are varied. A vernier dial and a 10-turn potentiometer are used for easy tuning and regeneration control. The metal ground plane of the PC board is connected to the metal enclosure using a single short wire.

Measured Parameters

For these measurements, the test frequency was 125 MHz. The test-generator output was connected directly to the receiver input using a short length of RG-59 cable.

AM Sensitivity: With the QUENCH-WAVEFORM (RQW) control set to 0 Ω, a 1 µV, 30% amplitude-modulated 1-kHz tone was clearly audible. This improved to 0.3 µV with a 100% modulated carrier.

FM Sensitivity: The QUENCH-WAVEFORM (RQW) control was set to 250 Ω (midscale). The test signal was FM modulated by a 1-kHz tone with 5-kHz deviation. At 125 MHz, a 0.7 µV signal was clearly audible. The sensitivity decreased at 160 MHz, but was still better than 2 µV.

Selectivity varied with input signal strength. In the AM mode (RQW set to 0 Ω), selectivity was about 250 kHz with a 2-µV input signal. In the FM mode (RQW set to 500 Ω, 125-MHz carrier, 1-kHz tone, 5-kHz deviation), selectivity was about 15-20 kHz for a 1-µV input signal; 80 kHz with a 5-µV signal and 250 kHz with a 10-µV signal.

Notice that these selectivity numbers are valid only if the operator carefully adjusts the regeneration to a level just above oscillation. As regeneration is increased, sensitivity improves while selectivity rapidly decreases. Both sensitivity and selectivity are slightly better (but similar) for the 38-54 MHz receiver.

UHF Reception

To build a receiver for UHF, two approaches may be used. The first is to use a small variable capacitor and a hairpin (single-turn) coil. Place these and the detector, along with the RF stage, on a small fiberglass board mounted several inches above the ground plane. Be careful to place the board far away from any metal object. The detector should also use a series LC circuit to extend the frequency range as high as possible.

A far easier approach that works quite well uses a UHF varactor tuner as a down-converter feeding a VHF receiver that functions as a tunable IF amplifier and detector. This is shown in Fig 15. UHF tuners may be salvaged from old VCRs and TV sets; they may often be purchased from mail-order electronics suppliers, as well.

These tuners operate over a range of approximately 450-910 MHz and have a broadband, 47-MHz output. This can be connected to the input of the 38-54 MHz receiver circuit of Fig 9, or any NBFM receiver covering that frequency range. The receiver then tunes the IF output of the converter. Since the UHF tuner has an output wider than 6 MHz, the actual tuning range will be many megahertz above and below the UHF tuner's range. Therefore, this arrangement lets you tune the amateur 70-cm band plus many police and other local stations at the low (450-MHz) end of the tuner's range. You can also receive the amateur 33-cm band and many other interesting stations at the 900-MHz end of the tuner's range. For best results, be sure that the +30-V tuning voltage is steady and does not drift with temperature.

Construction Guidelines

In building any of the receivers featured in this article, I highly recommend using FAR Circuits' PC board.[7] It has a metal ground plane on one side and it uses a very tight layout, with short, direct interconnections between components. This is essential for stable operation at VHF. Their board was designed for the two-band receiver circuit of Fig 13, but it can easily be used to build the circuits of Figs 9 and 12, as well. For these circuits, simply either omit the unused components or run short jumper wires on the board to complete the appropriate circuit.

When using the FAR Circuits board, it is *very* important to solder *all* ground leads to both the top and bottom of the PC board. This ensures that the ground plane on the top of the board is directly connected to the ground connections on the bottom. As each component with a ground connection is wired into the board, be sure to solder its ground connection to both sides of the board.

If you plan to use a hand-wired board, it is essential that all wiring around Q1 and Q2 is very compact, to minimize lead length and stray capacitance. Stray circuit capacitances and multiple ground paths can prevent the detector from oscillating. All wiring should use the shortest leads possible. It is also

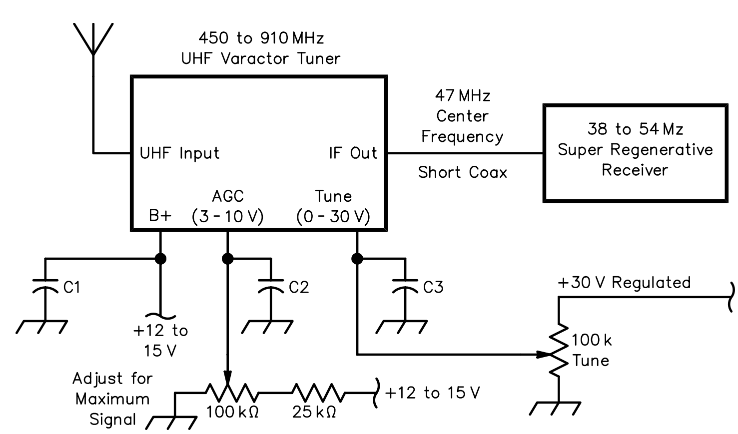

Fig 15—440 to 917 MHz reception using a UHF varactor tuner with a super-regen receiver.

vitally important that the super-regen detector's tuning coil be physically distant from other conductive objects—particularly chassis ground, the bottom and sides of the equipment box (if it is metal) and any shielding. If the coil were located too close to another object, loading would result, reducing the coil's Q and ruining the receiver's selectivity. Excessive loading can also prevent the detector from oscillating over part, or all, of its tuning range.

Be sure to locate the drains of JFETs Q1 and Q2 close together, allowing about one-quarter inch of space between them to install the gimmick capacitor. The main tuning coil should be wound using a piece of #14 AWG solid-copper wire—such as one wire from a one-foot length of #14/2 NM sheathed cable (Romex house wiring). Wind the coil around a standard wooden pencil, then slide the coil off the pencil and solder it into the PC board. Be sure to leave a 3/4-inch lead on each end of the coil to support it above the PC board.

These receivers may be mounted in small metal boxes, but always build the circuit and test it before placing it in the box. I find it best to mount the tuning capacitor directly on the circuit-board ground plane, then pass its shaft through an over-sized hole in the metal panel. When the capacitor is mounted directly to the panel, a ground loop is formed, and the detector usually fails to oscillate. The FAR Circuits PC board has a large section of ground plane to hold the tuning capacitor.

Mount all the other controls to the panel and connect them to the board with shielded cable. Connect only one end of the shield to ground and run a separate ground wire between the control and the PC board ground. This will help prevent ground loops.

Always build receiver circuits backwards: Start with the audio stage and wire the components from the speaker to the **VOLUME** control. Test this stage by advancing the control to midrange and touching the wiper: This should cause a buzz in the speaker. If the audio stage is not working, recheck its wiring. Measure the supply voltage and see that the voltage on pin 5 of the LM386 is half of the supply voltage. Be sure that bypass capacitors C14 and C15 are located close to pin 6 of the LM386; otherwise, the inductance of the wiring can isolate this pin from the bypassing and cause motor-boating (low-frequency oscillations).

After the audio stage is working, wire the detector and RF stage, but leave out gimmick capacitor C2. Set the **QUENCH-WAVEFORM** (**R_{QW}**) control (R6) to mid-range and advance the **REGEN** control (R3) most of the way. Adjust the **QUENCH FREQUENCY** (R5b) and **REGEN** controls until oscillation occurs. You should hear a loud rushing noise, which indicates super-regeneration. If your receiver includes the super-regen squelch circuit, switch the squelch circuit off during the initial testing.

In almost every case, the detector should oscillate strongly with C4 soldered to the center of tuning coil L2; some layouts may require this tap to be moved either side of center, however. Check that the detector oscillates over the entire tuning range. You may need to readjust R3 and R5b to keep the detector oscillating. If there are any holes in the tuning range (where oscillation stops), try moving L2 and L3 farther away from any surrounding objects. Next, install the gimmick capacitor.

Start by twisting a few turns, then check again that the receiver oscillates over its entire tuning range. Keep twisting the gimmick as much as you can without stopping the detector's oscillations. Then do a final oscillation check with a VHF antenna connected to the input jack.

Miscellaneous

For optimum performance from these receivers, use fresh batteries: Older batteries can have a high series resistance that changes the shape of the quench waveform. Two parallel-connected 9-V batteries are fine for portable operation. This provides a lower impedance than a single battery. Two series-connected 6-V lantern batteries will operate one of these receivers for many months under normal use, and you can often find twin-packs of these batteries for less than $10.

You can easily reduce the tuning range of these receivers to cover a single ham band by adding a couple of mica capacitors to the circuit: Add one in series with C3 and another in parallel with it. Experiment with their values until you achieve the desired band of frequencies. Similarly, the turns of L2 can be compressed or expanded—or turns can be added or removed—to raise or lower the entire tuning range.

Tuning the Receivers

For best performance, super-regen sets should have their regeneration levels reset each time their frequency is changed. In these receivers, the **REGEN** control changes the voltage that powers the detector. Higher detector voltages yield greater *sensitivity*, but reduce *selectivity*. In these self-quenched circuits, the **REGEN** control also affects the quench frequency. The **QUENCH-WAVEFORM** (**R_{QW}**) and **QUENCH-FREQUENCY** controls should both be adjusted for best NBFM reception. As a rule, the regeneration level should be kept fairly high on the 88-108 MHz FM broadcast band (wide-band FM mode) with **R_{QW}** set to 0 Ω. When listening to music, the **REGEN** level should be carefully adjusted for minimum distortion. On the 118-136 MHz aircraft band (AM mode), again set the **REGEN** level high and **R_{QW}** at 0 Ω. Tune-in a station, such as an air-traffic control tower; switch on the squelch and adjust its level so that the no-signal background noise is just muted.

When listening to stations on the 2-meter ham band (NBFM mode), increase **R_{QW}** to about midrange and set **REGEN** fairly high. After tuning in a station, reduce the **REGEN** setting until the audio level increases dramatically. Then retune the receiver and re-adjust the **REGEN** control for best reception. Operationally, **R_{QW}** creates a narrow-band window between the point where the detector squeals (**REGEN** level is too low) and the point where the NBFM audio level drops off rapidly (**REGEN** level too high). Increasing **R_{QW}** widens this region, but if too much resistance is used, the selectivity appears to become too great (attenuating the higher audio frequencies) and speech becomes difficult to understand. In general, **R_{QW}** needs to be advanced (more resistance) when receiving very strong signals. Adjusting the **QUENCH-FREQUENCY** control is also helpful in receiving weak NBFM stations.

Future Experimentation

I invite all radio amateurs to join with me in exploring this very exciting technology. Even today, there still remains a great deal that is unknown (or misunderstood) about super-regen circuits. For example, a superhet receiver with a whip antenna becomes much more sensitive when you place an operating super-regen next to it. Many of the basic circuit techniques outlined in this article could be used to develop easy-to-build experimental receivers at UHF or even microwave frequencies.

Other squelch methods are possible. Nat Bradley's method[8,9] amplifies the small change in dc bias of a JFET super-regen detector's source voltage that occurs between signal and no-signal conditions. This can be used to gate a JFET on and off, squelching the audio during no-signal conditions.

Since a super-regen detector's quenching oscillations contain the same modulation present in the received RF carrier, many new circuits could be developed that amplify, control or demodulate the quench frequency. In other words, the quench frequency could be processed in the same way as the IF of a superhet receiver. A true FM-discriminator or a PLL could possibly be used to demodulate the quench frequency and recover NBFM.

Acknowledgments

I would like to express my deepest thanks to David Quinn and Chuck Ayres for helping me with my super-regen and regenerative designs. My appreciation also to Mike Murphy, WB2UID, for his pioneering work on an early version of the super-regen squelch circuit.

Charles (Chuck) Kitchin, N1TEV is a hardware applications engineer at Analog Devices' Semiconductor division in Wilmington, Massachusetts. His main responsibilities include writing technical publications and developing new applications circuits. He has published over 60 technical articles, three books and a large number of application notes.

Chuck graduated with an ASET from Wentworth Institute in Boston. Afterwards, he continued studying electrical engineering at the University of Lowell's evening division. Chuck has been an avid radio builder and shortwave listener since childhood and a licensed radio amateur (General) for six years. His other hobbies include astronomy and oil painting.

References

[1]E. H. Armstrong, "Some Recent Developments in the Audion Receiver," *Proceedings of the Institute of Radio Engineers (IRE)* Vol 3, Number 4, September 1915, pp 215-247.

[2]E. H. Armstrong, "Some Recent Developments of Regenerative Circuits," *Proceedings of the Institute of Radio Engineers (IRE)* Vol 10, Number 4, August 1922, pp 244-260.

[3]H. Ataka, "On Super-Regeneration of an Ultra Short Wave Receiver," *Proceedings of the Institute of Radio Engineers (IRE)* Vol 23, Number 8, August 1935, pp 841-884.

[4]C. Kitchin, N1TEV, "Super-Regeneration: the Lost Technology," *Communications Quarterly*, Fall 1994, pp 27-40.

[5]J. Santangelo, "Coaxial-Line VHF Receivers," *QST*, March 1948, pp 20-23. Chambers, C. V., "A Coaxial-Line Receiver for 220 and 235 MHz," *QST*, June 1948, pp 25-28.

[6]D. DeMaw, W1FB, "Updating the 6 Meter Rush Box with an FET Front End", *QST*, July 1967, pp 11-12 and *The 1969 Radio Amateur's Handbook* (Newington, Connecticut: ARRL, 1968), pp 403-404.

[7]A PC board for the circuits of Figs 9, 12 or 13 is available from FAR Circuits for $8.00 each plus $1.50 shipping for up to three boards. There is a group-discount rate of 10% for 10 boards or more. You can contact FAR Circuits at 18N640 Field Ct, Dundee, IL, 60118-9269; tel 847-836-9148 (voice and fax); e-mail **Farcir@ais.net**; URL **http://www.cl.ais.net/~farcir/**.

[8]N. Bradley, ZL3VN, "Taming the Super Regenerative Detector," *Break-in Magazine*, November 1978, pp 410-415.

[9]N. Bradley, ZL3VN, "As Much for Even Less," *Break-in Magazine*, May 1979, pp 158-163.

Further Reading

C. Kitchin, N1TEV, "High Performance Regenerative Receiver Design," *QEX*, Nov/Dec 1998, pp 24-36.

C. Kitchin, N1TEV, "An Ultra Simple Receiver For 6 Meters," *QST*, Dec 1997, pp 39-41.

C. Kitchin, N1TEV, "Regenerative Receivers: Past And Present," *Communications Quarterly,* Fall 1995, pp 7-26.

A Simple UHF Remote Control System: Pt 2

Besides using a garage door opener to remotely key your rig, you can also use it to listen to your favorite SSB net while you have coffee on the patio.

By Sam Ulbing, N4UAU

In the previous issue of *QEX* (pp 32-39), I used a pair of Linx modules to assemble a remote CW keyer that allows some freedom of movement around the ham shack. I also noted that part of my busy mornings include listening to SSB and having coffee with my wife. She finds the patio more comfortable than the shack for her morning coffee, so I needed a way to listen to SSB while on the patio.

In Part 1, I noted that amateurs have many more privileges in the 440-MHz band than do commercial makers of unlicensed products. Table 1 shows some of the differences. Obviously, my remote keyer would have been illegal under unlicensed rules. So, too, would this Part 2 project, which makes use of voice transmission.

Fortunately, Linx also makes a set of modules (RM modules) that let me solve this problem. These modules, like those in Part 1, are recommended for applications such as garage door openers, remote control and protection alarms. The main difference is that these devices are designed to allow FSK data transmission (see Table 2). An FSK transmitter is a voltage-controlled, FM unit. When the modulation bandwidth is large enough and linear in nature, such a transmitter may be used for voice transmissions (a mode that is allowed for amateur use). These modules meet those requirements and, in fact, work very well for voice transmission.[1,2] The datasheet does not mention this use, probably because of the restrictions on unlicensed operation. The datasheet does state, though, that the units are SAW-based, double-conversion superhet FM devices (Fig 1). They are packaged as hybrid SIP modules; this actually makes it easier for the amateur to build.

A Remote Speaker

While these modules are larger, more power-hungry and costlier than those of Part 1, they do let me listen to analog SSB. Before I describe them, it is worth recalling that the modules in Part 1 have a maximum capability of 6000 WPM (5000 bits/sec). This is well above the speed that most hams

5200 NW 43rd St, Ste 102-177
Gainesville, FL 32606
n4uau@arrl.net
URL: http://n4uautoo.home.sprynet.com

[1]Notes appear on page 40.

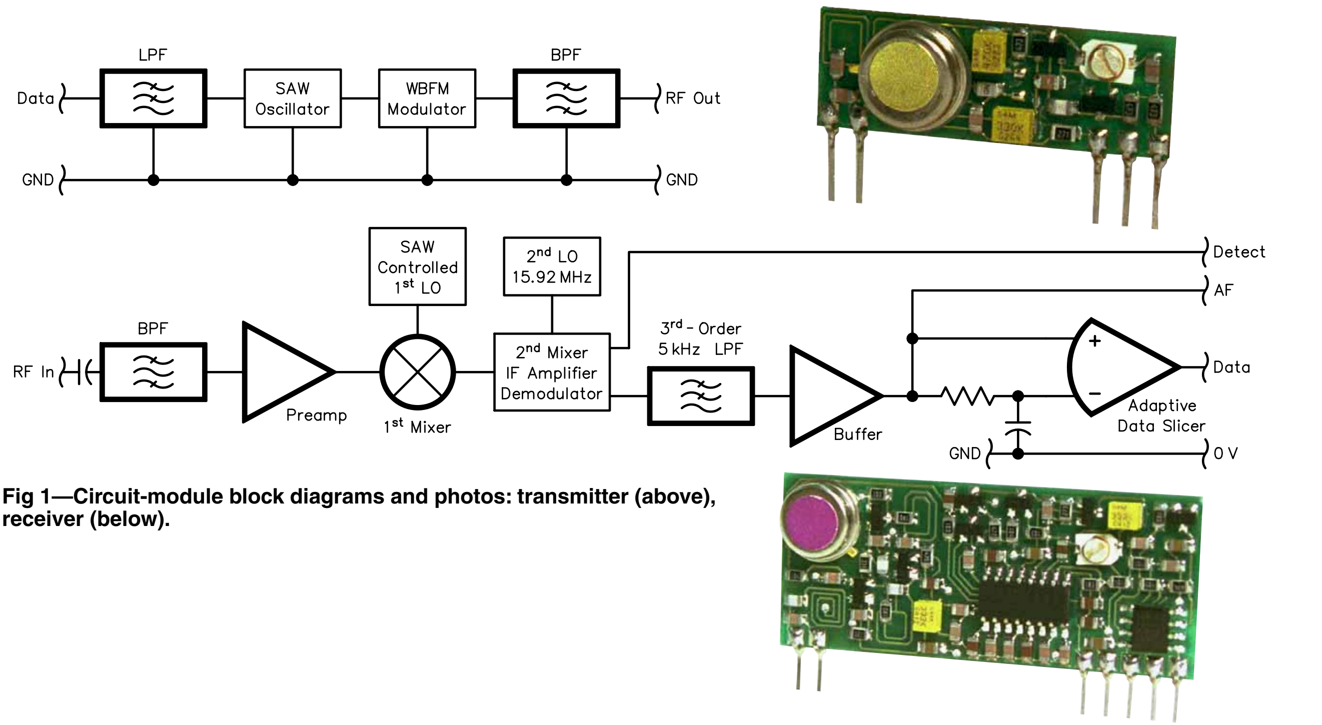

Fig 1—Circuit-module block diagrams and photos: transmitter (above), receiver (below).

speak. So why can't I use those modules for this project? The problem arises from the "obsolete" nature of the SSB transmissions; they are analog, not digital signals. (How do you like your new digital cell phone? They are so clear and noise-free! While the rest of the communications world is going digital, most hams still communicate via noisy, inefficient analog modes.)

Just as in Part 1, there were a lot of design considerations in making these circuits, but none of them required me to know anything about how a double-conversion superhet circuit works. Fig 2 shows the receiver and Fig 3 shows the transmitter for this project. A design goal for the receiver was to make it as small as possible; it fits into my shirt pocket and with a pair of headphones (or a single earpiece) it is quite unobtrusive. A design goal for the transmitter was a strong radiated signal. Since it is located in the shack, though, power consumption and size were only secondary considerations. This is the reverse of the design goals for the remote keyer, which was constrained to a small transmitter but allowed a larger receiver.

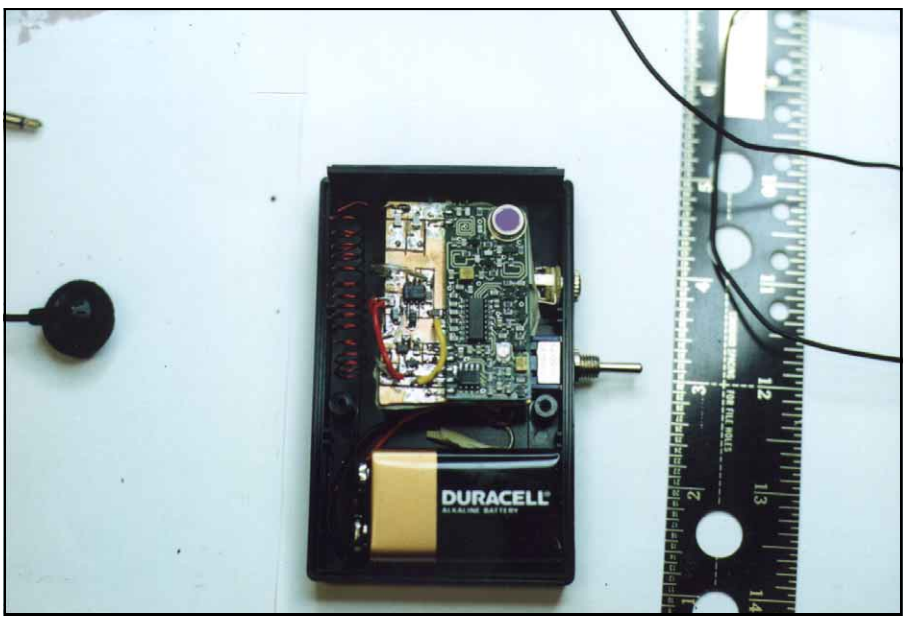

Fig 2—The audio receiver in its case. Notice the helical antenna inside the box (upper left). The text describes an antenna with better performance.

Transmitter Details

Fig 4 shows the block diagram of my transmitter. While it would be possible to connect the HF audio output directly to the UHF transmitter, it would not be operating legally because amateur operated transmitters must identify at least every 10 minutes. So my first design consideration was (again) how to program a microprocessor to do that. The software had to send my call sign every 10 minutes and mute the input from the HF rig while doing so; of course, it also had to keep track of the time. Again, while there are a number of ID circuits in the literature, practicality forced me to use the 87C750. Actually, this was not so bad because the '750 has 1k of ROM and the programs I wrote for the three projects all fit in a single microprocessor.

Fig 5 shows the schematic for this project. Pin 23 of U2 selects the program and, for the ID program, is not connected to ground. The ID speed is set at 20 WPM. The crystal is again a color-burst type. There are two outputs: Pin 4 goes high when it is time to ID and is used to mute the input from the HF rig; Pin 5 outputs my call sign in CW.

A multiplexer, U3, switches the input of the UHF transmitter between the HF audio and the ID input. Pins 9, 10 and 11 of U3 form a binary address to select which of eight input pins is connected to the multiplexer output at pin 3. Since I only have two inputs, I grounded pins 9 and 11. The high or low status of pin 10 selects between the input at pin 15 (the HF audio signal) and pin 13 (the ID from the '750). The output of U3 is routed to the transmitter. Because I use a single-sided power supply, the input to the multiplexer cannot go below 0 V. R1 and R2 bias the audio to 2.5 V to ensure that the input signal stays positive.

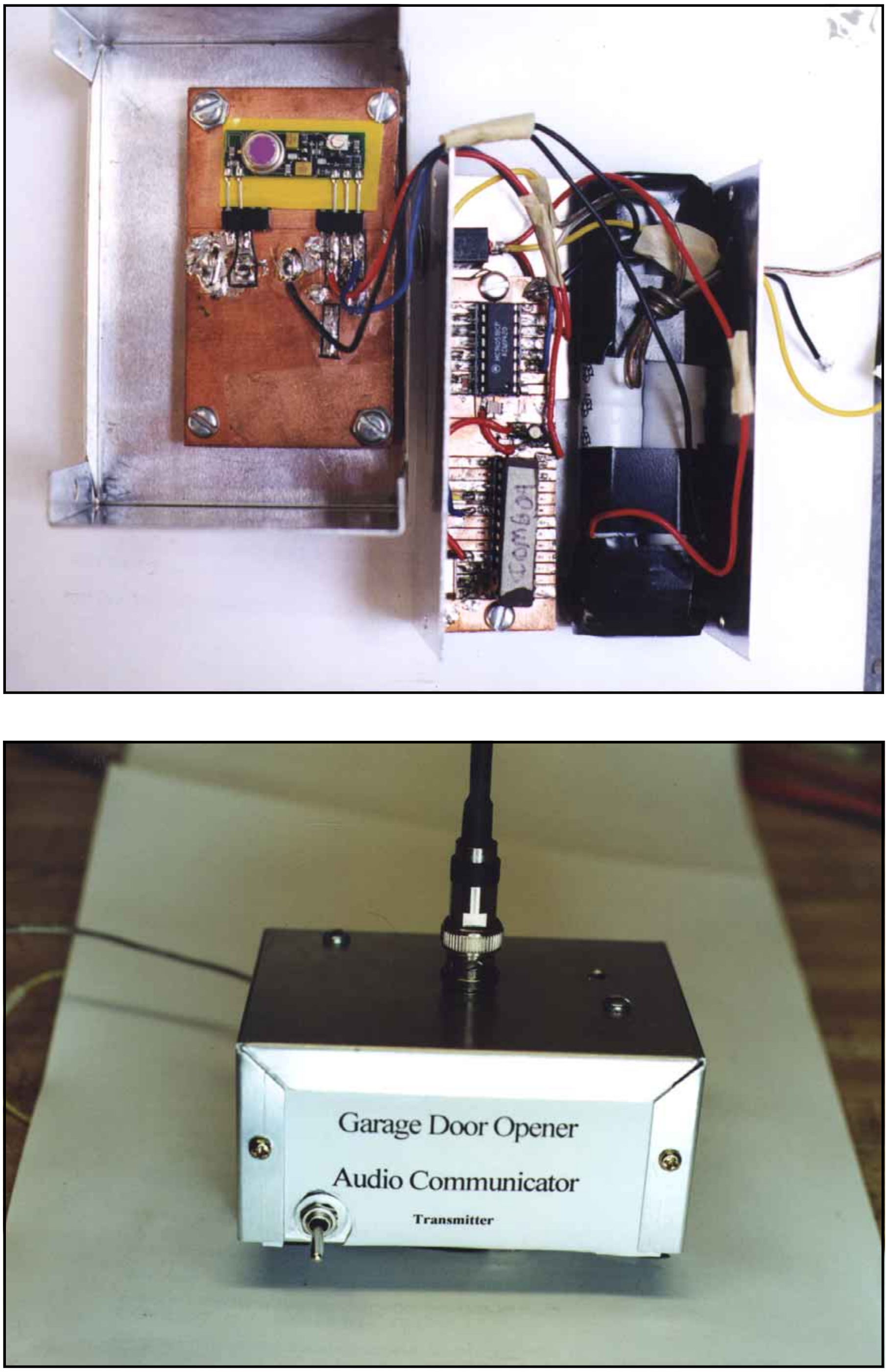

Fig 3—The audio garage door opener. Above, the transmitter module is on its own board and inserted into halves of a DIP socket (upper left center). The microprocessor and multiplexer are DIP ICs surface mounted to a copper-clad board (right center). Four NiCds are in a dark bundle to the right. Below is the finished product with a BNC connector and commercially made $\lambda/4$ antenna. The BNC allows for future antenna experiments.

Receiver Section

The circuit for the SSB receiver is a bit more complex (Figs 6 and 7), but it did not require any microprocessor design. In the block diagram, notice the mute (or squelch) block. It is possible to connect the receiver directly to an audio amplifier; but whenever the receiver circuit is on, it will try to demodulate a signal. If there is no transmitter signal, the receiver hunts to find one. The result is the familiar background noise you get when the squelch is open on your HT.[3] The Linx receiver module has a *detect* output pin that indicates when no transmit signal is present. It can drive a signal-strength indicator, which can be very useful for testing antennas (see below).

The *detect* output from U1 is an analog voltage that is 0.8 V below Vcc when no signal is present and 0.4 V below Vcc when a maximum-strength signal is detected. U2 is a comparator. The *detect* signal is fed to pin 4 of U2. A reference voltage of one diode drop (about 0.6 V) below Vcc is fed to pin 3. With no RF input, the pin-4 voltage is lower than the reference, and the output of the comparator is high. This output goes to the *shutdown* pin of the audio amplifier (U3, pin 1). When the voltage at this pin is high, the amplifier turns off, eliminating the hiss and reducing power consumption—an important consideration for this portable design.

The gain of U3, an LM4861, is set by R3 and R2 at about six. It would be possible to make one of the resistors a potentiometer to adjust the output volume, but I wanted to keep the circuit simple. I set the audio level by adjusting the volume of the HF rig. U3 will drive either headphones or a small speaker.[4]

When I made my prototype unit, I

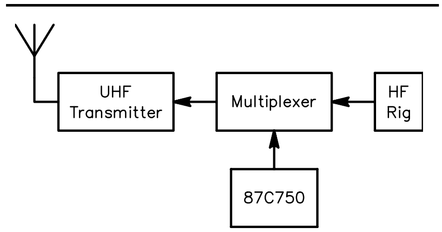

Fig 4—Transmitter block diagram.

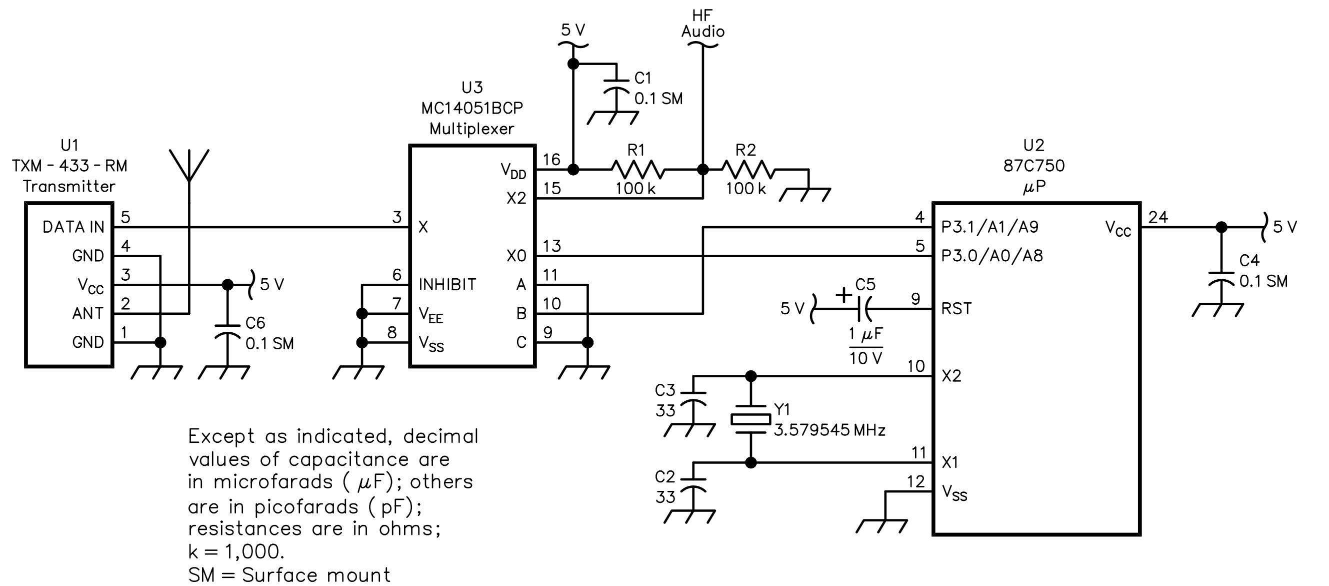

Fig 5—Transmitter schematic.

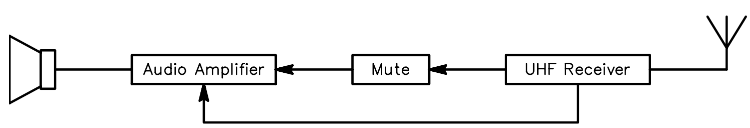

Fig 6—Receiver block diagram.

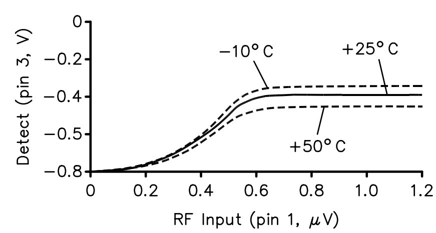

Fig 8—*Detect*-pin output (V) versus received signal strength (μV).

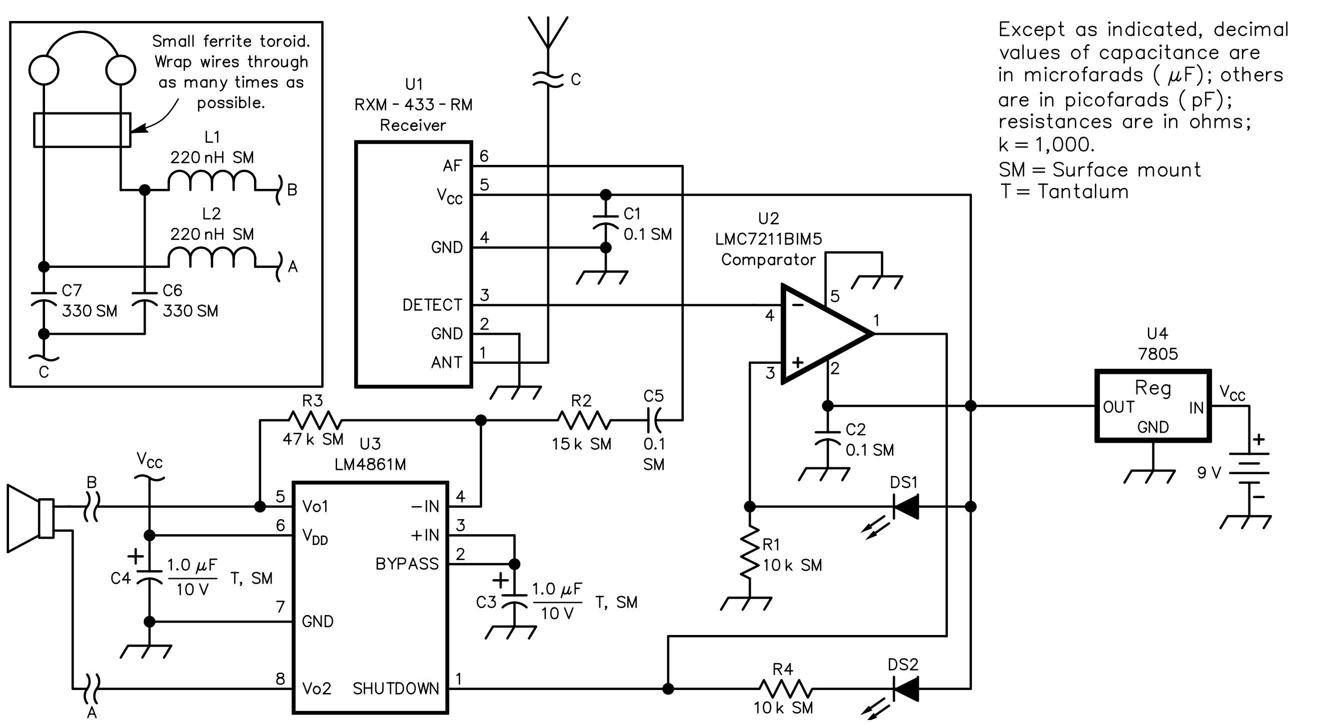

Fig 7—Receiver schematic.

splurged with power usage. I wanted to know if I was getting a signal from the transmitter, so I added a resistor and an LED to U2 pin 1; the LED lights when a signal is detected.

Building the Circuits

Building the transmitter is straightforward, as all the parts are in DIPs or SIPs. I used my PC-board-making method on a piece of double-sided board and soldered the transmitter SIP to the PC board. A bit of electrical tape ensures that the backside of the SIP is insulated from ground. Don't overheat the leads when soldering or internal connections are apt to come unsoldered. If you want, use one side of a DIP socket to mount the SIP.[5] That is bulkier but allows you to easily remove the SIP. I found that a standard SIP socket did *not* work, as the pin geometry is different. Notice in the photos that I put the transmitter module on a different board from the rest of the circuit. To allow antenna experimenting, I used a BNC antenna connector and an aluminum box to increase the ground-plane area.

To package the receiver, I used a plastic box with a 9-V battery compartment (see Fig 2). I trimmed the leads on the receiver SIP a little—to save space—and soldered it to the board. The rest of the parts are surface-mount (SM) devices because of their small size, low power and low voltage usage.

There is another reason for using SM parts: Recall that U2 is a comparator that determines when the input voltage is more or less than 0.6 V below Vcc. This requires the use of a "rail-to-rail" comparator. If you look at the specifications for commonly used comparators like the LM339, you will see that its input common-mode voltage extends only to Vcc – 2.0 V. That means when the input voltages are within 2 V of Vcc, the comparator will not work correctly. The only rail-to-rail comparators I know of are SM devices. Building the receiver is straightforward using SM construction, and if you did the

Antenna Technology Advances

I recently checked out the Linx Web page again to see what was new and discovered that UHF antenna technology is evidently advancing quite rapidly in the commercial area. Linx is announcing several small antennas. One that seems particularly interesting to me is their "Splatch" antenna shown here. Linx modestly calls it a "breakthrough in compact antenna technology" and judging by the size, I agree if it performs as well as they claim. Because it is a proprietary design, not much is said about it but I did find this in the data sheet.

> "This low-cost antenna utilizes a proprietary grounded-line technique to extract outstanding performance from a tiny surface-mount element. Unlike many compact antennas, the "Splatch" is highly immune to proximity effects, making it ideally suited to hand-held applications such as remote controls, pagers, and alert devices. The stable grounded-line design allows excellent performance to be obtained even by engineers lacking previous RF experience. The antenna's SMD package is appropriate for reflow or hand attachment. The antenna measures 1.1×0.5×0.062 inches (LWH) and exhibits a 50-ohm characteristic impedance and a VSWR of less than 1.9."

I hope to try out this little antenna soon to see how good it really is. I keep wondering why I learned about this antenna in the commercial literature rather than amateur literature. Unlike ICs, I should think that antenna manufacture is still suited for amateur design. Are we ignoring the UHF bands and letting our technological skills rust?—*Sam Ulbing, N4UAU*

Table 1—Privileges and Restrictions for Unlicensed Users versus Hams in the 440 MHz Band

	Unlicensed Operation	*Amateur Operation*
Power	Field Strength < 10,500 µV/m 3 meters from antenna	1.5 kW output
Allowed Transmissions	Control signals, commands, ID codes, radio control only during emergency	Any mode not expressly prohibited by Part 97
Duration of transmissions	Must not transmit continuously. Rules typically require that the silent period between brief transmissions be at least 30 times the transmission period.	No limit
Antenna	Must be either permanently attached or utilize a unique and proprietary connector to prevent the end user from changing the performance of the unit (App Note 00500)	No limit
Identification	None	Call sign at least every 10 minutes as specified in rules

Note: The FCC Part 15 rules that authorize periodic emitters are complex, with various permitted field strengths for different types of operation. For a good description of Part 15 rules of interest to Amateur Radio operators, see **http://www.arrl.org/tis/info/part15.html**.

projects in my *QST* SM article series,[6] you should have no problem with it. If you didn't, I suggest you review that series and try a few of the easier projects first.

For my remote receiver, I experimented with two antennas. One was a helical (a short, coiled whip—like a "rubber duck"—*Ed.*) antenna laid along side the circuit board inside the box (Fig 2). This is certainly a very neat arrangement—the kind of thing that garage-door-opener sender units use. The antenna worked well enough that I could listen to HF around my house, but as I moved around, I noticed many nulls where the signal would drop out. I also tried a vertical antenna built right into the headphone wires. This required a small modification to the circuit, which is shown in the inset of Fig 7. This antenna works a lot better than the helical antenna and I can copy the HF rig even while standing in the street in front of my house. There were only a few null points where the signal dropped out; these were probably caused by multipath effects. UHF antennas offer many experimental opportunities for the Amateur Radio operator because of their relatively small size.

Module Specifics

Linx datasheets tend to be a bit vague on many specifics, but here is a summary of some of the important points. The RM series devices are physically larger and more powerful than the LC series. The datasheets indicate ranges over 500 feet are possible. My first simple prototype consisted of a transmitter and receiver, each mounted on a 6×3-inch ground plane. With the transmitter on a table in the living room, I took the receiver a block down the street and around a corner before I got deterioration in the audio. I wonder what distance I could get if I hooked the transmitter to a five-element Yagi or 10-dB corner reflector.

Input voltage range is specified as 3.9 to 9 V for both the receiver and transmitter. At 6 V, the transmitter draws 6 mA, rising to 10 mA at 9 V. The receiver draws 11 to 17 mA depending on its voltage. It works well with both my 5-V power supply and four series connected NiCds.

Modulation bandwidth is specified as 0 to 10 kHz, although it appears that linearity drops off a bit at the limits. This is perfect for voice communications with a 3 or 4 kHz maximum deviation. Be aware that the Linx modules are not reverse-polarity protected: A protection diode

Table 2—LC versus RM Module Characteristics

Feature	*LC Modules*	*RM Modules*
Power*	–4 to +4 dBm (nominal –1 dBm)	10,000 µV/m at 6.00 Vcc and a loop antenna at 3 meters
Mode	On-Off	Voltage Controlled oscillator, FM
Max Data Rate	5000 bps	10,000 bps
Vcc	2.7 to 5.5	3.9 to 9
I max Xmtr	6 mA	17 mA
I max Rcvr	8 mA	17 mA
Size	About: 0.8" by 0.6" Rcvr 0.5" by 0.4" Xmtr	About: 1.8" by 0.8" Rcvr 1.2" by 0.4" Xmtr

*per Linx App Note 00125: The legal unlicensed field strength at 440 MHz is about 10,500 µV/m at 3 m; but most transmitter modules, including those manufactured by Linx, have an output level that is sufficient to produce a radiated RF level that is non-compliant. It is purposefully set high to allow the use of low-profile, inefficient antenna styles. The use of attenuation pads is otherwise recommended to meet compliance limits.

Table 3—Notes Regarding Small Antennas shown in Fig 9

Fig	*Name*	*Relative Gain (dB)*	*Notes*
A	Standard Whip	0	Best if ground plane is λ/4-radius circle Best if element perpendicular to ground plane
B	RFM Loaded Whip	–3	Shortened antenna on a small ground plane Performance nearly equal to Standard Whip
C	Helical	–18	Coil is 14 turns of #22 AWG
D	Helical	–5.5	Alternate orientation of Fig 9D
E	Spiral	–10	Wire length is a little shorter than λ/4 Requires no ground plane Start with 19-mm-square area and coil wire into it; trim to resonance Gain and impedance depend on ground-plane size, that shown is small
F	Short Printed Stub	–13	Impedance ≈ 10 Ω as shown (stub near ground plane) Hand effects will increase impedance, if it's hand-held Wide traces reduce resistive losses A longer trace and less inductance improve performance if not near conductive objects
G	Loop	–18	Larger loops yield more gain
H	Semi-Loop	–15	End is capacitively coupled to transmitter Tuning not critical Hand effects improve performance Group electronics and battery in center ground area
I	Folded Dipole	0	Relatively high gain Board thickness and dielectric constant affect resonance Impedance (≈ 50 Ω)

is recommended in the power source. Apparently, the data input wants to be dc biased at Vcc/2, as the frequency-shift graph shows no deviation at midpoint bias. I have also used the modules with no dc bias, and they appear to work that way as well.

There are three outputs for the receiver. The audio output is dc-coupled to the demodulator, so be sure to use a dc-blocking capacitor in line. A second output is an internal data

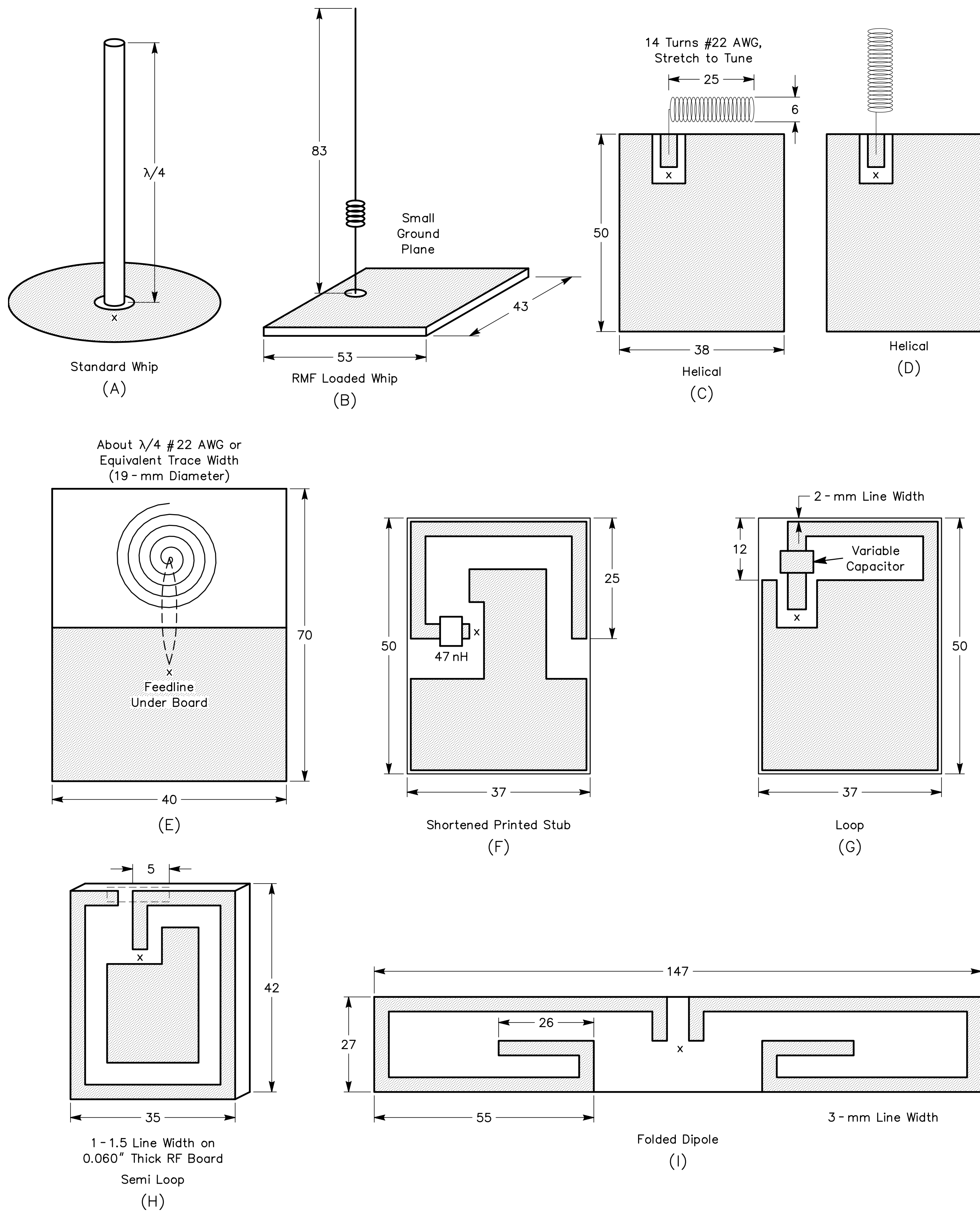

Fig 9—Several antenna configurations described in RFM Application Note AN36 "Antennas for Low Power Applications" (see Note 8 and Table 3). For all antennas shown: f_0 = 433.9 MHz and measurements are in millimeters.

slicer, normally used to drive a digital decoder. I left it unconnected for this project, but for those who want to try a digital FSK wireless link, it is available. The third output is the *detect* output. It is the output I used to trigger my mute circuit. It can do more: Fig 8 shows the *detect* voltage (with respect to Vcc) as a function of the RF input voltage. Using a voltmeter connected between the *detect* and Vcc, you get a signal-strength meter. This can be a very handy feature if you want to experiment with antennas.

Some Ideas for Low-Profile Antennas

Antennas have always been a favorite area for experimentation by hams. While there are many positive-gain antennas shown in the ARRL literature—Yagi, phased verticals, corner reflector, Sterba arrays and so forth—I could not find any low-profile, negative-gain antennas. I was able to find some information on this kind of antenna at various Web sites.[7] If you want to experiment in this area, that is a place to start. (For a late minute news flash see the sidebar "Antenna Technology Advances.") By using a low-gain, low-profile remote antenna and a larger, high-gain antenna at the transmitter in the shack, a positive gain figure can be achieved overall, while still having a small remote unit. Keep in mind that range is proportional to the field strength, hence to the square root of the antenna power gain. Thus, while a 3-dB increase doubles the power, you need a 6-dB change to double the range.

The Linx Technology datasheets describe three basic kinds of antennas: whips (or vertical), helicals and loops. RF Monolithics gives some specific examples and the measured results of their prototypes.[8] Fig 9 and Table 3 show a few of them. Below is a summary of their attributes.

Whips

- Exceptional performance
- Easy to build
- Size can be reduced with base loading
- Size is relatively large
- Easily detuned by nearby objects, especially at the hot end
- Length: about 6-inches (150 mm) at 433.9 MHz
- Range possible with LC modules: > 300 ft
- Impedance: 35 Ω when vertical, 20 Ω if angled at 45°, 10 Ω if horizontal over ground plane. This yields an SWR of 5:1 and a 2.6-dB loss.

Helicals

- Good efficiency for the small size
- Good choice for concealed internal antenna
- Placement very important due to detuning by close objects
- High Q, spacing of coils has major impact on performance
- Some directional effects.
- Range possible with LC modules: 200 ft

Loops

- Excellent immunity to proximity detuning
- Easily concealed
- Difficult to match and tune without expensive equipment
- Untuned, can have very high SWR and may induce harmonics
- Low gain—range possible with LC modules: 100 ft
- Larger loops have better gain
- No ground-plane needed
- Needs a capacitor or inductor to tune
- Omnidirectional

The RF Monolithics application note also shows a magnetic antenna, common for radar uses and some patch antenna designs as well. Their example is only for 900 MHz because they consider them too bulky for the uses they had in mind at lower frequencies. For amateur use, it might be interesting to scale these antennas to the 434-MHz range. The only magnetic antenna I have seen in ham literature was in an ARRL *Antenna Compendium* a few years ago.[9] By providing some articles on the subject, hams with some technical expertise could do much to advance the state of our hobby.

What Next?

The previous projects are one-way communication devices. Next time, I will show a bidirectional CW system I built. With it I can listen to CW on a remote speaker in another room and still send when I hear my call. This circuit has some new design challenges because I wanted to do it all on a single frequency within the ham band. It also required the use of a TR circuit. In the meantime, if you want to experiment with the above-described project, consider hooking it to a voice-recognition chip and your garage-door-opener circuit. You could command it to open with an "Open sesame" and maybe a genie will appear! In any case, don't forget to ID when you use it.

Notes

[1]The bandwidth of these modules is given in the datasheet graph of frequency shift versus modulation voltage as ±25 kHz for a 0 to 10 V modulation. The table of characteristics shows a 3 dB modulation bandwidth of 0 to 10 kHz. Since both far exceed normal voice communication, the module seems a natural for such an amateur application.

[2]Small quantities of Linx parts can be purchased from RF Digital Corp, 2029 Verdugo Blvd # 750, Montrose, CA 91020; tel 818-541-7622, fax 818-541-7644; e-mail **info@rfdigital.com**; URL **http://www.rfdigital.com/**. Notice that this information is different from that published in Part 1.

[3]Of course, if you have the transmitter on whenever the receiver is on, you will not have this problem unless you move beyond the transmitter range. A mute circuit is not absolutely necessary.

[4]For more details on the LM4861 see "SMALL, A Surface Mount Amplifier that's Little and Loud" *QST,* June 1996, pp 41, 42 and 68.

[5]I used a Dremel cutoff tool to slice a DIP socket in half, lengthwise, making it a SIP socket.

[6]"Surface Mount Technology You Can Work with It!" Pt 1 *QST*, Apr 1999, p 33; Pt 2 May, p 48; Pt 3 Jun, p 34; Pt 4 Jul, p 38.

[7]Linx Technology, Inc, 575 SE Ashley Pl, Grants Pass, OR 97526; tel 800-736-6677, fax 541-471-6251; **www.linxtechnologies.com**. RF Monolithics, Dallas, Texas, **www.rfm.com**; Micrel, Inc, 1849 Fortune Dr, San Jose, CA 95131; tel 408-944-0800; **www.micrel.com** are just two companies involved in this area. Both of these sites and the Linx site have a wealth of technical information available as free downloads.

[8]RFM Application Note AN36 "Antennas for Low Power Applications" (by Kent Smith) has a lot of useful information on low profile antennas and is available at **http://www.rfm.com/corp/appdata/antenna.pdf**.

[9]R. E. Prack, K5RP, "Magnetic Radiators-Low Profile Paired Verticals for HF," *The ARRL Antenna Compendium*, Vol 2, (Newington, Connecticut: ARRL, 1989) p 39. Order No 2545, $14. ARRL publications are available from your local ARRL dealer or directly from the ARRL. Check out the full ARRL publications line at **http://www.arrl.org/catalog**.

An Improved Switched-Capacitor Filter

Here's a cure for unwanted harmonic responses in these easy-to-build filters.

By Chen Ping, BA1HAM

When making an audio CW-tone filter or a Doppler direction finder, a sharp band-pass filter is often needed. An active filter employing operational amplifiers may give very good characteristics; however, it requires carefully calculated and very accurate components that are not always readily available. The job may be especially difficult if the center frequency of the passband is to be changed occasionally. In many cases, a switched-capacitor filter (SCF) is a good choice.[1]

A diagram of a typical SCF is shown in Fig 1. Semiconductor switch S1 is driven by clock signals, and sampling capacitors C1-C8 are connected to point A, in turn, at each clock cycle. If the input signal has the same frequency as the clock, each capacitor will be charged to the same voltage during each cycle, via R1. Therefore, point A's waveform will resemble the original signal (see Fig 2). At input frequencies different from the clock's, the capacitors will reach voltages not related to a fixed phase interval of the clock cycle; they will sometimes be positive, sometimes negative in a seemingly random pattern. Voltages reaching point A will be canceled and

[1]M. Kossor, WA2EBY, "A Digital Commutating Filter," *QEX*, May/Jun 1999, pp 3-8.

Chinese Radio Sports Association
No. 9 Tiantan Neidongli
Beijing 100061, China
ba1ham@amsat.org

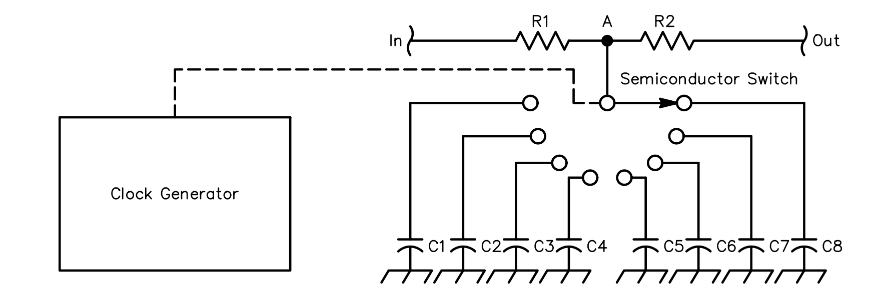

Fig 1—A typical switched-capacitor (commutating) band-pass filter.

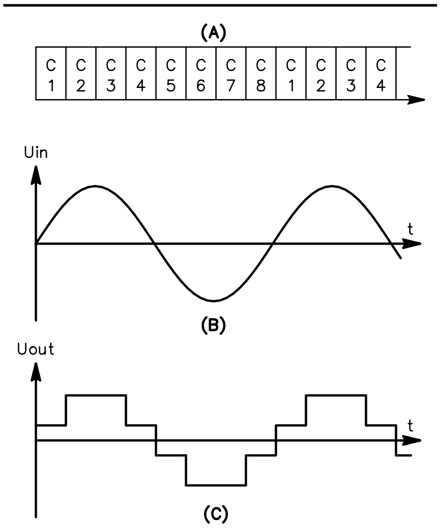

Fig 2—Signals in the SCF of Fig 1. The input signal is a sine wave at the center frequency of the filter. (A) shows the capacitor-selection timing, (B) the input signal and (C) the output signal.

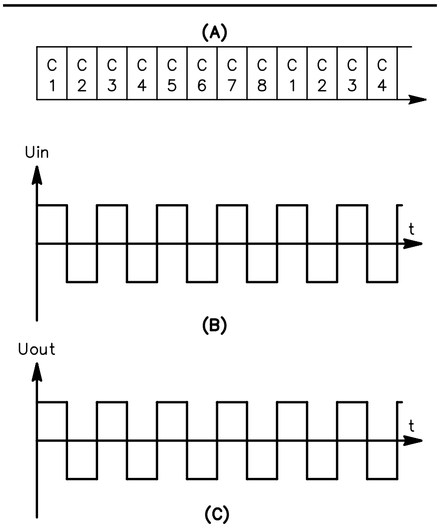

Fig 3—This is the even-order harmonic response of the SCF of Fig 1. The input and output are square waves at four times the center frequency of the filter. (A) shows the capacitor-selection timing, (B) the input signal and (C) the output signal.

the net voltage there will be zero. In this way, only signals harmonically related to the clock frequency are passed: The SCF acts like a resonant band-pass filter. Its center frequency is determined by the clock frequency, which may easily be changed. To make the output signal smooth, no less than four capacitors are normally used. Usually, it is eight or more.

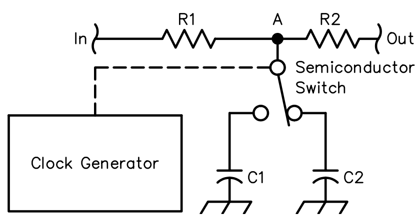

Fig 4—An SCF with two capacitors.

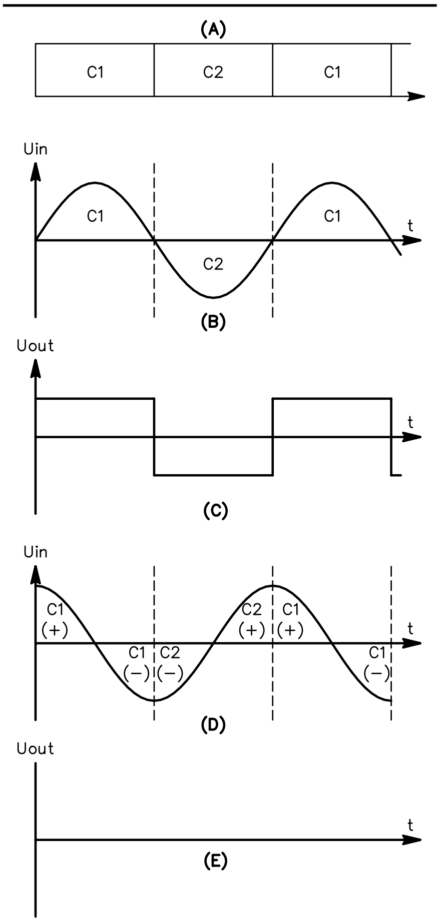

Fig 5—Signals in a two-capacitor SCF. (A) shows the capacitor-selection timing, (B) an input signal in phase with the clock, (C) the output signal for (B) shows that the output is always a square wave. (D) shows an input signal leading the clock by 90°, (E) the output signal for (D) shows that there is no output, phase sensitivity.

This simple SCF circuit, however, has a problem: It suffers from severe harmonic response. As an example, consider the eight-capacitor case. Suppose a signal with a frequency four times that of the center frequency, F_c, appears at the SCF input with a certain phase. C1 is charged by the first positive half cycle, C2 by the first negative half cycle, C3 by the second positive half cycle, and so forth. The result is that a square wave of frequency $4F_c$ will appear at point A. This shows that signals at the clock's fourth harmonic may pass easily through the SCF.

In fact, it can be shown that signals having harmonic numbers equal to any of the integer factors of the number of capacitors may pass. If six capacitors were used, 2nd- and 3rd-harmonic responses would pass; with 16 capacitors, we would see 2nd-, 4th- and 8th-harmonic responses. Using more capacitors may create more undesired responses.

From this, we may surmise that using an odd or prime number of capacitors avoids that situation. Experiment indeed shows that harmonic responses are somewhat reduced in those cases; but usually, it is not very convenient to use an odd number of capacitors. In a typical Doppler direction finder, for example, four or eight antennas are switched to an FM receiver during each

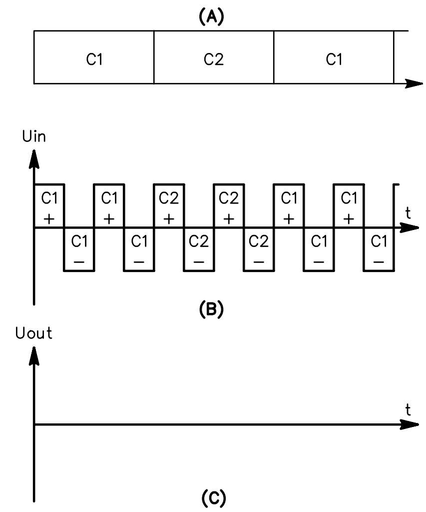

Fig 6—Even-order harmonic response of a two-capacitor SCF. (A) shows the capacitor-selection timing, (B) the input signal and (C) the output signal.

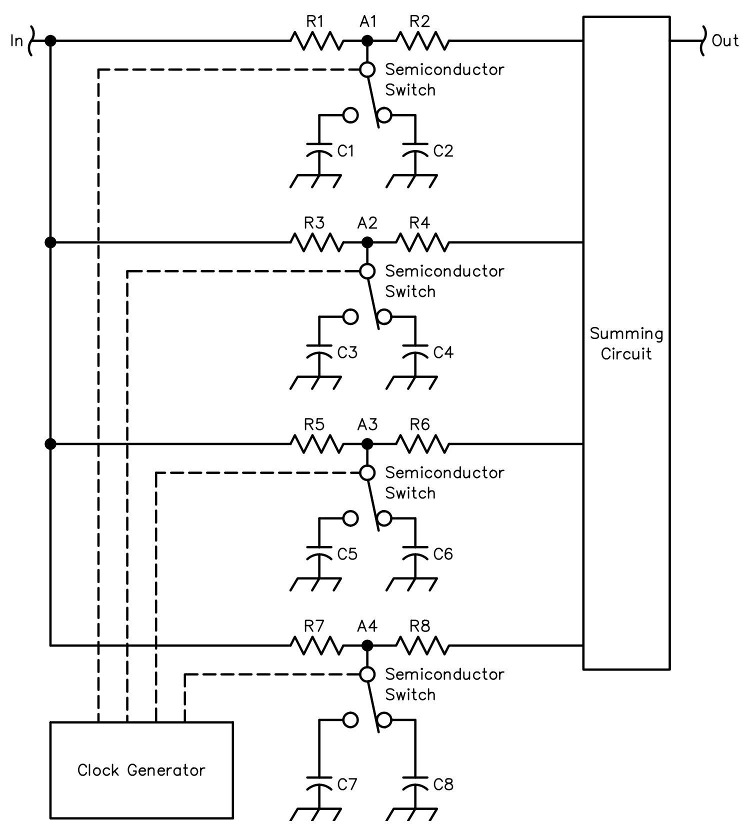

Fig 7—A four-channel, two-capacitor SCF.

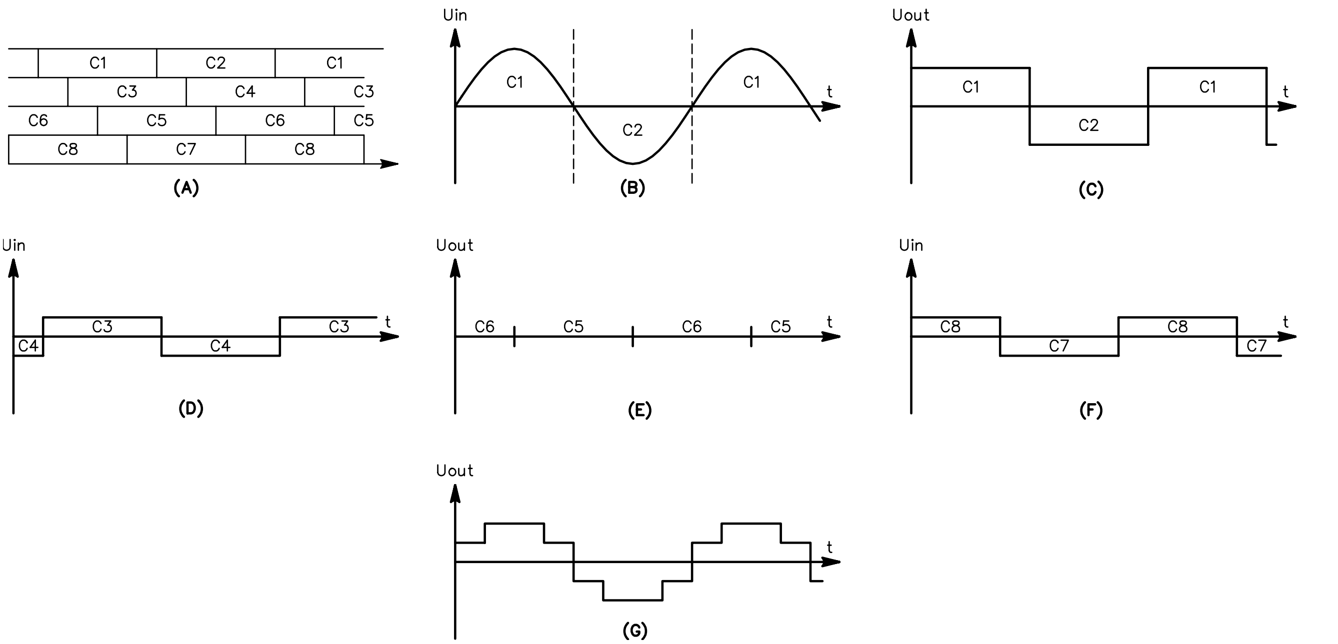

Fig 8—Signals in the filter of Fig 7. (A) shows the capacitor-selection timing, (B) the input signal, (C) the output signal at channel 1, (D) the output signal at channel 2, (E) the output signal at channel 3, (F) the output signal at channel 4 and (G) the output signal.

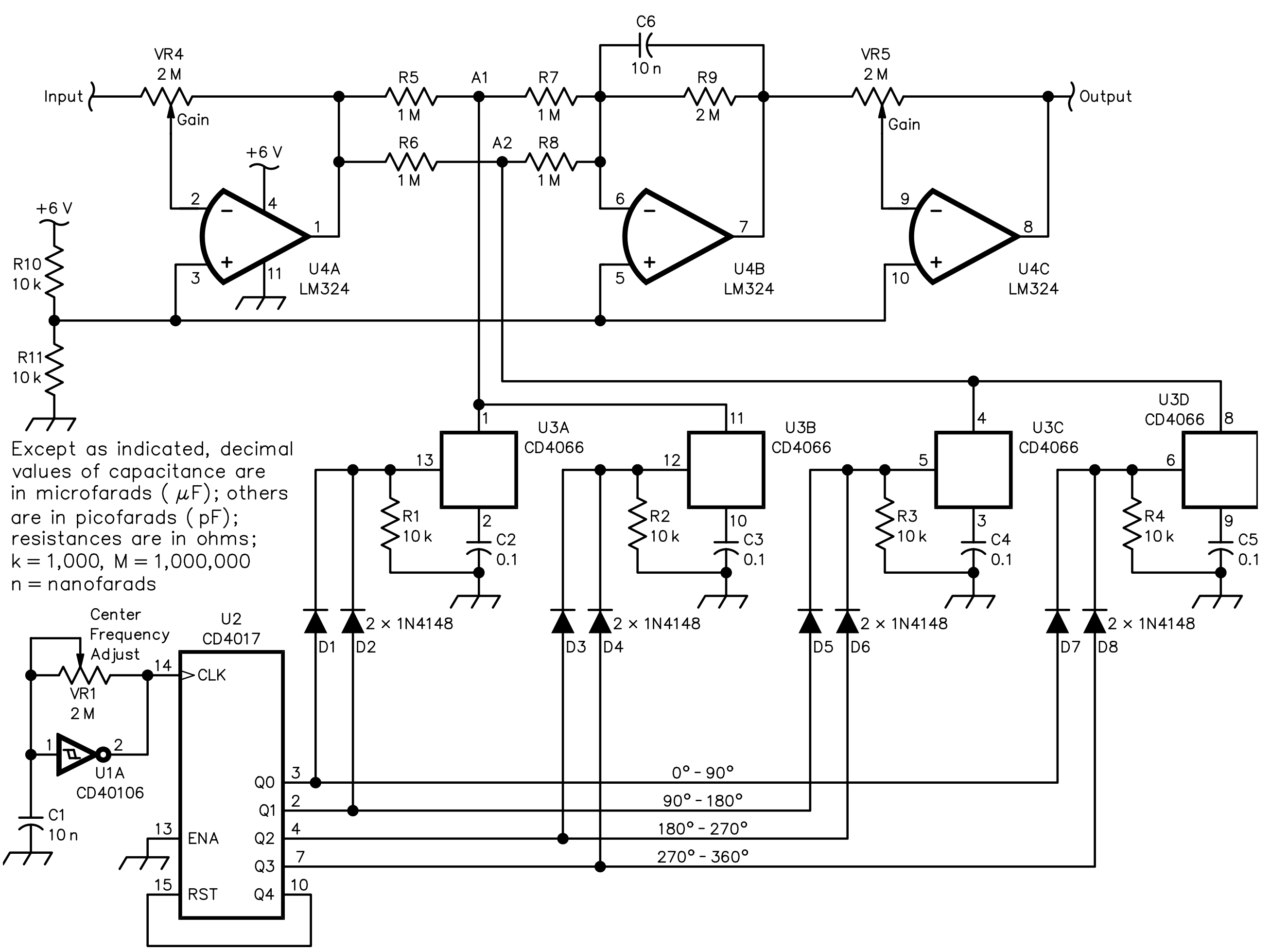

Fig 9—Schematic diagram of a practical two-channel, two-capacitor SCF.

cycle. It is much easier to use the same clock source to drive both the antennas and the SCF than to generate a separate odd number of switching pulses during each cycle. In this case, we must look for other ways to kill the SCF's harmonic responses.

How about reducing the number of capacitors to only two, as shown in Fig 4? Now, no harmonic responses are produced (see Fig 6), but two new side effects arise. One is that the two-capacitor SCF's output signal is *always* a square-wave, rich in harmonics. Even when the original input signal is a clean sine wave, the output is a square wave. The other new problem is that the two-capacitor SCF is extremely phase-sensitive. Assuming that the frequency of the input signal is exactly equal to the filter's center frequency and its phase is just right, one capacitor is charged to the maximum positive peak of the input and the other to its maximum negative peak. The output signal is a square wave of maximum amplitude. In contrast, when the input signal is 90° different, both capacitors will sample the input signal at the zero-crossings, producing no output what-

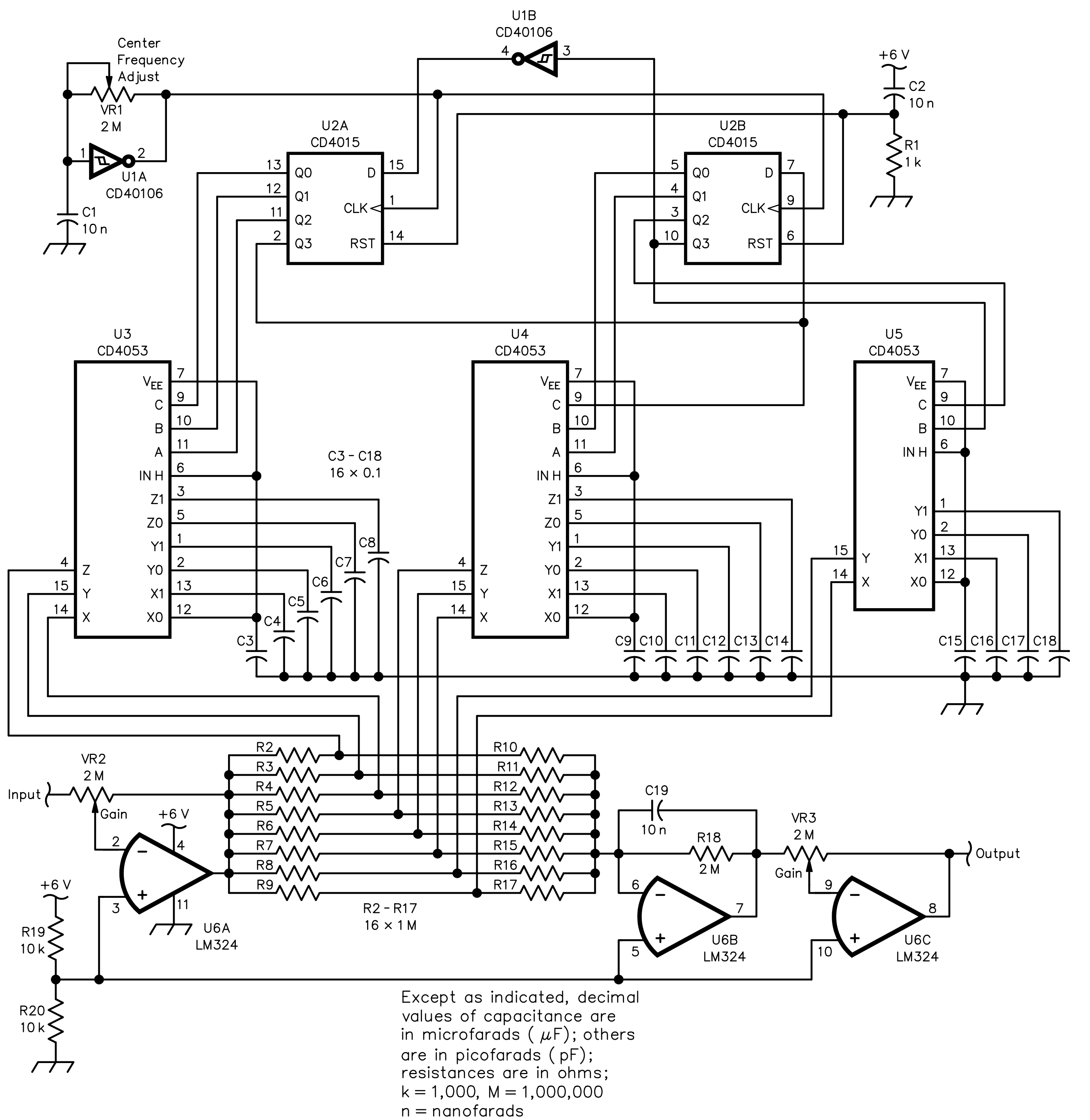

Fig 10—Schematic diagram of a practical 16-channel, two-capacitor SCF.

ever. This makes the output amplitude greatly dependent on input phase. In fact, the behavior of a two-capacitor SCF is very much like a CW demodulator: When the input signal frequency is close to the SCF center frequency, the output signal is amplitude-modulated at the difference (beat) frequency.

After some consideration and experiments, I found a good solution that overcomes the above problems. The concept is to use several parallel channels of two-capacitor filters, each driven in a different phase. (See Fig 7.) The output signals of all channels are summed by an op amp. In this multi-channel system, the worst case occurs when one channel is completely "out of phase." The rest of the channels will still work; the filter is much less phase-sensitive. Moreover, even if the input contains distortion, the output is still a step-wise, sampled signal that may easily be smoothed into sine waves.

Fig 8 illustrates the operation of a four-channel, two-capacitor SCF filter bank. Figs 9 and 10 show two actual experimental circuits of the improved SCF that I tested.

IC1 in Fig 9 produces the main clock; this drives IC2 to produce four individual clock phases during each cycle. The cycle frequency is equal to the center frequency of the filter. Each step represents a quarter cycle of the center frequency: 0-90°, 90-180°, 180-270° and 270-360°. IC2's output at each step feeds a CMOS switch, IC3, so that capacitors C2-C5 are connected to points A1-A4 during the four phases, respectively. IC4A is a pre-amplifier and IC4C is a post-amplifier; their gains may be adjusted by VR2 and VR3 to meet requirements. IC4B is a summing circuit that adds the channel outputs. The capacitor between the input and output of IC4B smoothes the waveform of the final output.

IC1A of Fig 10 generates the main clock at eight times the filter's center frequency. IC2A and IC2B generate eight square-wave signals to control the DPDT CMOS switches of IC3, IC4 and IC5. Each control signal differs from its neighbors by 1/8 cycle. C3-C18 are the sampling capacitors. Their values and those of R2-R17 determine the Q of the band-pass filter. Greater R/C values increase the Q. Compared to an ordin-ary SCF circuit, the harmonic respon-ses of this eight-channel, two-capacitor SCF are negligible. The final output signal is always cleaner at the center frequency.

I hope this improved switched-capacitor filter will help you in your applications.

Chen Ping, BA1HAM, is Chinese, born in 1944. Chen started reading radio books and making simple BC receivers when he was 8 years old. He joined an amateur high-speed telegraphy (HST) training course in 1958, while in middle school. From 1961 through 1967, he studied at the Radio and Electronic Department of Tsing Hua University, Beijing. There, he was active as Radio Sport Team leader of the university and achieved the Nation Master Class of Radio Direction Finding in 1964. Chen received his first call sign, BZ1HAM, when China first resumed issuing individual Amateur Radio call signs in 1989. After working as a refinery designer and computer engineer in the petroleum industry for 20 years, he was moved to the sports department to dedicate himself to the promotion of Amateur Radio in the country. Currently he works as the chief engineer in Sky Path Telecom Research Institute under the sports department, which mainly develops electronic kits for kids.

Radio Line-of-Sight Paths from the USGS Digital-Elevation Database

Looking for UHF/VHF terrestrial DX? Let this Web server and the USGS check proposed propagation paths for you.

By Matt Reilly, KB1VC

[This article was originally published in the Proceedings of the 25th Eastern VHF/UHF Conference of the Eastern VHF/UHF Society and North East Weak Signal Group.[1]—Ed.]

Eventually, every microwave operator is left scratching his head wondering about the "contact that got away." Was it the local QRM? Was it an inversion? Was it gremlins in the receiver? Was there a big hunk of rock in the way?

It is hard to know if the local QRM made a difference. Weather comes and goes: who knows what the atmosphere was doing at the time? Of course, there were gremlins in the receiver—that's where they live—but you've made many contacts with that receiver. We'll never know the answer to the imponderables, but we can find out if there was a big rock in the way.

The United States Geological Survey has provided access (via the Web) to a huge database of digitized topographic maps. While one could show that two points are on a line-of-sight path by drawing lines on paper topographic maps (many of us have done this), digitized maps offer us the opportunity to automate what is normally a very tedious job. There is a Web-based service that produces line-of-sight plots for paths between any two points in the continental United States.

What is "Line-of-sight"?

In general, a directional radio wave propagating in a vacuum travels in a straight line. Like light, however, the paths of radio waves can be bent when they pass through non-uniform media. This effect can be demonstrated quite simply with light, by looking through a glass of water. The image seen through the glass is distorted by the change in refractive index from air, to glass, to water and back. There are many ways of explaining this phenomenon. They are all related by Maxwell's equations, and we know that Maxwell's equations apply equally well to radio waves and light waves.

Nevertheless, through what "non-uniform" media are these radio waves propagating? The non-uniformity is in the atmosphere. The refractive index of a medium is a function of its

[1]Order No 760-1, $15. ARRL publications are available from your local ARRL dealer or directly from the ARRL. Check out the full ARRL publications line at http://www.arrl.org/catalog/.

7 Conant Dr
Stow, MA 01775
matthew.reilly@compaq.com

permittivity (dielectric constant) and its permeability. In all but the most bizarre circumstances, air contains the same amount of ferrous material as free space, so its permeability is pretty much that of free space. Its dielectric constant, however, is influenced by temperature, humidity and pressure. As altitude increases, the density of the atmosphere decreases. As such, its dielectric constant approaches that of free-space—it decreases relative to air at see level. The presence of water vapor increases the dielectric constant. Cold air has a higher dielectric constant than warm air. When all of these are accounted for, the general trend is that the dielectric constant decreases as altitude increases.

When a wave propagates through a medium whose refractive index is gradually but steadily changing, the wave bends. In extreme cases, where the refractive index changes abruptly, the wave is reflected. This is what makes "ducting" work. Since the refractive index of the atmosphere decreases with altitude, a wave pointed into the sky will encounter a gradually changing atmosphere and its path will be bent *toward the surface of the earth.*

This effect was explored rather thoroughly by the folks at the MIT Radiation Laboratory back in the 1940s. (Volume 13, *Propagation of Short Radio Waves,* has a very readable treatment of this material in Chapter 1.) They discovered that, while the amount of bending varies with atmospheric conditions, the path of a radio wave propagating in the atmosphere is fairly approximated by an arc of a radius 4/3 times that of the earth. The approximation holds reasonably well up through X band. The consequence of this can be seen in Fig 1, a plot of the "terrain" between two points separated by water.

The two points in the figure are separated by about 85 km. The left-hand station is at 120 meters elevation, and the right-hand station is at 115 meters. If the earth were flat, the two stations would clearly have a line-of-sight path. When we accurately represent the earth's curvature (labeled "true-earth") the visual path between the two points is obstructed. If we assume that the earth's apparent radius is 33% larger (to account for bending of the path), then the two points are on a line of sight.

Path curvature is, of course, not the entire story when it comes to "over the horizon" propagation. Tropospheric "ducting" in the presence of temperature/humidity inversions can substantially enhance a microwave path that is deemed "obstructed" by the simple approximation presented here. Scatter, diffraction and other phenomena can also improve an otherwise obstructed path. Similarly, paths that look good relative to a line-of-sight plot may well be obstructed by objects that are not shown on maps, such as buildings, trees or grain elevators. Nevertheless, an understanding of the topography between two points can give us an idea of whether a contact will be possible, or unlikely.

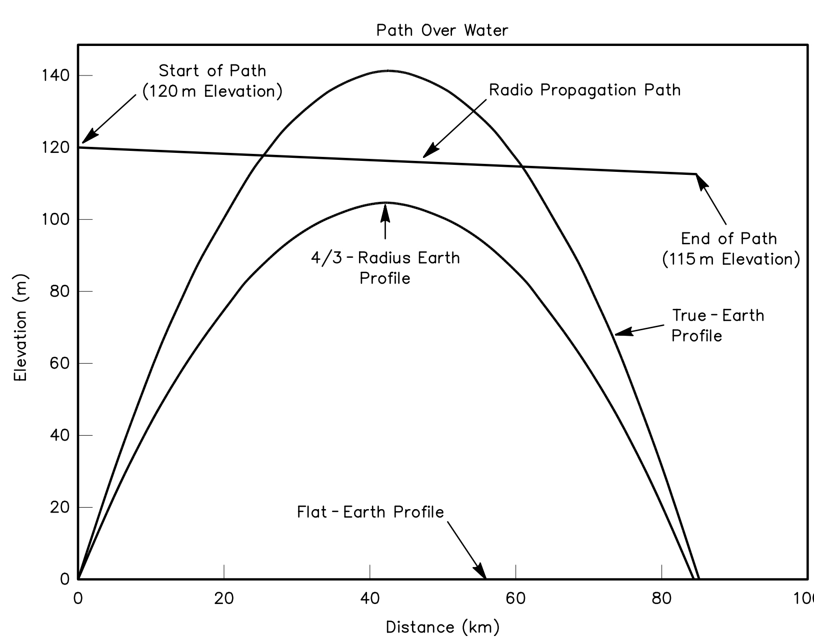

Fig 1—4/3-radius versus true-earth versus flat-earth profiles for two points separated by 85 km.

The Digital-Elevation Maps

The United States Geological Service provides Internet access to a set of digitized topographic maps that cover most of the continental US. Each map in the set represents a square of one degree in each direction. These are referred to as "Digital Elevation Maps" or the DEM database. Each map is stored in its own file. Each file contains 1200 lines of 1200 points each. This amounts to a point every three arc-seconds (about 90 meters, or so, in the Northeast). The maps are not without error or flaw, but they are nearly exhaustive—that is, they cover the entire "lower 48" and then some. The elevation at each of the 1,440,000 points in each map is in meters, with a resolution of approximately three meters.

There are 956 maps in the set. As stored at the USGS, they are quite large. The raw files are amenable to compression however. (The USGS Web site now has all the files stored in compressed format.) The compression technique used by the USGS is rather generic and doesn't account for the rather flat nature of most terrain. Applying additional loss-less compression to the data sets helps. Reformatted and recompressed, all 956 maps consume approximately 600 MB of disk space.

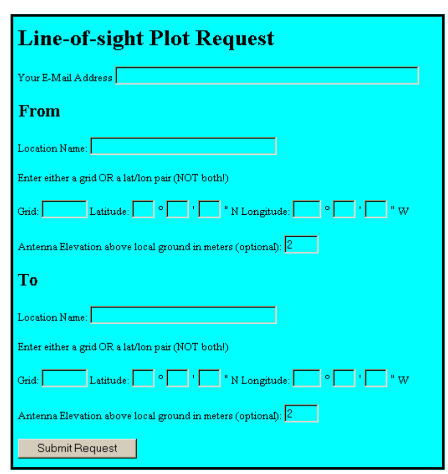

Fig 2—The request form.

The USGS also provides digitized topographic maps that are not in raster form. These are digital versions of the familiar topographic (topo) maps, showing contour lines of equal elevation at intervals of a few meters or so. When this work was started several years ago, these maps were not yet widely available. Their "vector" form makes their utility for plotting line-of-sight paths somewhat marginal, however they may promise better accuracy than the current DEM database. In the future, I'll try to translate these vector-form maps into raster form.

The Server

So, we have maps and we know how to warp the terrain slice to model radio propagation. The rest should be a mere matter of calculating—and so it is. I have set up a server to provide line-of-sight plots free of charge for amateur use only. You need only fill in a Web form with the required information and the server will provide a GIF-formatted plot of the terrain between any two points in the continental United States.

The computing task is, however, rather formidable. So, rather than calculating the path in real time, the user's information is stored for later retrieval by a "batch" server that satisfies all requests via e-mail. The server currently gathers all currently unfilled requests at 2:00 AM Eastern Time. Each response is e-mailed to an address supplied by the user as GIF encoded plot compatible with most network mail readers.

The Request Form

To request a plot, connect to **http://www.tiac.net/users/reilly/los_form.html**, which presents a summary of the service and some background information. At the bottom of the information page, click the "Plot Request" button to reach the actual request form shown in Fig 2.

Users must know a few things before making a request:

1. *A valid return e-mail address:* The Web form may not recognize badly formed addresses, so the user may not be notified if the address is incorrect.

2. *A name for the "starting" location:* This can be any name, but must be no longer than 40 characters.

3. *The six-character Maidenhead locator grid or the latitude and longitude of the starting location:* If the user enters a latitude/longitude (lat/lon) pair, the plot will start from that point. Otherwise, the user must enter a six-character grid location. The server will start the path from the highest point in that grid square.

4. *The elevation of the antenna at the starting location:* If the antenna at the starting point is 6 meters above the local terrain, the user should enter "6."

5. *A name for the "ending" location*

6. *The six-character grid or lat/lon pair for the ending location.*

7. *The elevation of the ending location.*

After filling out the form, click the "Submit Request" button. If any required entry has been omitted, you will be directed back to try again. If all is well, you will be asked to confirm the request. A confirmed request will be entered in the queue and serviced at a later time.

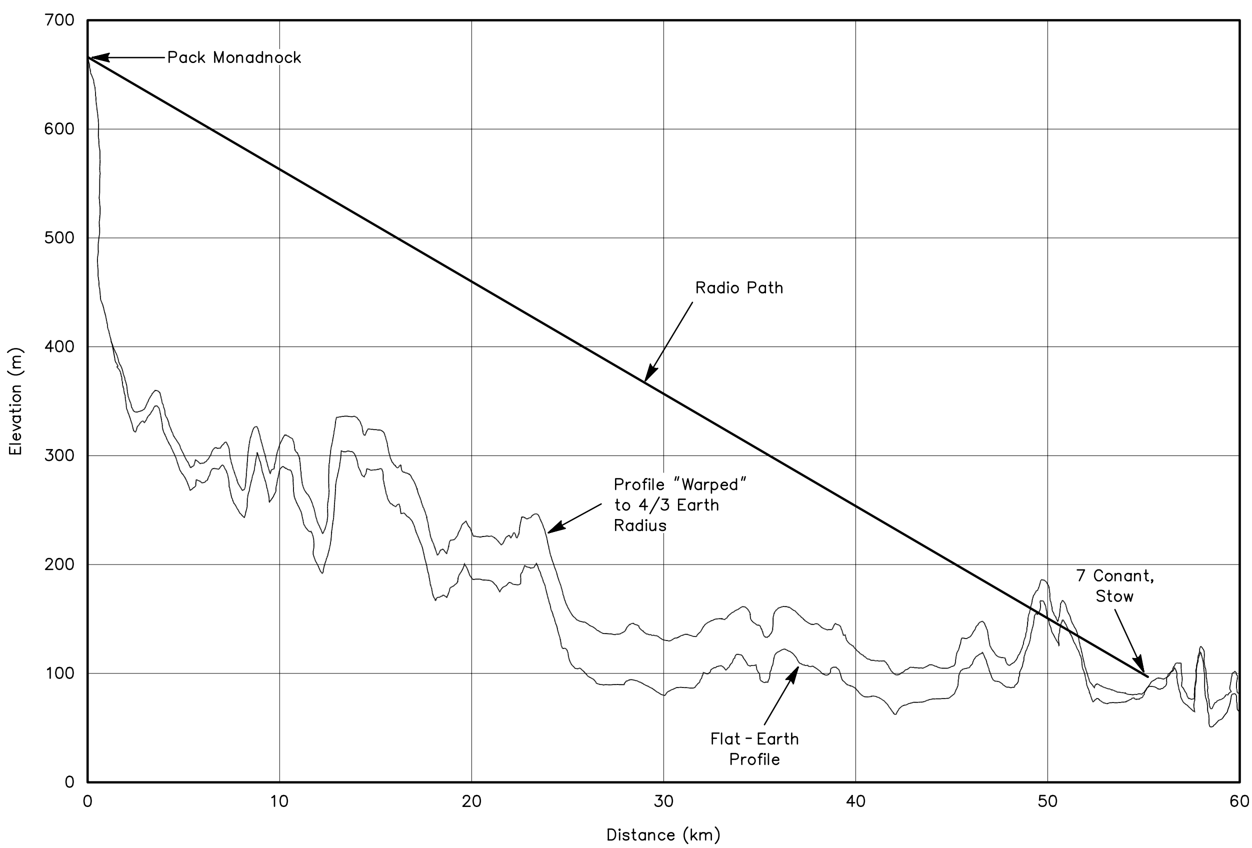

Fig 3—A sample line-of-sight plot from Pack Monadnock (42°53'10" N, 71° 51' 58" W), New Hampshire, to the author's home (42° 27' 18" N, 71° 32' 13" W). (The path is obstructed.)

The Response

Within a day or two after posting a request, you will get a response via e-mail. (The server batch job runs every morning, but Murphy works the night shift at the ISP that hosts the Web pages, so there are occasional delays.) The server gathers all unfilled requests, creates the plot files and sends each answer as a MIME encapsulated image that can be read by almost all modern PC-based mail readers. The plot is attached to the mail message: The service does not work for users with mail systems that do not allow such attachments. A plot sent in response to a Web request is shown in Fig 3. Note that the path is obstructed for both a "flat earth" assumption and the "warped" approximation. Because the plot shows the earth's surface in "warped space," we can draw a line from the peak of Pack Monadnock so as to clear the obstruction 50 km from the start. Thus determining that the path would be unobstructed if the tower at 7 Conant Dr were just 50 meters taller. Given local building codes, it would be more profitable to move the antenna or wait for anomalous propagation.

Ideally, the service would be provided in real time. As it turns out, however, the size of the map database, the magnitude of the computing task and the cost of ISP service all argue against real-time responses. During the initial trials of the service, the server has been very reliable, responding to each request within 24 hours. The server process is entirely automatic in that requests are satisfied without any human intervention. At the end of each night's run, the server sends the maintainer a log, which is reviewed as part of the continuing "bug search" activity. (The programs that generate the profile plots are laced with "consistency checkers" that report anomalous conditions to the maintainer.)

The plot may show that the path is obstructed, but remember that many obstructed paths, in fact, work almost all the time. WBlFKF and WA1MBA regularly communicate between their homes on a 10-GHz path that is obstructed by Mount Wachusett.

Nitty Gritty Details

Line-of-sight plots are produced from the starting and ending locations and the large set of digital-elevation maps. Between request and result, a number of operations take place.

First, the input coordinates are examined. If the location for the start or end point was supplied as a Maidenhead grid, the highest-point program scans the map database to find the highest point within the grid square. (It does this by scanning the region of the digital elevation map containing the Grid Square. If the region is perfectly flat, the resulting point will be in the northeast comer of the grid.) The result of the scan is a new start/end point specified in terms of lat/lon.

Given the start and end points, the next step is to make a list of all the map sections that contain some part of the path. Since there are over 900 map files, we don't want to scan each one. For example, if we know that the path is between two points in Texas, we will not need to scan the maps for New England or Oregon. This is actually a more-dicey proposition than it seems. As an example, take the path from EM99bx to FM29xx shown in Fig 4. A simple "flat earth" view of map intersections would allow us to draw a "bounding box" with EM99bx at the northwest corner and FM29xx at the southeast corner. Intersecting this bounding box with the known maps would yield a list of maps that cover EM99, FM09, FM19 and FM29. In fact, the actual great-circle route will very likely cross over into EN90, FN00, FN10 and FN20. For this reason, the map-intersections program uses the great-circle route between the start and end points to make a list of maps that fall along the path.

The *dirprof* or directional-profile program scans each map for points that fall under the great circle path. First, it makes a vector of points along the path spaced at 100-meter intervals. Each point (P) is specified as a lat/lon pair and the highest elevation found so far in the database along with the point at which it was found. This allows the program to find the elevation of the grid point nearest to each point (P) along the path. The maps are scanned in raster format, one line at a time. Each line represents a scan along a constant longitude. When a raster line is found to intersect the path, the program finds the closest point (P) on the path. If the point on the raster line is closer to (P) than any previously encountered raster point, then the elevation for (P) is updated. (Interpolation would be a better choice, and this may be incorporated in a later version.) After scanning all appropriate maps, the *dirprof* program writes a table to its output. Column one is the distance along the propagation path, and column two contains the respective elevation at that point.

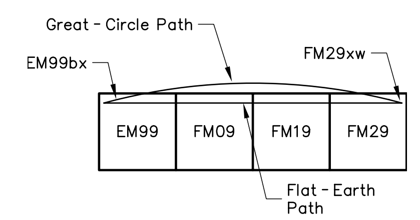

Fig 4—The great-circle path between EM99bx and FM29xw intersects maps outside the "flat-earth" path.

This table is a flat-earth view of the earth. To correct this view, the *rotwarp* or rotational-warp program reads the output of *dirprof* and transforms it into the 4/3-earth view that is more useful. This transformation however, can often cause the graph to look rather odd, as the starting location is plotted at the "correct" elevation, but the end location may be depressed below 0-meter elevation if it is "over the horizon." This is merely an artificial rotation of the view that was caused by the algorithm that corrects for earth curvature. This is corrected by rotating the plot so that elevations at the start and end points can be read directly from the graph.

The output of the *rotwarp* program is then sent to the *gnuplot* plotting program to produce the GIF output. The final plot contains a flat-earth profile as well as the 4/3-earth profile. The flat-earth profile can act as an aid to identifying any obstruction, as the elevation axis provides a true measure of elevation for the flat-earth view. On the 4/3-earth path, the elevation axis is only accurate at the start and end points.

Conclusions, Cautions and Tedious Stuff

The programs that produce the plots were written over a period of three years or so. The result comes from what could charitably called an "organic" approach that some have called "tinker-toy" engineering. The analogy is apt, as the plots are produced by a series of programs, each feeding its output to the next program's input. The bearing and distance calculation code is based on the *BD* program by Michael Gwen (W9IP) and Paul Wade (WlGHZ). Much of the format-translation code (to translate between grids and various lat/lon formats) was originally written for a laptop/notebook interface to a GPS that I developed in 1996. The plots themselves are drawn by *gnuplot* a widely used freeware plotting program. The actual profile scanner was written and modified over a period of two years as I found and fixed various "behavioral anomalies." The whole collection is tied together with about 500 lines of Perl. The Perl code is used to coordinate the half-dozen programs that participate in building a plot.

At the start, the code was written with an eye to optimizing *every* calculation to reduce the runtime of the map-scanning program. Though this offered an interesting set of problems and puzzles to solve, the effort was largely unnecessary. Most paths can be calculated within a second or two on a high performance Compaq Alpha workstation. (Though the runtime is much, much longer on Intel-based computers due to their relatively poor floating-point performance.) The bulk of the time that is required to service a request is consumed in actually mailing the response back to the user. (The server connects to the network via a 28-kbps dialup link.) It takes about 10 seconds to push a request through the relatively low-bandwidth channel from the server to the rest of the network.

As with any programs, there are still bugs waiting to be discovered. Some plots will have "gaps" that show up as very deep holes in the ground. These are manifestations of a bug of unknown cause. For this, and many other reasons, the copyright to these plots is owned by Matthew Reilly. Under the terms of the copyright, commercial use of any sort is prohibited. Subject to this restriction, the plots may be reprinted, distributed, used and republished in any Amateur Radio related forum. Users of the service must agree that the author, his associates, employers past and present, neighbors and future issue assume no liability for any use, abuse, errors, disappointment, injury, damage, discomfort, sadness or indigestion resulting from the use or existence of the plot server, its programs, constituent parts or input data sets.

No effort was made to make the code portable to Windows or Windows/NT environments. All the code was developed under Linux, and it makes heavy use of the multiprogramming facilities provided by Unix operating systems. The source-code pool for the plotting routines is available from the author upon request.

For those with high bandwidth connections, or a lot of time on their hands, the digital elevation maps are available from the USGS at **ftp://edcftp.cr.usgs.gov/pub/data/DEM/250/**. I have no doubt that we can do many interesting things with this information: The effort described here has just brushed the surface. □□

RF

By Zack Lau, W1VT

Feeding a Dipole with TV Twin lead

Portable QRP operation has become much more popular as technology has improved. Not only are QRP kits smaller and lighter today, but the performance of many of the radios are quite reasonable, even in crowded band conditions. For instance, I used a pair of single-band 2-W transceivers to operate the 1999 CW Sweepstakes on 40 and 20 meters. It took just 2$^1/_2$ hours to get my pin for working 100 contacts, a rate of 40 per hour. These simple superhetrodyne transceivers are available from Small Wonder Labs.[1] However, with a radio weighing just 11 oz, one begins to re-assess the weight of antenna and feedline. For instance, 50 ft of RG-174 with BNC connectors weighs just 8 oz, but has a loss of nearly 2 dB. RG-58 would lower the loss to 0.85 dB, according to specifications, but the weight would be up to 21 oz, nearly twice that of the rig.

One clever solution, popularized by Jerry Hall, K1TD, and Jay Rusgrove, W1VD, is to feed a dipole with lightweight TV twin lead.[2] They used a folded dipole made out of twin lead—the impedance step up provides a good match to 300-Ω transmission line. Matching at the transmitter end is done with a capacitor and a short section of twin lead—a single tuned circuit. This improves the performance to weight ratio, as long as the feedline is kept clean. Roy Lewallen, W7EL, found that TV twin lead becomes significantly more lossy when it gets wet or dirty.[3] The need to use twin lead to make the dipole is a bit of a disadvantage, however. Thin wire works just fine as 20-meter dipole elements in portable applications. Using Roy's measurement of 1.5 lbs/100 ft, the folded dipole takes another 8 oz of twin lead, for a total of 21 oz. This still compares favorably to the RG-58 solution.

Why not use a matching network at either end of a piece of twin lead? This would eliminate the need for making the dipole out of twin lead. Yes, you can. However, you are forming a double-tuned circuit—each network interacts with the other. More importantly, the degree of interaction is controlled by the feedline—the length of the feedline becomes a significant factor in determining the bandwidth over which the feedline appears transparent. As shown in Fig 1, I found that the matching network designed by Jay and Jerry works amazing well with 566 inches of 300-Ω twin lead—the 30-dB-return-loss bandwidth is 1.3 MHz. Reducing the feedline from 566 to 370 inches reduced the bandwidth to just 200 kHz. For most purposes, a 30-dB return loss has a negligible effect in amateur systems. Fortunately, the narrower bandwidth is still wide enough for most amateur purposes.

Why stop at attempting to make the feedline transparent? Why not optimize the feedline to minimize the SWR of the system? With computer simulators, it is relatively straightforward to obtain impedance plots at various antenna heights. The feedline can then be optimized to obtain a reasonable compromise over the anticipated dipole heights. Obviously, this may be expecting too much at the typical ham station with lots of interacting antennas, but a portable antenna can often be placed far from interfering objects.

I find that I can easily install a dipole 35 or 40 feet up, just by tossing lead weights attached to monofilament fishing line into trees. However, there

[1]Notes appear on page 55.

225 Main St
Newington, CT 06111-1494
zlau@arrl.org

are times when there just aren't convenient trees, so I end up with a dipole just 25 or 30 feet up. Fig 2 shows an *EZNEC* (with an *NEC-4* computation engine) plot of a dipole simulated at heights of 25, 30, 35, and 40 feet. I plotted these in *Amateur Radio Designer*. I can easily add a lossy transmission line and some capacitors to see the effect on system performance. Simultaneously viewing the plots at different heights makes it easier to design the antenna system for a variety of field situations. Fig 3 shows the performance of the improved system. A good SWR is obtained over a variety of expected antenna heights.

Will we see more system designs in the new Millenium? In the past, some design concepts were difficult to publish because there were just too many questions that needed to be answered for each installation. No author has enough time to custom design antennas for each and every reader. With the ready availability of computer software, however, it becomes much more feasible for readers to tailor a design to their needs, particularly if designs are presented in convenient building blocks. Readers may mix and match building blocks, then perform the desired optimizations.

Or, will we see designs intended to be good compromises over a wide variety of conditions? Instead of looking for the ultimate in directivity or efficiency, perhaps designers will use modern tools to simplify the installation and tuning of antennas. Not only can we make sure that the antenna will work in a variety of typical operating situations, but we can study the interaction of the antenna with the environment. This may lead to more intuitive tune up procedures based on theory, instead of empirical cut and try.

Modeling the Hall and Rusgrove Matching Section

There is just enough information in the article to figure out the design. While the velocity factor of the open-stub twin lead is missing, it is easily calculated based on the transmission-line equivalent provided for the capacitor.

Frequency = 14.175 MHz

Capacitance = 76 pF

Capacitive reactance, X_C is $1/(2\pi fC)$, or 147.7 Ω.

X_C is also $Z_0\mathrm{Cot}(L)$, where Z_0 is the characteristic impedance of the line and L is the line length, in units that match your trig calculator. Most hams use degrees, while mathematicians often find radians more useful.

$\mathrm{Cot}(L) = (147.7\ \Omega)/(300\ \Omega)$

$L = 63.8°$

Thus, the 118.5-inch stub has an electrical length of 63.8°.

The equation for calculating the length of the stub is:

$\lambda(L°)/(360°)vf$ = stub length

Alternately,

vf = (stub length) $360°/((L°)\lambda)$

Substituting,

vf = 118.5 inches 360° /(63.8°) (833 inches))

$vf = 0.803$

The design can also be modeled in *ARRL Radio Designer*. The first choice is the best element model. I prefer to use the coaxial-cable model, CAB, since it offers more accuracy in modeling attenuation over a range of frequencies.

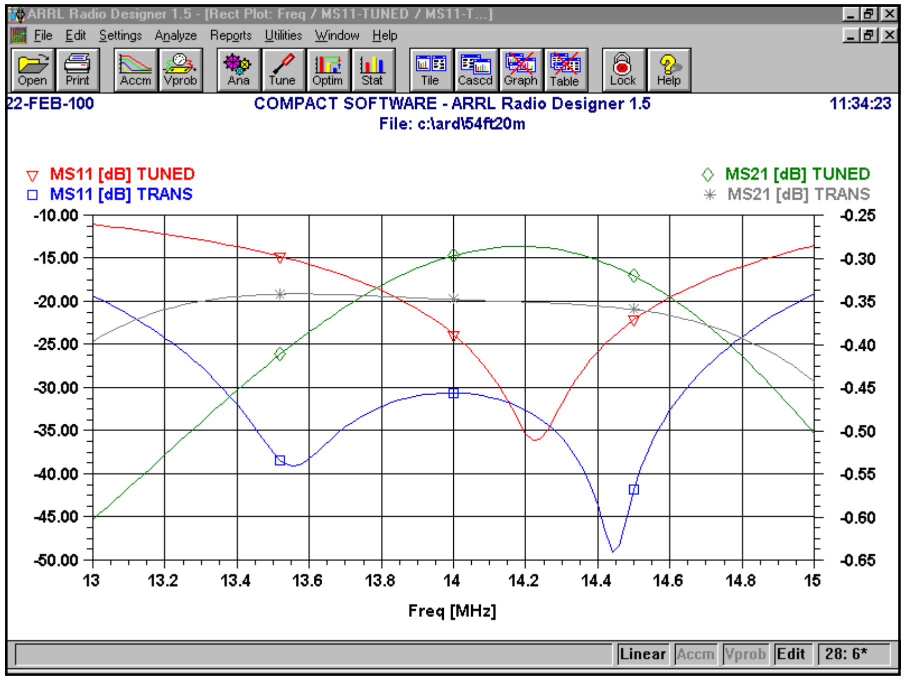

Fig 1—Response plots of the matching network designed by W1VD and K1TD with 566 (TRANS) and 370 (TUNED) inches of 300-Ω twin lead.

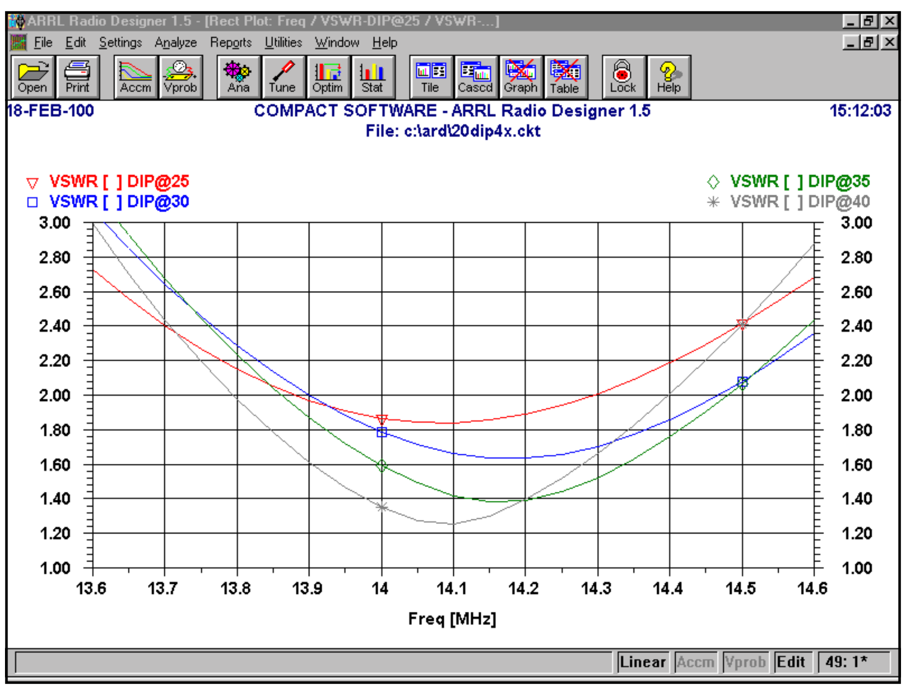

Fig 2—An *EZNEC* (with an *NEC-4* computation engine) plot of a dipole simulated at heights of 25, 30, 35 and 40 feet, plotted in *ARRL Radio Designer*.

This isn't surprising, since the TRL model assumes that the loss is purely resistive conductor loss, while the CAB model includes another term, proportional to frequency, for modeling dielectric loss. As a result, the TRL model is overly optimistic at high frequencies, if adjusted for a precise simulation at a lower frequency. This is shown in Table 1.[4]

The CAB model does have a problem—I've seen frequency-offset errors if you assume the shield and center conductors are equivalent. For instance, a 1-meter shorted $\lambda/4$ acts as an open circuit at 67 MHz, instead of 75 MHz, as predicted by theory. Fortunately, there are two very simple solutions. The most obvious is to model the parallel line as two coaxial cables. The second is to install a 1:1 transformer to make the transmission line a "floating" component. Either of these two equivalents can be used to more accurately model shorted transmission-line stubs.

It is quite easy to model the parallel

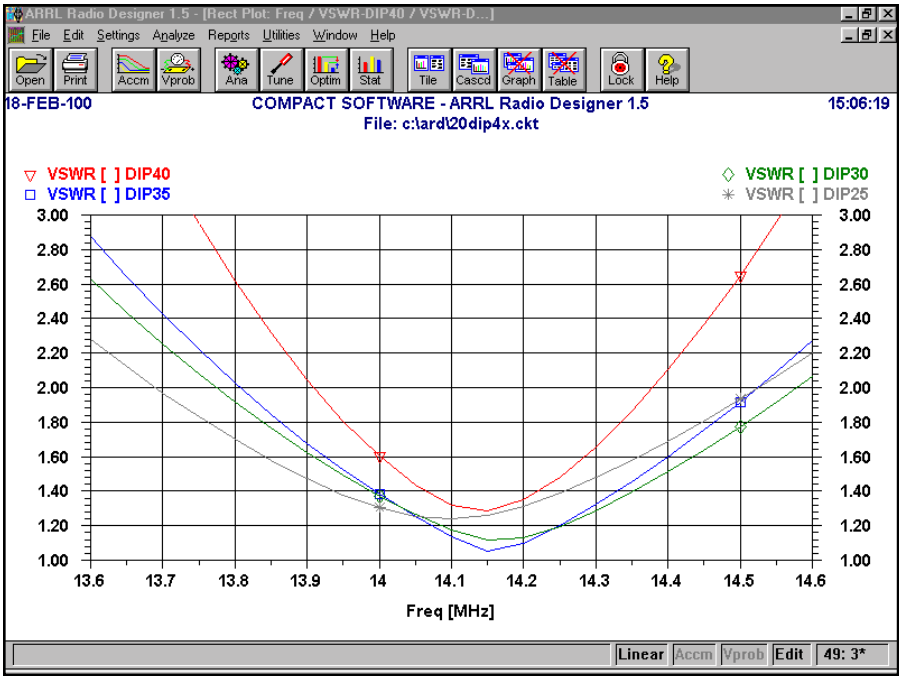

Fig 3—Performance of the improved antenna and feedline system.

Table 1—Loss of TV Twin Lead

TRLINE uses the less accurate TRL model. LINE is the "coaxial cable model." 2LINE uses two coax cables to produce an accurate model.
Compact Software - ARRL Radio Designer 1.5 18-FEB-100 13:39:31
File: c:\ard\tvlead.ckt

Freq (MHz)	*MS21 (dB) TRLINE*	*MS21 (dB) LINE*	*MS21 (dB) 2LINE*
3.500	–0.21	–0.21	–0.21
7.000	–0.30	–0.30	–0.30
14.000	–0.42	–0.43	–0.43
21.000	–0.51	–0.54	–0.54
28.000	–0.59	–0.62	–0.62
30.000	–0.61	–0.65	–0.65
50.000	–0.79	–0.85	–0.85
100.000	–1.12	–1.24	–1.24
144.000	–1.35	–1.51	–1.51
200.000	–1.59	–1.82	–1.82
400.000	–2.24	–2.71	–2.71

Table 2—Accurately Modeling a Shorted Coaxial Transmission-Line Stub

The SC model unsuccessfully tries to float a coax shield, producing inaccurate results at 75 MHz.
Compact Software - ARRL Radio Designer 1.5 18-FEB-100 13:51:25
File: c:\compact\sc.ckt

Freq (MHz)	*MS11 (dB) SC2CAB*	*MS21 (dB) SC2CAB*	*MS11 (dB) SCTRF*	*MS21 (dB) SCTRF*	*MS11 (dB) SC*	*MS21 (dB) SC*
50.000	–0.16	–14.49	–0.16	–14.49	–0.05	–19.02
53.785	–0.11	–16.11	–0.11	–16.11	–0.03	–21.50
57.856	–0.07	–18.14	–0.07	–18.14	–0.01	–25.04
62.235	–0.04	–20.86	–0.04	–20.86	–0.00	–31.35
66.945	–0.01	–24.98	–0.01	–24.98	–0.00	–50.59
72.012	–0.00	–33.75	–0.00	–33.75	–0.01	–29.20
74.000	–0.00	–43.58	–0.00	–43.58	–0.01	–26.55
74.500	–0.00	–50.09	–0.00	–50.09	–0.01	–25.99
75.000	–0.00	–68.82	–0.00	–68.82	–0.01	–25.47
75.500	–0.00	–48.28	–0.00	–48.28	–0.01	–24.97
76.000	–0.00	–42.67	–0.00	–42.67	–0.02	–24.50
77.463	–0.00	–35.10	–0.00	–35.10	–0.02	–23.25
83.326	–0.02	–24.58	–0.02	–24.58	–0.05	–19.47
89.633	–0.05	–19.55	–0.05	–19.55	–0.10	–16.56
96.418	–0.11	–15.97	–0.11	–15.97	–0.17	–14.06
103.716	–0.22	–13.01	–0.22	–13.01	–0.30	–11.74
111.566	–0.43	–10.28	–0.43	–10.28	–0.52	–9.46
120.010	–0.84	–7.57	–0.84	–7.57	–0.95	–7.08
129.094	–1.80	–4.70	–1.80	–4.70	–1.92	–4.46
138.865	–4.78	–1.76	–4.78	–1.76	–4.90	–1.70
149.376	–29.71	–0.00	–29.71	–0.00	–29.72	–0.00
160.682	–4.91	–1.69	–4.91	–1.69	–4.81	–1.74
172.844	–1.49	–5.38	–1.49	–5.38	–1.40	–5.61
185.927	–0.51	–9.53	–0.51	–9.53	–0.46	–10.01
200.000	–0.16	–14.53	–0.16	–14.53	–0.13	–15.45

Table 3—The Single-Tuned Matching Network Using a Transmission-Line Stub.

Compact Software - ARRL Radio Designer 1.5 18-FEB-100 14:02:58
File: c:\ard\jjmatch.ckt

Freq (MHz)	*MS11 (dB) TLMATCH*	*MS21 (dB) TLMATCH*
13.000	–12.10	–0.39
13.098	–12.70	–0.36
13.197	–13.39	–0.33
13.297	–14.17	–0.30
13.398	–15.06	–0.27
13.499	–16.12	–0.24
13.601	–17.37	–0.21
13.704	–18.92	–0.19
13.807	–20.90	–0.18
13.912	–23.59	–0.16
14.017	–27.66	–0.16
14.123	–35.17	–0.15
14.175	–39.00	–0.16
14.230	–34.81	–0.16
14.337	–27.03	–0.17
14.446	–22.63	–0.19
14.555	–19.60	–0.22
14.665	–17.29	–0.26
14.776	–15.40	–0.31
14.887	–13.81	–0.38
15.000	–12.44	–0.46

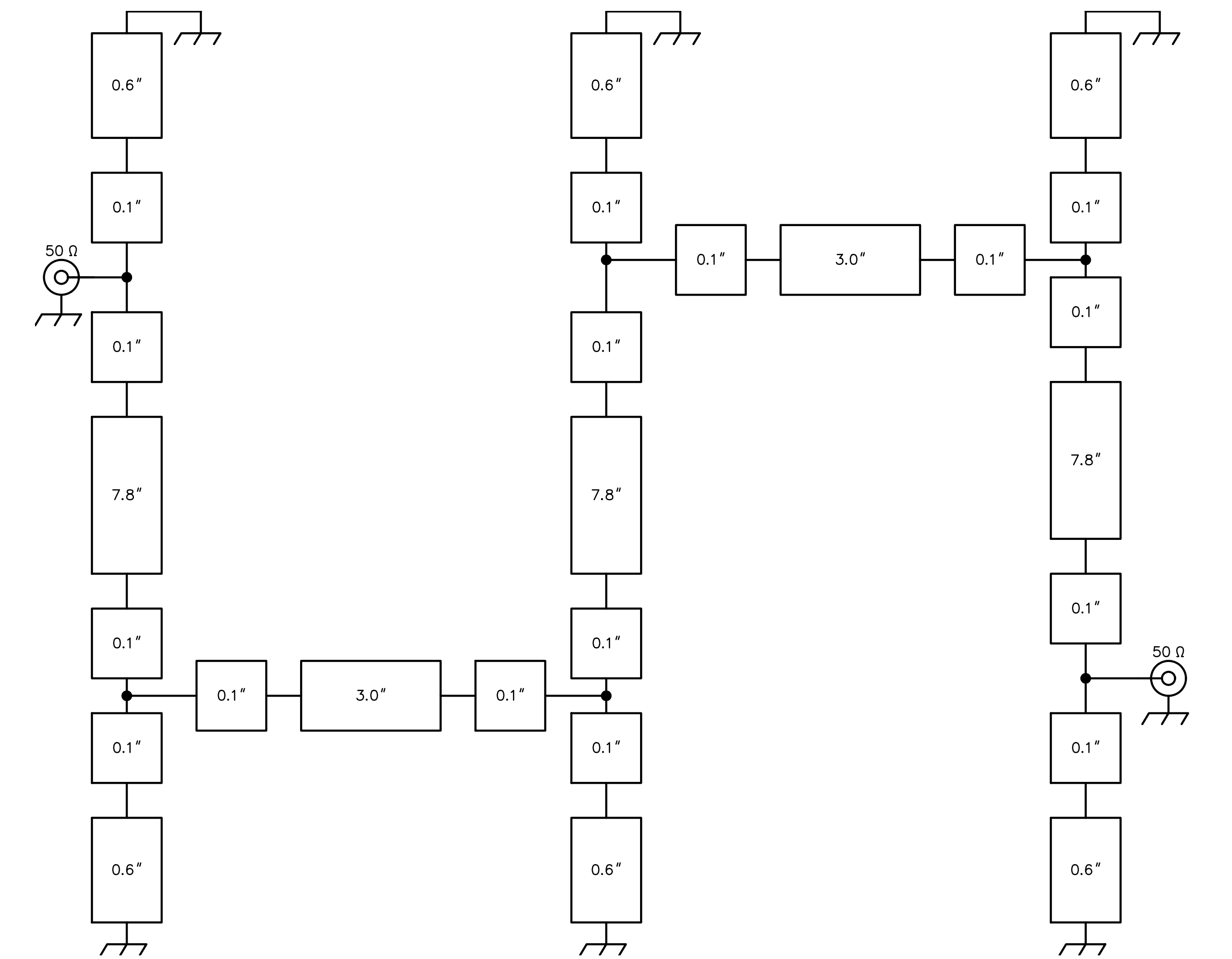

(Above) Fig 4—A construction diagram of the 70-cm BPF for 434.5 MHz with a 23-MHz bandwidth. The lengths shown are shield lengths for the UT-141A. The center conductor extends 0.1 inch beyond the shield at each end of each piece.

line as two coaxial cables. The impedance of each coaxial cable is half the impedance of the parallel line. The attenuation constants are even easier—they are unchanged, as shown in Table 1. Table 2 shows all three situations—the frequency-offset problem, using a transformer for isolation and modeling the cable as two parallel coaxial cables.

Table 3 shows the result of modeling the 50 to 300 Ω matching circuit in ARD after the return loss is optimized for best return loss at 14.175 MHz. Not surprisingly, the optimum velocity factor is 0.803.

You can also see this in ARD if you adjust the velocity factor to optimize the return loss at 14.175 MHz. The results are shown in Table 1.

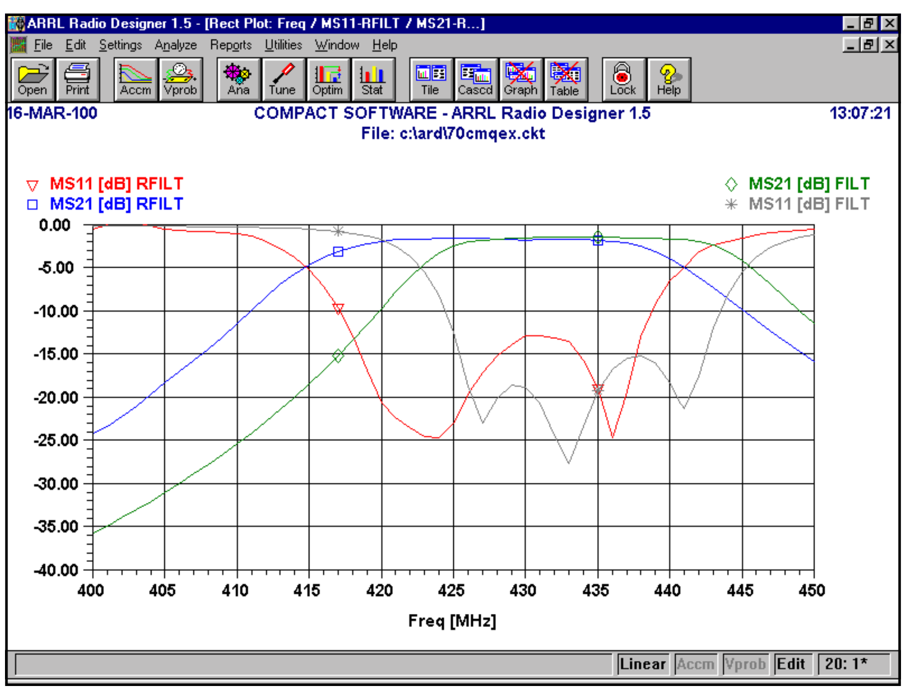

Fig 5—ARD performance plots for the 70-cm BPF. FILT is simulated, while RFILT is the measured filter response

No-Tune 70-cm Bandpass Filter

Here is a 70-cm no-tune bandpass filter than can be built using ordinary hand tools (see Fig 4). It is made out of accurately cut sections of UT-141A semi-rigid 50-Ω coax. The design isn't new—it is based on the same idea used in the 2-meter bandpass filter published in the May 2000 *QST*.[5]

The design was done empirically on *ARRL Radio Designer*.[6] The coupling lines and tap points were designed for the best pass-band shape to cover 423 MHz to 446 MHz, while the length of the resonators was adjusted for the desired center frequency. The half-wave resonators are shorted at either end by soldering the center conductor to the coax, just like the *QST* version.

There are two changes compared to the *QST* filter—another half-wave resonator is added for steeper skirts, compared to a two-resonator filter. Also, the input and output couplings are on either side of the resonant transmission lines, for a more symmetrical passband. This is desirable, to eliminate unwanted signals lower in frequency. In the 2-meter case, all the unwanted signals were just above the passband. If this filter were used in a typical transverter, LO and opposite-sideband signals would occur below the passband. High-order mixing products would occur above the passband.

The measured performance is quite reasonable, less than 2 dB of insertion loss and 13 dB of return loss at 432 MHz (see Fig 5). The center frequency is about 7 MHz low, representing a shift of 1.5%. With a bandwidth of 6%, the passband still covers the 432 to 436 MHz portion of the band popular for SSB/CW work. Weak-signal work can be found around 432 MHz, while satellite operation is around 436 MHz. Unfortunately, the rejection to a 404 MHz LO is about 10 dB worse with this passband shift, so additional filtering is required if your mixer has significant LO leakage. For instance, the popular SBL-1 and SBL-1X mixers have about 34 dB of LO-to-RF leakage, according to the Mini-Circuits data book.

How bad is this? With a 7 dBm LO, the leakage is –27 dBm. Typically, a mixer will have –4 dBm of input or be tested with a pair of –10 dBm tones. With 6 dB of mixer loss, the output signal is –10 dBm. This is only 17 dB stronger than the LO leakage. Filter attenuation of 18 dB will reduce the LO leakage to –35 dB. Thus, additional filtering will be required. The need for an extra filter isn't necessarily a problem—I'd advise against trying to do everything with a single filter. Leakage around filters is a significant problem in RF design—it doesn't take much to radiate a signal around filters.

A disadvantage of this filter is the time-consuming construction—it does take some work to accurately cut the semi-rigid sections by hand. However, this is mitigated by the self-shielding nature of the filter. Printed-circuit-board filters can be quite time consuming to properly shield.

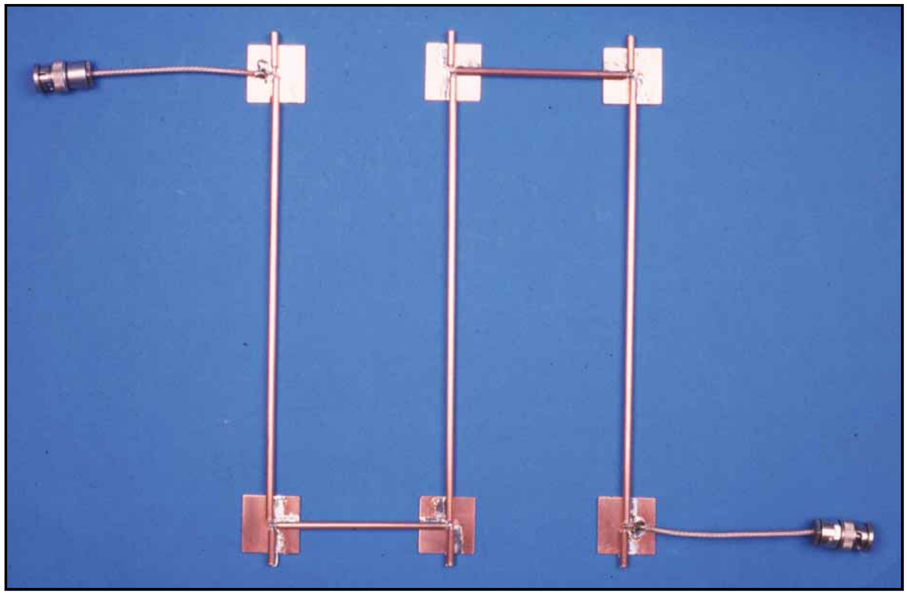

Fig 6—423 MHz to 446 MHz no-tune bandpass filter made out of UT-141A semi-rigid coax.

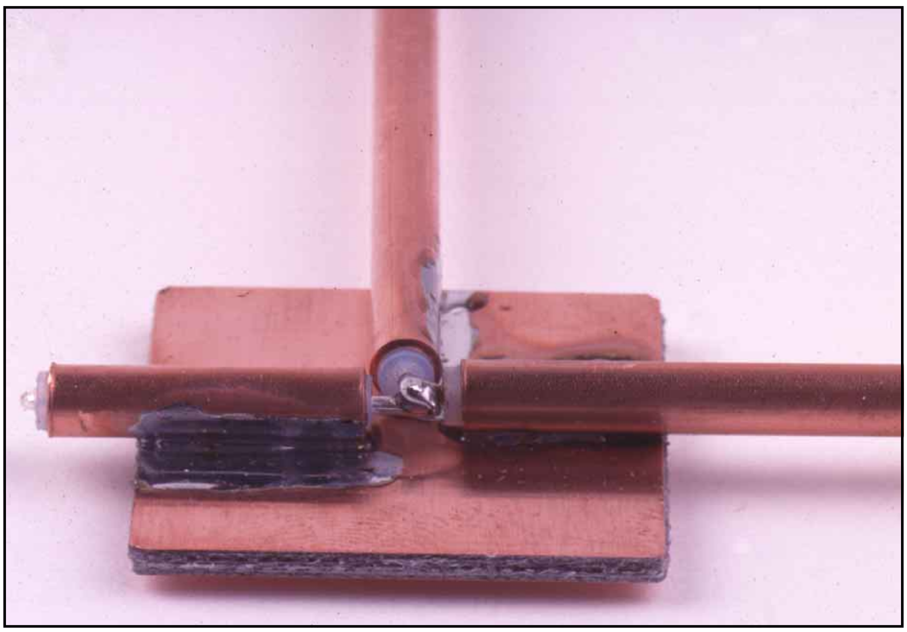

Fig 7—Close-up of the T-connections between the coax sections.

Notes

[1]Small Wonder Labs SWL-40+ and SWL-20+; URL **http://www.smallwonderlabs.com/**.

[2]*The ARRL Handbook* "Simple Antennas for HF Portable Operation," 1981 pp 10-13 to 14, 1982-84 p 10-14, 1985 p 33-16, 1986-89, 92, 93 p 33-14, 1990-91 p 33-11.

[3]R. Lewallen, W7EL, "Antenna Feed Lines for Portable Use," *QST*, Feb 1982, pp 51-52.

[4]ARD files to generate Figures 1, 2 and 3 and Tables 1, 2 and 3 (TwinLead.txt) are available as a download package from the ARRL Web **http://www.arrl.org/files/qex/**.Look for 00RF09.ZIP.

[5]Lau, Zack, W1VT, "A No-Tune 2-Meter Bandpass Filter," *QST*, May 2000, pp 54-55.

[6]You can download the ARD file (70cmQEX.ckt) to model this filter from the ARRL Web **http://www.arrl.org/files.qex/**. Look for 00RF09.ZIP.

Tech Notes

It is an honor to be part of the QEX/ Communications Quarterly *magazine and being allowed to continue the Tech Notes column in this new forum. I hope the column is both as popular and informative to our new readers as it was in* Communications Quarterly *for the past several years. I hope to spotlight short articles that are not quite large enough to be run as full feature-length articles. This month's Tech Note is by Rick Littlefield, K1BQT, and describes a simple method for constructing tuned coaxial baluns. If you have a small project, or a just a better way to do something, we would be pleased to review your material for possible use in Tech Notes.*—Peter Bertini, K1ZJH, *QEX* Contributing Editor; **k1zjh@arrl.org**

Lightweight Resonant-Trap Baluns

Baluns come in many types, but all serve the same fundamental purpose—to electrically disengage the exterior surface of a coaxial feed line from an antenna element. A "trap balun" is similar to a traditional SRF (series-resonant) coaxial feed-line choke, except lumped C is added in parallel with the inductor to reduce coil size and weight. Smaller size means less wind load and feedpoint sag for suspended-wire dipoles—especially on lower-frequency bands where wound coaxial chokes may become quite large. On the negative side, the addition of lumped C reduces useful bandwidth and provides a lower blocking impedance, compared to an optimized SRF choke. However, these drawbacks have little impact on 50-Ω monoband-dipole installations.

Construction

The traps described here use RG-58 cable wound on short lengths of 2-inch (ID) Schedule-40 thin-wall PVC "pressure pipe." This pipe is inexpensive and readily available from most well stocked hardware stores. For coax, I recommend RG-58A. This cable has a stranded center conductor that provides better flexibility for winding and better immunity against breakage or migration. Use only good quality dipped silver-mica capacitors in the circuit.

L/C values for each trap were determined experimentally using a dip meter and strings of standard-value capacitors (see Table 1). My objective is to resonate each inductor with a string of four to six standard-value 500-V dipped mica capacitors of equal value. This would ensure uniform RF current distribution across the string and provide a rating of 2000 to 3000 dc volts. Since RF-breakdown voltage is usually much lower than published dc ratings, a healthy safety margin is required.

Coil lengths are provided in Table 1. It is very important to prevent kinks in the coax. To reduce this tendency, bore entry holes straight through the forms, then slowly tilt the drill to elongate the hole in the proper direction for cable entry. Before winding, install a tie-wrap on the cable (inside the form) to prevent it from pulling through the entry hole and loosening the coil. If you use a continuous length of RG-58 for both feed line and balun, thread the specified length (from Table 1) of cable up through the lower hole in the form. Then wind from the bottom to the top. Insert the remaining cable through the top hole in the form and secure it in place with another tie wrap. Be especially careful to avoid kinks or sharp bends—center-conductor migration can quickly destroy the cable's breakdown-voltage rating.

Construction details for a typical trap balun are shown in Fig 2. When dressing the cable, prepare a pigtail sufficient to accommodate flexing. The antenna wire for each dipole leg should be immobilized inside the form

Table 1—Component Data for HF Trap Baluns

Band	*Turns*	*Capacitors**	*Hole Spacing*	*RG58 Length*
80	26	5, 470 pF	5 1/8"	19'
40	13	5, 330 pF	2 9/16"	9' 6"
30	10	4, 200 pF	1 15/16"	7' 6"
30	10	6, 300 pF	1 15/16"	7' 6"
20	9	4, 100 pF	1 3/4"	7'
20	9	6, 150 pF	1 3/4"	7'
17	7	5, 120 pF	1 3/8"	5' 6"
15	6	5, 100 pF	1 3/16"	5'
12	5	5, 100 pF	1"	4' 6"
10	4	5, 100 pF	13/16"	3'6"

*All capacitors are 500-V silver mica (see text).

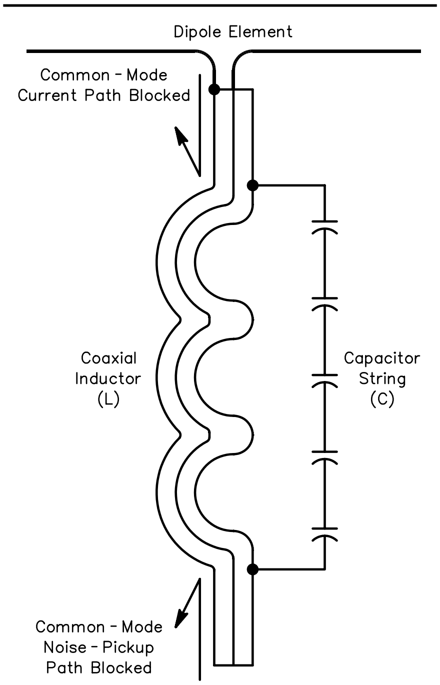

Fig 1—When a trap balun is installed at the feedpoint, the tuned L/C circuit presents high blocking impedance to break the current path.

to minimize stress and movement. Use a large gob of "plumber's goop," or clamp the wire with a large flat washer to hold it securely in place.

When making up the capacitor chain, space the caps equally through the center of the coil. Prepare the lower (feed line) end of the coil by girdling the PVC jacket close to where it enters the center of the form, as shown in Fig 1. Remove about 1/8-inch of the jacket and carefully tin the exposed copper braid, being careful not to melt through the dielectric underneath. Then, tin the lower capacitor lead, form it to conform to the cable and tack solder it onto the shield. Coat the joint with sealant to protect it from condensation and corrosion. Solder the top end of the capacitor string to the shield pigtail, making the connection as close to the cable's entry point as possible.

Feel free to modify the construction to suit your particular application. If you use eyebolts or other metallic hardware, however, spend the extra money for brass or stainless. For longer dipoles, I recommend using a PVC end cap at the top to add lateral strength. To minimize weight, you can shorten the cap by about 3/4-inch with a hacksaw. Install the cap using Genova Cement to ensure a strong chemical bond. Be sure to stress-relieve the coax by installing a nylon cable clamp at the bottom of the form.

Power Rating

To "smoke-test" these traps, I tested three of them on low SWR antennas at 1 kW for several minutes each, without failure. However, this power level exceeds RG-58 ratings, so I don't recommend doing so at your station! My cable was brand new and the traps were "freshly wound." If anything, coaxial cable should be derated because of the potential for center-conductor migration in windings. A power limit of around 300 W seems sensible. If you want to build a high-power version, I recommend using RG-58 Teflon-jacketed plenum cable on a 4-inch form. In addition, the capacitor strings should be 1000-V rather than 500-V capacitors. At the opposite end of the spectrum, you could use RG-176 on a small-diameter form with a single resonating capacitor for QRP versions.

It's relatively easy to check trap resonance with a dip meter. However, because low-cost dippers often have poor frequency calibration and may "pull" under load, I find it helpful to spot the actual dip-meter frequency with a receiver. If your capacitor string is slightly high in frequency, you may add a small-value capacitor in parallel with one in the string to trim it. At 80 and 40 meters, traps should be tuned near mid-band. Tuning is less critical from 30-meters up.

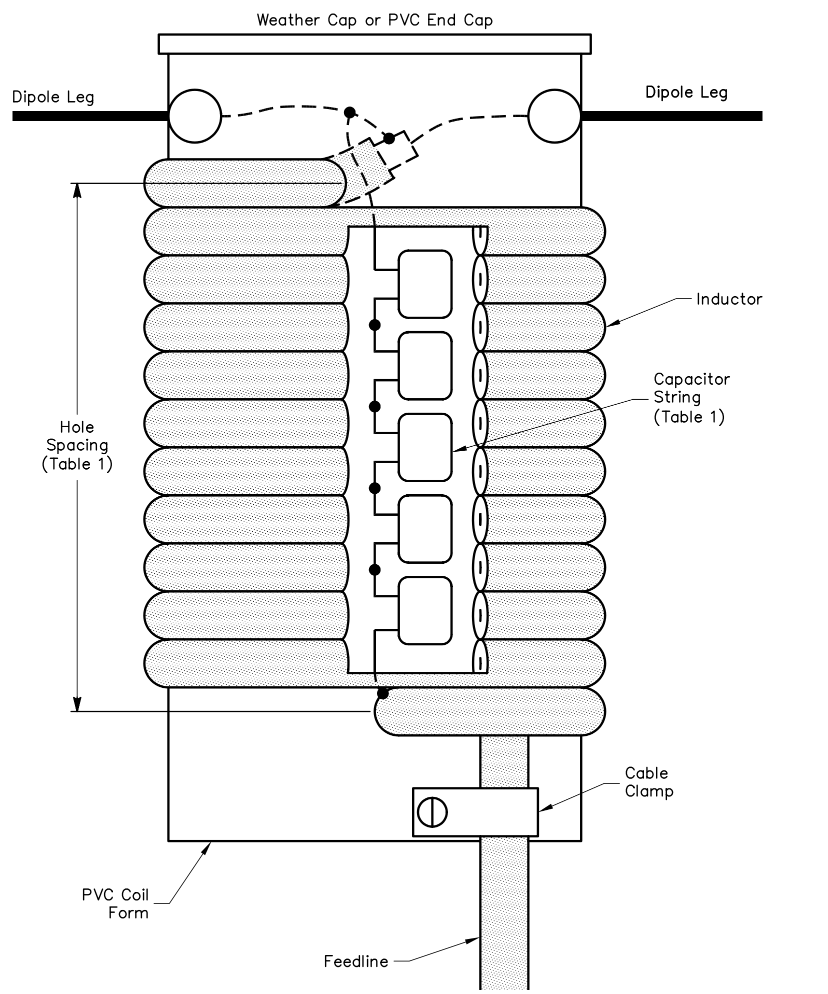

Fig 2—Construction details for a typical trap balun. The capacitor string is installed inside the form and routed down through the center. A weather cap keeps rain and snow out.

Feed-Line Traps and Mutual Coupling

Keep in mind that baluns prevent common-mode feed-line radiation problems resulting from *direct coupling* (the physical connection of the feedline shield's exterior surface to the feedpoint). They do not protect the line from becoming energized through *mutual coupling* to the antenna element. This condition most often occurs when the feed line must be routed under one leg of the antenna. If you cannot route the feed line to depart from the antenna at a right angle, you may reduce mutual coupling by dropping the feed straight to the ground and running it at—or below—ground level. Close proximity to earth, a lossy medium, raises the shield's surge impedance and reduces its efficiency as a radiator. Finally, as a last barrier, install a string of ferrite sleeves or tape several coils of coax together where the line enters the building to provide additional suppression.

Conclusion

Many of today's consumer electronic devices not only "fold up" when exposed to high levels of RF, they also radiate a fair amount of spurious noise on the ham bands. Virtually any well-designed balun will provide a measure of relief from this problem by breaking the circuit where these unhappy RFI exchanges takes place! The trap balun is one more way to get the job done, and it may be a great low-cost solution for monoband applications where weight is a factor.—*Rick Littlefield, K1BQT, 109A McDaniel Shore Dr, Barrington, NH 03825-3003; e-mail* **k1bqt@aol.com**

Upcoming Conferences

2000 ARRL/TAPR Digital Communications Conference

The 19th Annual ARRL and TAPR Digital Communications Conference will be held September 22-24 in Orlando, Florida—just minutes from the Orlando International Airport!

The ARRL and TAPR Digital Communications Conference is an international forum for radio amateurs in digital communications, networking and related technologies to meet, publish their work and present new ideas and techniques for discussion. Presenters and attendees will have the opportunity to exchange ideas and learn about recent hardware and software advances, theories, experimental results and practical applications. Chairing this year's event is Steve Stroh, N8GNJ, recently named as *CQ* magazine's digital editor.

The Digital Communications Conference is not just for digital experts, but also for digitally-oriented amateurs at all levels of experience.

As in years past, an entire session strand with beginning, intermediate and advanced presentations on selected topics in digital communications will be offered. Topics will include APRS, Satellite Communications, TCP/IP, Digital Radio, Spread Spectrum and other introductory subjects.

Two symposia/seminars will be held which allow those with additional time and interest to make the most of the Conference. For those who may have interest in just one symposium or seminar, registration for the conference is not required to attend these activities. This allows maximum flexibility for those who may want to participate during the Digital Communications Conference, but do not have an entire weekend to devote to the event.

The Fourth APRS National Symposium will be held on Friday and will be moderated by Steve Dimse, K4HG (the developer of *javAPRS*). Many APRS software authors, such as Bob Bruninga, WB4APR (the father of APRS), Keith Sproul, WU2Z, Mark Sproul, KB2ICI (the developers of *MacAPRS* and *WinAPRS*), Brent Hildebrand, KH2Z (the developer of *APRSPLUS*), Mike Musick, N0QBF (developer of *PocketAPRS*) and other nationally known APRS leaders are expected to be on hand.

The DCC banquet is Saturday night. A guest speaker will speak after the banquet and a prize drawing will top the evening. The grand prize is a Palm VII Personal Digital Assistant.

The Sunday morning seminar will focus on PIC development, design and programming. This five-and-a-half hour seminar will focus on the things you need to know now in order to understand and begin to participate in PIC development.

The 2000 ARRL and TAPR Digital Communications Conference local cohosts will be the Lake Monroe Amateur Radio Society (**http://www.qsl.net/lmars/**), Orange County ARES/RACES (**http://evcom.net/~jvoisin/ares.htm**), Seminole County ARES/RACES (**http://www.geocities.com/capecanaveral/launchpad/4773**) and the Orlando Amateur Radio Club (**http://www.oarc.org/**).

The Packet Radio User Group of Japan will be the International co-host for the third year running. PRUG will host an informal social Friday evening before their seminar and symposium is held. Visit **http://www.prug.or.jp** for more information about PRUG.

Conference presentations, meetings and seminars will be held at the Orlando Airport Marriott. It is highly recommended that you book your room prior to arriving. A special DCC room rate of $89/single and $89/double per night has been blocked for 50 rooms and is available until September 1. Once the 50 rooms have been reserved, room rates will increase. The hotel provides transportation to and from the Orlando International Airport.

To contact the Orlando Airport Marriott: write 7499 Augusta Dr, Orlando, FL 32822; call 407-851-9000, fax 407-857-6211; or visit the URL **http://marriotthotels.com/MCOAP/**.

A registration form and conference and hotel information, may be obtained by contacting Tucson Amateur Packet Radio, tel 940-383-0000, fax 940-566-2544; e-mail **tapr@tapr.org**; **http://www.tapr.org**.

Conference registration includes a copy of the conference *Proceedings*, sessions, meetings and lunch on Saturday. Registrations received before September 1 are $45. After September 1 or at the door, registration is $55. The banquet is $30. The Fourth Annual APRS National Symposium on Friday is $25. The Sunday Seminar on PIC Design, Development and Programming is $20.

Microwave Update 2000

Microwave Update 2000 will be held 29 through 30 September 2000 at the Holiday Inn Select, Bucks County just north of Philadelphia, Pennsylvania.

This year, Microwave Update will be hosted by the Mt Airy VHF Radio Club, Inc ("The Pack Rats"). The Holiday Inn Select, Bucks County will be providing accommodations for the event. This is a 215-room full-service hotel with a restaurant, lounge, indoor pool, fitness room and so on. It is centrally located between the Bucks County countryside and historic Philadelphia. We will have full use of the conference center Friday and Saturday. Two smaller meeting rooms will be available for the evening flea market(s).

For those of you who are unfamiliar, the Pack Rats are a group of VHF and Above enthusiasts with a 44-year history. The club was started by a small group from Philadelphia with the sole purpose of promoting VHF activity. The club has sponsored one of the area's best hamfests (Hamarama) for the past 28 years and has hosted the Mid-Atlantic States VHF Conference since 1975. The Packrats provide beacons on 10 VHF/Microwave bands from 50 MHz through 10 GHz and are active in all VHF contests.

Room rates will be in the low to mid $80s. There is no additional charge for double occupancy. We have blocked out 100 rooms under the key code "Microwave Update." The rooms will be held for us until September 7th. This might sound like many rooms, but don't wait until the last minute to make your reservation. This is a busy area. Contact Holiday Inn Select, Bucks County 4700 Street Rd Trevose, PA 19053; tel 215-364-2000 800-HOLIDAY; URL **www.basshotels.com/holiday-inn**.

In addition to ham activities, we are tentatively planning some extra-curricular activities for family members. Most attractions can be reached in less than 1 hour. Here is a partial list of proposed activities:

- Atlantic City Casino bus trips
- Franklin Mills Outlet Mall
- Liberty Bell & Old Philadelphia
- NJ State Aquarium
- Philadelphia Park Race Track
- Sesame Place
- Valley Forge National Park

Of course, it wouldn't be Microwave Update without the surplus tour. There are more new and surplus houses within a 50-mile radius around the Holiday Inn than you will be able to visit in one day. This includes new equipment because Down East Microwave factory tours will be on the list. There will be evening flea markets at the hotel and don't forget Hamarama on Sunday. Please add flashlights to your packing list. The doors to the Pack Rat hamfest (Hamarama) open Sunday at 8 AM, but Hamarama has always been known for the "flashlight shopping."

Noise Figure testing will be provided as well as an equipment tune-up clinic.

Advance Registration is $40 with forms available at the Web site listed below. Send registration to Microwave Update, PO Box 682, Hatboro, PA 19040. Hamarama and Dinner tickets will be available at the door.

For more information contact **JohnKB3XG@aol.com** and visit the Packrats Web page for the latest news on Microwave Update 2000 at **http://www.ij.net/packrats/MUD_2000/mud.html**.

Northwest VHF/UHF Conference

A Pacific Northwest VHF UHF Conference will take place this year thanks to the efforts of Arnie Jensen, W7DSA. The date is Saturday, September 23rd at the Village Inn at 535 South Hwy in the city of St Helen. For more information, contact Arnie at **n7yag@columbia-center.org** or Jim Christensen, K7ND, at **K7ND@worldnet.att.net**.

Letters to the Editor

Impedance Matching: Interpreting the Virtual Short Circuit (*Communications Quarterly*, Fall 1999)

Dear Editor,

In this article, Steven Best, VE9SRB, discusses reflection mechanics that are basic to all impedance-matching operations. He asserts that the explanation of wave mechanics appearing in my book *Reflections—Transmission Lines and Antennas* and in the Mar/Apr 1998 *QEX* article I authored ("Examining the Mechanics of Wave Interference in Impedance Matching") is incorrect.

In an attempt to prove my explanation wrong, Dr. Best included several pages of erroneous mathematical calculations, resulting from misuse of a basic concept of transmission-line theory. The text accompanying his math contains grossly incorrect statements concerning conjugate matching and reflection mechanics. His statements assert that my understanding of various aspects of conjugate matching is incorrect, and they also imply that the basis for my explanation of reflection mechanics is simply my invention.

To the contrary, the material I presented appeared in engineering texts as early as 1943. An eloquent presentation of the reflection mechanics basic to impedance matching appears in MIT physics professor J. C. Slater's book, *Microwave Transmission*, (McGraw-Hill, 1943). Another presentation with rigorous mathematical proof by the eminent microwave engineer Andrew Alford of the Harvard Radio Research Laboratory staff appears in *Very High-Frequency Techniques*, Vol 1, (McGraw-Hill, 1947).

I reported this material to the ham community in *QST* (October 1973), repeated it in *Reflections* and in revised form in Mar/Apr 1998 *QEX*. The material paraphrased from the above engineering texts was presented without altering the concepts and without adding any concept of my own. Below, I explain why Dr. Best's statements are wrong, and how he mistakenly arrived at them.

Dr. Best based some of his statements on the results of his Appendix B. However, a vital calculation and the procedure appearing there are both flawed: He used an incorrect mathematical premise and technical procedure to obtain the network output impedance, *ZN*, 71.13 + j77.82 Ω. Had he started with the correct premise and used the right procedure, explained below, he would have obtained 58.32 + j85.85 Ω for *ZN*, the *conjugate* of the line input impedance Z_{IN}, 58.32 – j85.85 Ω. These errors are a major factor in Dr. Best's disagreement with certain portions of my published material. As will be seen later, this calculation was unnecessary.

Now to explain: In Appendix A of his article, he first determined the correct values of the T-network parameters (C-L-C) required to match line impedance Z_{IN}, 58.32 –j85.85 Ω at the input of the antenna line to a 50-Ω network input impedance. He calculated the network parameters starting with Z_{IN}, then transformed that impedance to the network input impedance using the correct attenuation factor (positive) and the correct output-to-input phase relationship, also positive. However, it should be first understood that starting with the line input impedance Z_{IN} for calculating the network parameters, Z_{IN} immediately establishes the network output impedance *ZN*, 58.32 + j85.85 Ω, as the conjugate of Z_{IN}, 58.32 –j85.85, a given. No calculation is necessary—simply a reversal of sign. This relationship follows from the Maximum Power Transfer Theorem that says maximum available power will be delivered when there is a conjugate match at the junction of the network output and its load, in this case the antenna line. However, as we shall see, because the correct impedance *ZN* is already a given, his pages of math are superfluous.

First, recalling from his Appendix A, transforming the load (line impedance Z_{IN}) through the network to the input yielded the 50-Ω input impedance. Conversely, transforming the input impedance through the network going in the opposite direction from input to load, we end up where we started, at the load, line impedance, Z_{IN}. In addition, when transforming from input to load, both the attenuation factor and the input-output phase relationship must also be reversed—from positive to negative. This procedure is easily clarified and verified by visually tracing the corresponding load-to-input and back to load plotted on the Smith chart, including the gradual inward spiral while going toward the input to account for attenuation.

Dr. Best's first procedural error occurred when reversing the direction of impedance transformation in the belief that he was returning to the output impedance *ZN*, not Z_{IN}. Remember, the network (and the equation for his calculation) transforms impedance from network input to network *load*, not from input to network *output*.

His second procedural error also occurred when reversing the direction of the impedance transformation—he failed to reverse the attenuation factor and the phase. The result? The incorrect value he obtained for the network output impedance *ZN*. Consequently, he assumed that a re-reflection occurs at the junction. Since he believes that reflection has a coefficient ρ with magnitude of only 0.56, he concluded that total re-reflection does not occur there. Indeed it doesn't! In reality, total re-reflection of the reflected waves occurs at the *input of the network*, the matching point, where the reflection coefficient is 1.0 to the reflected waves but the reflection coefficient is 0.0 to the source waves, thus no reflection of source waves occurs. There is no partial re-reflection at the network-output line-input junction as he claims.

This phenomenon is explained in the Alford and Slater engineering references noted earlier. All this preoccupation with output impedance *ZN* is unwarranted. On entering the network rearward, output impedance *ZN* is transparent to the reflected waves, and they travel on rearward through *ZN* to become totally re-reflected at the matching point, the network input. Here the reflection coefficient is 1.0 because of the virtual short circuit established by the wave interference as explained in the references cited above, in *Reflections* and in my *QEX* article.

The effect of network attenuation only reduces the power available at the network output relative to that delivered to the network input, and has no effect on the network output impedance when designed to match the impedance of the load. This refutes Dr. Best's claim that a conjugate match can never exist at the network output if the network contains attenuation, because he asserts that the output impedance changes with attenuation. *—Walter Maxwell, W2DU, 234 Cranor Ave, DeLand, FL;* **w2du@iag.net**

Dear Editor

I have read Walter Maxwell's (W2DU) comments regarding my article. The basis of his criticism is that he believes the method that I use to determine the output impedance of a T network is incorrect. In his letter, he further describes the impedance-reversal transformation technique that he uses to determine the output impedance of a T network. Using his calculation methods, Mr. Maxwell determines that the output impedance of a "lossy" T network is the conjugate of the load impedance connected at the T-network output when an impedance match exists at the T-network input. A review of impedance transformation concepts will demonstrate that the material presented in my article is correct and that Mr. Maxwell's criticism of my work is unjustified.

Consider the basic transmission line system shown in Fig 1, where a T-network circuit is used to match the input impedance of a transmission line, Z_{IN}, to the transmission line's characteristic impedance Z_0. A known load impedance, Z_L, is connected at the end of the transmission line. In this discussion, it is assumed that the T-network circuit components are "lossy."

The first impedance-transformation procedure is used to determine the input impedance to the transmission line, Z_{IN}, from the known load impedance Z_L. The load impedance Z_L can be transformed to the transmission-line input to determine Z_{IN} using the following generalized transmission line formula for input impedance:

$$Z_{IN}=Z_0\left[\frac{\frac{Z_L}{Z_0}+\tanh(\gamma L)}{1+\frac{Z_L}{Z_0}\tanh(\gamma L)}\right] \quad \text{(Eq 1)}$$

where L is the length of the transmission line and γ is the transmission-line propagation factor given by $\gamma = \alpha + j\beta$. The term α is the transmission-line attenuation factor in nepers/meter and β is the transmission-line phase-shift factor given by $2\pi/\lambda$. In this calculation, both the transmission-line attenuation and phase-shift factors are "positive."

An impedance-reversal transformation procedure can be used to determine the load impedance, Z_L, connected at the end of the transmission line beginning with the input impedance of the transmission line, Z_{IN}. In this case, Eq 1 is rewritten in a reverse manner as follows:

$$Z_L=Z_0\left[\frac{\frac{Z_{IN}}{Z_0}+\tanh(-\gamma L)}{1+\frac{Z_{IN}}{Z_0}\tanh(-\gamma L)}\right] \quad \text{(Eq 2)}$$

It is critically important to note that with this impedance-reversal transformation procedure, the sign of both the attenuation and phase-shift factors must be reversed or set "negative." If the impedance-reversal transform-ation procedure is performed with only the sign of the attenuation factor set negative in Eq 2, the resulting value determined for Z_L is meaningless. However, in the special case where Z_{IN} to the transmission line is purely resistive (a Z_0 match not being necess-ary), using Eq 2 with only the sign of the attenuation factor set negative results in the conjugate of Z_L being determined. This is mathematically interesting but other than the fact that the conjugate of Z_L is determined, it is physically meaningless.

A somewhat similar impedance transformation procedure can also be used with the T-network circuit. In this case, we begin with the load impedance connected at the T-network output, which is the input impedance of the transmission line, Z_{IN}. The first objective is to determine the input impedance to the T network, Z_{NET}. Determination of Z_{NET} is accomplished using simple circuit-theory equations. In the general case, the T-network circuit elements are "lossy" and have an element impedance in the form of Z = R + jX. The circuit calculations used to determine Z_{NET} are performed as follows:

$$Z_1=Z_{C2}+Z_{IN}$$
$$Z_2=\frac{Z_1 Z_{IND}}{Z_1+Z_{IND}} \quad \text{(Eq 3)}$$
$$Z_{NET}=Z_2+Z_{C1}$$

where Z_{C1} is the impedance of capacitor C1, Z_{IND} is the impedance of inductor L and Z_{C2} is the impedance of capacitor C2.

An impedance-reversal calculation procedure can be used to determine the load impedance connected at the T-network output, Z_{IN}, beginning with T-network input impedance Z_{NET}. In this case, the formulas in Eq 3 are rewritten in a reverse manner as follows:

$$Z_1=(-Z_{C1})+Z_{NET}$$
$$Z_2=\frac{Z_1(-Z_{IND})}{Z_1+(-Z_{IND})} \quad \text{(Eq 4)}$$
$$Z_{IN}=Z_2+(-Z_{C2})$$

Again, the sign of both the resistance and reactance in each network component must be reversed or set negative. As with the transmission-line calculations, using the impedance-reversal transformation calculation with only the sign of the resistance set negative in Eq 4 results in a meaningless value of Z_{IN}. However, in the special case where the T-network input impedance, Z_{NET}, is purely resistive (a Z_0 match not being necessary), using Eq 4 with only the signs of the resistances set negative results in the conjugate of Z_{IN} being determined.

Determination of Z_{OUT} of a T-network circuit is actually very straightforward and is accomplished using the same circuit theory concepts used to determine the forward input impedance Z_{NET}. To determine Z_{OUT}, we move our viewpoint to the output side of the T network and, looking rearward into it, perform the same simple impedance calculations beginning with the impedance "terminating" the network input. This impedance is defined as Z_S in Fig 1. This impedance should not be confused with the T-network input impedance, as these two impedances are generally not equal to one another.

The T-network output impedance is simply determined as follows:

$$Z_1=Z_{C1}+Z_S$$
$$Z_2=\frac{Z_1 Z_{IND}}{Z_1+Z_{IND}} \quad \text{(Eq 5)}$$
$$Z_{OUT}=Z_2+Z_{C2}$$

In my article, I used Eq 5 to determine the output impedance of the T-network circuit described in my example. In the T-network circuit described in my article, the following circuit component impedance values were used in the calculation:

Z_{C1} = 0.51 $-j$205.56 Ω,

Z_{IND} = 1.55 + j116.41 Ω and

Z_{C2} = 0.38 $-j$150.15 Ω.

In my calculations, I assumed $Z_S = Z_0$. This assumption is unrelated to the fact that the input impedance of the matched T network is also equal to Z_0. In practice, the value of Z_S will be a function of the transmitter and the characteristics of any transmission line connecting the transmitter and the T network.

The procedure Mr. Maxwell uses to determine the output impedance of the T network is actually the procedure that should be used to determine the load impedance connected at the T-network output. He makes an error in only setting the resistance of each network component negative in his impedance-reversal calculations. This is the reason that he calculates an "output impedance" equal to the conjugate of the transmission-line input impedance.

Mr. Maxwell's description of my procedural method is incorrect and does not represent the calculation technique I used in my analysis. Further, he asserts that it is a given that the output impedance of the T network is the conjugate of Z_{IN} simply

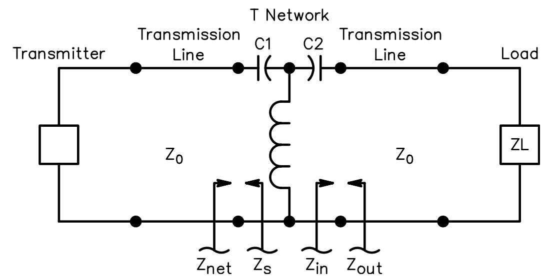

Fig 1—Basic transmission-line system with T-network matching circuit.

because an impedance match is established at the network input. He states that this follows from the maximum-power-transfer theorem. I agree that maximum power transfer will occur to the load when a conjugate match exists between the network output and load; however, an impedance match at the network input does not, in itself, establish a conjugate match at the output in a lossy network.

Mr. Maxwell also states that the output impedance of the network is transparent to reflected waves and that they are totally re-reflected through the creation of a "virtual short circuit." In transmission-line systems, reflections are created at any physical impedance discontinuity. This is the basis of all transmission-line theory. Unless the impedance seen by a traveling wave is equal to Z_0, a reflection is created. To state otherwise is a direct contradiction of generally accepted transmission-line theory and practice. *—Dr. Steven R. Best, VE9SRB, 48 Perimeter Rd, Manchester, NH 03103;* **sbest@cushcraft.com**

Dear Editor,

I will demonstrate below that the criticism appearing in my letter is both justified and correct, and that the material in Steve's article is incorrect.

Best states "If the impedance reversal transformation procedure is performed with only the sign of the attenuation factor set negative in Eq 2, the resulting value determined for Z_L is meaningless." That is not true. First, we are dealing with Z_{OUT}, not Z_L. Second, the resulting value with only the sign of the attenuation set negative is the output impedance of the network, Z_{OUT}, the conjugate of the line input impedance. Third, the value is not meaningless for the reason just stated. A special case is not necessary here for the conjugate of Z_L to be determined with only the sign of attenuation factor set negative. The conjugate of Z_L is determined in this case whatever the value of Z_L. And it is certainly not physically meaningless. Best's other statements about transformations involving reversing the sign of only resistance are therefore also incorrect.

Here is the crucial point that Steve misses: If there is loss in the network, the value obtained looking rearward into the network will not be the impedance at the output of the network when used to deliver power to its load. Looking rearward into the network determines the input impedance of the network at the terminals that were formerly the output terminals, because now the former input terminals are the output terminals. The impedance-transformation directions are reversed and the measurement is again going from load to input. Thus a measurement at the new input terminals uses the same signs (positive) of phase and attenuation factor in going from the new output terminals to the new input terminals. Consequently, measurement also involves attenuation in the wrong direction to obtain the true output impedance going in the original direction. The correct output impedance of the network can only be determined by calculation, using positive phase and negative attenuation factor unless the network is loss less. Using both negative phase and attenuation factors yields the load impedance. Changing the phase to positive and leaving the attenuation negative reverses the sign of the load impedance to obtain its conjugate, the network output impedance.

Let me recite the rules of signs for making impedance transformations on networks and lines. It will be helpful in understanding the basis for these sign rules to remember that in transforming from load to input, due to network or line attenuation, both the magnitude of the reflected waves and the SWR decrease, and when transforming from input to load the magnitude and SWR increase.

1. When transforming in the direction from load to input the attenuation is always positive.

2. When transforming in the direction from input to load the attenuation is always negative.

3. When transforming load impedance to input impedance both phase and attenuation are positive.

4. When transforming input impedance to load impedance both phase and attenuation are negative.

5. When transforming input impedance to output impedance phase is positive and attenuation is negative.

It must be kept in mind that in going from input to output, both reflection coefficient and SWR increase. For both output impedance and load impedance to follow the changes in reflection coefficient and SWR accordingly during the transformation from input to output, the attenuation factor must be negative. If the attenuation factor is positive the reflection coefficient and SWR decrease, as in going from load to input. When Steve uses positive attenuation, as he does above, what he believes is the network output impedance is really the input impedance with the network terminals reversed with the input terminated. Consequently, using positive attenuation factor gives a meaningless value with respect to the use of the network with its intended output terminals feeding the transmission line. The correct network output impedance is the conjugate of the input impedance of the transmission line, and can be determined only by using negative attenuation factor and positive phase when transforming the network input impedance to the output.

This error in using positive attenuation factor to determine the network output impedance is also the reason Steve believes that no conjugate match can exist when the network has loss. We know that conjugate matches occur in network operation, but if we were to follow Steve's concepts, there would never be a conjugate match in practice, because there are no loss-less networks.*—Walter Maxwell, W2DU*

Doug,

I would like to add a few brief comments regarding the pi network as a follow-up to my letter to the editor in the May/June *QEX*. The example considered was for 2000 Ω input, a 50-Ω load, and an operating Q of 12. The question occurs: How does the output impedance of the pi network, looking backward from the 50-Ω load, vary as *rp*, the tube's loss-less dynamic output resistance (the slope of the plate V-I curves) varies? Note that the network presents a 2000-Ω plate load, which is assumed to be correct for the range of *rp* values shown in Fig 2.

Let *rp* vary between 1000 and 5000 Ω. Fig 2 shows the resistance, reactance and magnitude of the pi

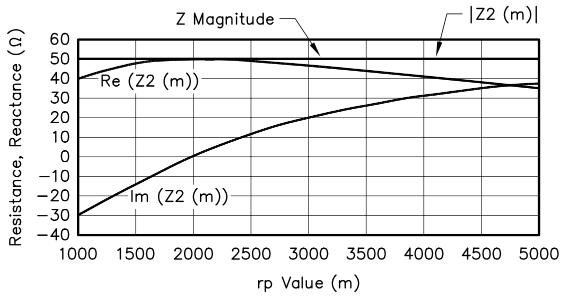

Fig 2—The resistance, reactance and magnitude of a pi network's output impedance.

network's output impedance. The following items are noticed:

- The magnitude remains close to 50 Ω.
- This is also approximately the value that the load-pull test (45-55 Ω) gives.
- For an *rp* of 2000 Ω, the output impedance at the coax connector becomes complex. The values of series R and X are shown.

The conclusion is that a *magnitude-only* measurement of the output impedance (at the coax) cannot be used to determine *rp*. On the basis of this magnitude measurement, one would believe that *rp* is actually very close to 2000 Ω, the same value as the 2000-Ω value of pi-network input resistance, regardless of the *actual* value of *rp*.

The comments of Fred Telewski, WA7TZY, are appreciated.—*William E. Sabin, W0IYH, 1400 Harold Dr SE, Cedar Rapids, IA, 52403;* **sabinw@mwci.net**

A Regulated 2400-V Power Supply (Jul/Aug 1999)

Thanks to Brad, WB9BPF, who found another error that had gone by me entirely. Figure 2 on page 52 shows a resistor from the emitter of Q4 (2N3904) to the emitter of Q3 (2N2646) UJT as 403 k. Since 403 k is a standard precision value, Brad used it and his UJT won't fire! That resistor should be 4.3 k.

By the way, I have been using the linear every day for a month and I am so very pleased. When I run 200-300 W you would swear the needle is glued to the meter face! There are three of these supplies working locally. One is 4600 V!—*Al Williams, VE6AXW, 13436 114 St NW, Edmonton, AB T5E 5E6;* **alwill1@telusplanet.net**

Next Issue in QEX/Communications Quarterly

It's been said that hindsight is 20-20; looking ahead isn't always so easy. Next time, we'll reprint a fascinating bit of foresight from 1963 (!) by Warren Bruene, W5OLY, along with his updated prognosis of the state of Amateur Radio art. We think it will be interesting for future "optometrists" to look back on our doings as we slip into a new century.

In case you didn't know, Robert Brown, NM7M, is a 160-meter fan and a DXer. He takes a look at a particular path that seems to hold significant promise for top-banders during the new season. Bill Sabin, W0IYH, contributes some application and analysis of thermistors as used in transceiver design. VFO builders will be particularly interested. M. A. Chapman, KI6BP, brings us his 30-meter QRP transceiver design.